



Cape Peninsula
University of Technology

**EFFICIENCY PLAN FOR A LARGE INTERCONNECTED URBAN RING MAIN
NETWORK UNDER CONTINGENCY CONDITIONS**

by

JULIA DHIMBULUKWENI IINDOMBO

Thesis submitted in fulfilment of the requirements for the degree

Master of Technology: Electrical Engineering

in the Faculty of Engineering

at the Cape Peninsula University of Technology

Supervisor: Prof. G. Atkinson-Hope

**Cape Town
November 2011**

CPUT Copyright Information

The dissertation/thesis may not be published either in part (in scholarly, scientific or technical journals), or as a whole (as a monograph), unless permission has been obtained from the university

DECLARATION

I, Julia Dhimbulukweni lindombo, declare that the contents of this dissertation/thesis represent my own unaided work, and that the dissertation/thesis has not previously been submitted for academic examination towards any qualification. Furthermore, it represents my own opinions and not necessarily those of the Cape Peninsula University of Technology.

Signed

Date

ACKNOWLEDGEMENTS

- I give thanks to the Lord, my God for his blessings and for guiding me towards my achievements. His love is never ending and his grace is beyond our knowledge.
- I would like to express my deepest gratitude and appreciation to my supervisor, Prof G Atkinson-Hope, for his expert advice, encouragement and commitment during this project.
- I wish to thank the Namibia Power Company (NamPower) for granting me bursary
- I wish to thank the Cape Peninsula University of Technology, for granting me a bursary, to pay for my Masters Degree.

- Special thanks are due to my uncle Mr. G. Enkara for his encouragement and valuable help throughout this project.
- I am also grateful to the Cape Peninsula University of Technology, Centre of Power System Research (CPSR) for availing simulation software packages and a computer laboratory to assist me in completing my investigations leading to my contribution to the field of electrical power engineering.
- My heartfelt thanks go out to my family and my friends who had the foresight to provide the support, background and encouragement for my education.

ABSTRACT

In a situation, where there is a shortage of power generation or the power stations are operating with a very low reserve margin, as is typically the current position in South Africa, there is a need to operate distribution network at the highest possible efficiency by utilising network power loss reduction techniques. Such techniques are especially important when contingencies occur as they tend to increase loss, reduce efficiencies and cause power supplies to such networks to increase. This increase can cause the network or multiples of such networks to be load shed as the power stations do not have the reserve margins to meet this increased demand. The ideal situation would thus be to minimise network loss and in so doing decrease the amount of power needed and possibly avoid load shedding. Thus, there is a need to study efficiency, network loss reduction under contingency conditions and this is the focus of the research.

Most large urban distribution networks are operated as ring main networks. Ring networks are considered to have less power loss. However, a major component in a ring network can cause the loss to substantially increase; resulting in power shortage in the network. There is an urgency to eliminate high network loss.

An efficiency plan was developed for a large ring network that reduces the loss so that its input power can be decreased. In this way, the available power existing due to the contingency can be more evenly spread, and the number of ring main networks to be load shed could be reduced.

The efficiency investigation looks into two possible techniques used for power loss reduction, which are network reconfiguration and capacitor addition. Three case studies were conducted on an interconnected ring main distribution network. This network had two ring main networks, Ring main network 1 and Ring main network 2. The first case study considered a loss of a primary U/G cable in Ring main network 1; the second case study considered the loss of a substation infeed in Ring main network 1 and the third case study considered two simultaneously occurring contingency cases, the loss of a substation infeed in Ring main network 1 and loss of a primary U/G Cable in Ring main network 2. Additional studies were done in case studies 1 and 2 in which the transients caused by capacitor switching were investigated and measured. The network was simulated using the DIgSILENT and PSCAD power system software packages. DIgSILENT is a tool used mainly for steady-state whereas PSCAD is a time-domain package used for studying transients.

From the investigations conducted, the developed efficiency plan for a large ring main network under contingency conditions was shown to be effective. It can be easily adapted for

investigations of other ring networks as well as interconnected ring networks as is demonstrated in the work. The efficiency plan is thus recommended for application in this important field as it will help to prevent load shedding, especially in the situation where power stations are operating with low reserve margins.

TABLE OF CONTENTS

DECLARATION	ii
ACKNOWLEDGEMENTS	iii
ABSTRACT	iv
TABLE OF CONTENTS	vi
SYMBOLS	xi
CHAPTER ONE: INTRODUCTION	1
1.1 Background	1
1.2 Shortcomings and need for research	1
1.3 Objective of research	2
1.4 Outline of the thesis	3
CHAPTER TWO: POWER IN AC CIRCUITS	4
2. Introduction	4
2.1 Power in a resistive circuit	4
2.1.1 Power in a Inductive circuit	6
2.1.2 Power in a capacitive circuit	7
2.1.3 Circuit with Resistance and Reactance	8
2.1.4 Reactive power	9
2.1.5 Complex power	10
2.1.6 Power factor (PF)	10
2.1.7 Active and reactive currents	11
2.2 Reactive power in distribution networks	12
2.2.1 Shunt capacitors	12
2.2.2 Benefits of shunt capacitors	12
2.3 Transients and capacitor switching	15
2.4 Summary	18
CHAPTER THREE: DISTRIBUTION NETWORK THEORY AND OPERATION	19
3. Overview of a distribution system	19
3.1 Types of distribution systems	20
3.1.1 Radial feeder system	20
3.1.2 Ring main feeder systems	21
3.1.3 Interconnected distribution system	22
3.2 Components of a distribution network	23
3.2.1 Underground cables (U/G cables)	23
3.2.2 Overhead lines	25
3.2.3 Power transformer	26
3.2.4 Circuit breakers and switches	30
3.3 Operational constraints of a distribution network	31
3.3.1 Supply frequency standard	31
3.3.2 Voltage standards	31
3.3.3 Conductor current carrying capacity	32
3.4 Summary	32
CHAPTER FOUR: LOAD FLOW	33
4. Power flow analysis	33
4.1 Methods for power flow solution in a ring main network	33
4.2 Bus classification	36

4.3	Formulation methods for load flow solutions	37
4.3.1	DlgSILENT powerfactory	38
4.3.2	PSCAD	38
4.4	Summary	38
CHAPTER FIVE: CONTINGENCY ANALYSIS		39
5.	Overview	39
5.1	Contingency analysis methodology.....	40
5.1.1	Contingency case	40
5.1.2	Reserve margin	42
5.2	Summary	42
CHAPTER SIX: ENERGY EFFICIENCY TECHNIQUES		43
6.	Overview	43
6.1	Techniques used for power loss reduction.....	43
6.1.1	Re-conductoring	43
6.1.2	Load balancing	44
6.1.3	Capacitor Addition	44
6.1.4	Replacement of old and obsolete equipment	44
6.1.5	Reconfiguring the network	44
6.1.6	Energy Management Systems (EMS).....	45
6.2	Practical choices for power loss reduction	46
6.3	Benefits of improving efficiency	46
6.4	Summary	46
CHAPTER SEVEN: EFFICIENCY PLAN OF INTERCONNECTED RING MAIN NETWORK.....		47
7.	Overview	47
7.1	Development of the efficiency plan work flow diagram.....	47
7.2	Efficiency plan Methodology	49
7.2.1	U/G cable outage.....	50
7.2.2	Substation infeed outage	52
7.3	Capacitor switching voltage transients measurements.....	52
7.4	Summary	53
CHAPTER EIGHT: APPLICATION OF EFFICIENCY PLAN		54
8.	Overview	54
8.1	Case study 1	54
8.2	Case study 2	61
8.3	Case study 3	65
8.4	Summary	71
CHAPTER NINE: ANALYSIS OF RESULTS AND EVALUATION OF EFFICIENCY WORK PLAN		72
9.	Introduction.....	72
9.1	Case study 1	72
9.1.1	Analysis of RM1 voltage profile.....	72
9.1.2	Analysis of RM1 cable loadings	73
9.1.3	RM1 Volt-drop calculations.....	73
9.1.4	Analysis of RM1 overall power loss	73
9.1.5	Analysis of RM1 overall efficiency.....	75
9.1.6	Transient studies	75

9.2	Case study 2	76
9.2.1	RM1 Voltage profile	76
9.2.2	RM1 Cable loading	76
9.2.3	RM1 volt-drop calculations	77
9.2.4	RM1 Power loss analysis.....	77
9.2.5	RM1 Overall Efficiency	78
9.2.6	Transient studies	79
9.3	Case study 3	80
9.3.1	RM1 Voltage profile	80
9.3.2	RM2 Voltage profile	80
9.3.3	Cable loading for RM1	81
9.3.4	Cable loading for RM2.....	81
9.3.5	RM1 and RM2 volt-drop calculations	82
9.3.6	Analysis of Power loss of RM1	82
9.3.7	Analysis of RM2 Power losses.....	83
9.3.8	RM1 Overall efficiency.....	83
9.3.9	RM2 Overall efficiency.....	84
9.4	Discussion of significant findings arising from the existing and proposed optimal configurations in this research.....	84
9.5	Summary.....	85

CHAPTER TEN: CONCLUSIONS, RECOMMENDATIONS AND FUTURE WORK 86

REFERENCES.....	88
APPENDIX A	91
APPENDIX B	97
APPENDIX C	101
APPENDIX D	104

LIST OF FIGURES

Figure 2.1: Resistive circuit	4
Figure 2.2: Relationship between v , i and p in a resistor	5
Figure 2.3: Inductive circuit	6
Figure 2.4: Relationship between v , i and p in an inductor	6
Figure 2.5: Capacitive circuit.....	7
Figure 2.6: Relationship between v , i and p in a capacitor	8
Figure 2.7: Power triangle for an inductive load	10
Figure 2.8: Currents in different circuits	11
Figure 2.9: Circuit representation.....	13
Figure 2.10: Relationship between power loss and power factor.....	15
Figure 2.11: Capacitor switching equivalent circuit.....	16
Figure 2.12: Oscillogram of total capacitor voltage transient component.....	17
Figure 2.13: Transient and steady-state components at the oscillogram	18
Figure 3.1: Overview of the power system from generation to load's switch.....	20
Figure 3.2: Radial feeder system	21
Figure 3.3: Ring main feeder system	22
Figure 3.4: Typical interconnected ring main network	22
Figure 3.5: Single equivalent circuit of a power cable.....	23
Figure 3.6: A transformer	27
Figure 3.7: Equivalent circuit of a practical single-phase 2-winding transformer.....	28
Figure 3.8: Efficiency curve.....	30
Figure 4.1: Power flow between two sources	34
Figure 4.2: Power phasor diagram.....	34
Figure 4.3: Summary of power flow directions.....	35
Figure 5.1: Contingency analysis methodology	40
Figure 5.2: One-line diagram of a typical interconnected network	41
Figure 6.1: Schematic diagram of a primary circuit of a distribution system	45
Figure 7.1: Large urban interconnected ring main networks RM1 and RM2	48
Figure 7.2: Efficiency plan: work flow diagram	49
Figure 8.1: Case study 1 Single line diagram after the removal of Cable 1A	56
Figure 8.2: Case study 1 optimal configuration	59
Figure 8.3: Case study 2 single line diagram after VS1 is removed.....	62
Figure 8.4: Case study 2 optimal configuration	63
Figure 8.5: Case study 3 Single line diagram after the removal of VS RM1 and cable 3B....	66
Figure 8.6: case study 3 optimal configuration	68
Figure 9.1: RM1 voltage profiles for case study 1	72
Figure 9.2: RM1 cable loadings for case study 1.....	73
Figure 9.3: RM1 Power losses for case study 1	74
Figure 9.4: RM1 Overall efficiency for case study 1	75
Figure 9.5: Voltage waveforms at bus LV1 during capacitor switching at station BUSHV5...	75
Figure 9.6: RM1 voltage profiles for case study 2	76
Figure 9.7: RM1 cable loadings for case study 2.....	77
Figure 9.8: RM1 Power losses for case study 2	78
Figure 9.9: RM1 Overall efficiency for case study 2	79
Figure 9.10: Voltage waveforms at bus LV3 during capacitor switching at station BUSHV5.	79
Figure 9.11: Voltage profiles of Case study 3 for RM1	80
Figure 9.12: Voltage profiles of case study 3 for RM2	80
Figure 9.13: Cable loadings of case study 3 for RM1	81
Figure 9.14: Cable loadings of case study 3 for RM2	81
Figure 9.15: RM1 Power losses for case study 3	82
Figure 9.16: RM2 Power losses for case study 3	83
Figure 9.17: RM1 Overall efficiency for case study 3	83
Figure 9.18: RM2 Overall efficiency for case study 3	84
Figure A.1: Linear load modelling.....	92
Figure A.2:Transformer modelling.....	93

Figure A.3: Cable modelling.....	95
Figure A.4: Voltage source modelling	95
Figure A.5: Busbar modelling.....	96
Figure A.6: Capacitor modelling.....	96
Figure B.1: Ideal voltage source	97
Figure B.2: Transformer modelling.....	97
Figure B.3: Busbar modelling.....	98
Figure B.4: Cable modelling.....	98
Figure B.5: Linear load modelling.....	99
Figure B.6: Capacitor modelling.....	99
Figure B.7: Circuit breaker modelling.....	100
Figure D.1: RM2 Voltage profile for case study 2.....	104
Figure D.2: RM2 cable loadings for case study 2.....	105
Figure D.3: RM2 Power losses for case study 2.....	105
Figure D.4: RM2 Overall efficiency for case study 2.....	106

LIST OF TABLES

Table 4.1: Power flow buses and variables.....	37
Table 7.1: South African National Voltage Limits LV busbar	51
Table 7.2: Limits for cables	51
Table 8.1: RM1 load bus voltage levels	54
Table 8.2: RM1 Cable loading of RM1	55
Table 8.3: RM1 Load bus voltage levels due to removal of Cable 1A.....	57
Table 8.4: RM1 Cable loading due to removal of Cable 1A.....	57
Table 8.5: Load bus voltage levels for the optimal configuration	59
Table 8.6: Cable loadings for the optimal configuration.....	60
Table 8.7: Peak voltage levels at the RM1 load buses during capacitor switching	61
Table 8.8: RM1 load bus voltage levels for the optimal configuration.....	63
Table 8.9: RM1 cable loadings for the optimal configuration	64
Table 8.10: Peak voltage levels of the RM1 load buses during capacitor switching	65
Table 8.11: RM2 Load bus voltage levels due to removal of Cable 3B.....	66
Table 8.12: RM2 Cable loadings due to the removal of Cable 3B	67
Table 8.13: RM1 Load bus voltage levels for the optimum configuration.....	69
Table 8.14: RM1 Cable loadings for the optimum configuration	69
Table 8.15: RM2 load bus voltage levels for the optimum configuration.....	70
Table 8.16: RM2 Cable loadings for the optimum configuration	71
Table 9.1: Highest volt-drop for the different configurations of RM1	73
Table 9.2: Highest volt-drop for the different configurations of RM1	77
Table 9.3: Highest volt-drop for the different configurations of RM1	82
Table 9.4: Highest volt-drop for the different configurations of RM2	82
Table A.1: Load Specifications.....	91
Table A.2: Transformers Specifications	93
Table A.3: U/G cable Specifications.....	94
Table C.1: Normal operating voltage profile for RM2.....	101
Table C.2: Normal operating cable loadings for RM2	101
Table C.3: RM2 Load bus voltage levels.....	102
Table C.4: RM2 Cable loadings	102
Table D.1: RM2's highest volt-drop obtained for the different configurations.....	105

SYMBOLS

%	Percentage
A	Unit of current
AC	Alternating Current
C	Capacitance
CPUT	Cape Peninsula University of Technology
E₁	Primary voltage
E₂	Secondary voltage
EMS	Energy management systems
f₁	Fundamental frequency
HV	High Voltage
Hz	Unit of frequency
I	Current
I_{rms}	Root mean square current
K_{pu}	Voltage dependency index for P
K_{qu}	Voltage dependency index for Q
L	Inductance
L_{MAGNETISING}	Magnetising inductance
LV	Low Voltage
PF	Power factor
P_{in}	Input power
PLC	Paper Insulated Lead Covered Cable
P_L	Power loss
P_o	Operating real power
P_{out}	Output power
P_r	Rated real power
Q	Reactive power
Q_o	Operating reactive power
Q_r	Rated reactive power
R	Resistance
R_p	Primary resistance
R_s	Secondary resistance
SCADA	Supervisory Control and Data Acquisition
t	Time
V	Unit for voltage
V_{max}	Maximum voltage
V_{min}	Minimum voltage
V_{rms}	Root mean square voltage

X_C	Capacitive reactance
X_L	Inductive reactance
X_m	magnetising reactance
X_p	Primary reactance
X_s	Secondary reactance
Z	Impedance
Ω	Unit of resistance

CHAPTER ONE INTRODUCTION

1.1 Background

Saving electrical power has become a major challenge worldwide. However due to the increase in environmental concerns the expansion of power stations that use traditional energy resources, such as coal, nuclear, oil etc., are being considered to be put on hold, forcing existing transmission and/or distribution networks to be used more efficiently (Mohamed & Lee, 2006:2388). Researchers have shown that a reduction of power loss in the network is much more beneficial than the increase in generation capacity. (Lupescu & Leca, 2008:1). According to Fourie (2004:10), power losses in networks represent 6-8% of the cost of generated electricity. Thus, there is a need to conduct energy studies to improve efficiencies of the power systems.

Traditionally, a well designed network serves its purpose best when it is working under normal operating conditions and power loss are kept at a minimum. Failure of a major component in a ring main network, such as a substation infeed or main distribution line can cause a network to go into an unacceptable state of operation requiring contingency analysis. In this contingency state, the network operators must attempt to control the network defensively, that is, to make the input power to the ring main network as small as possible, by using techniques to decrease losses. This reduction in power drawn by the ring main network will mean less power needs to be supplied by power stations to this network, making more available for other networks, despite the contingency being in effect.

1.2 Shortcomings and need for research

Many approaches regarding power loss reduction in distribution systems have been proposed over the years. Some researchers used optimization methods, while others used expert systems, or heuristic methods. Many of these methods were developed for radial networks, which are simpler for investigations, however most large urban distribution networks are not operated as radial networks. Also localised areas of a national grid, called "distribution" comprises of many interconnected large urban ring main networks. When operated together they pose great challenges in regard to power loss reduction. Some of the methods applied to reduce loss in radial systems cannot be applied to the power loss analysis of ring main networks. Further, although ring main networks are believed to have less power loss compared to radial networks, loss of an important component in a ring main network can cause an increase in power loss. This may cause a power shortage in the network. There is also a limited explanation of efficient operation under contingency conditions. There are also no studies found in literature on the efficient operation of a large urban network comprising multiple ring main networks. This is a shortcoming in literature.

Thus, there is a need to develop a plan for such a network that shows how to deliver electrical power to loads efficiently under contingency conditions. This is the focus of the work reported herein.

1.3 Objective of research

The objective of this research is to investigate a large urban network comprising multiple ring main networks and develop an efficiency plan for various contingency cases, while ensuring that network constraints are respected. The developed efficiency plan can be used as guidance by network operators to enable them to deliver power to loads efficiently under contingency conditions and in so doing to help reduce the power intake to the ring main network and the impact on generation capacity. This is especially relevant if the overall power system is running with a small reserve margin as this will make extra power available that could help other networks to continue operating which otherwise may need to be load shed, inconveniencing customers.

i) Importance of this research

Under contingency operations the losses in a network generally increase above that occurring under normal operations. The importance of this project is to ensure that the power lost in ring main networks due to contingency conditions should no longer be ignored. This will help network operators and energy conservationists to determine the power loss in the network and assist them with measures that can be taken to reduce these losses.

ii) Contributions

The contributions of this work to power loss reduction and improved efficiency are:

a) Identification and selection of power loss reduction techniques

Literature based on power loss reduction in distribution networks is reviewed. From the review various techniques used for power loss minimization are identified. These techniques were rated from the most effective to the least effective so that the most appropriate technology can be selected. Their effectiveness were evaluated for power loss reduction and improved efficiency in a large urban interconnected ring main network.

b) Efficiency plan

An efficiency plan, in a form of a flow chart, which is unique, is developed for conducting the investigations.

c) Case studies

A large urban interconnected ring main distribution network is identified for investigations and one software package and its models are used to conduct load flow case studies under

normal and contingency operating conditions incorporating the selected power loss reduction techniques and a second time domain software package is used for studying capacitor switching transients, when capacitors are selected as the technology technique to be used for power loss reduction.

d) Analysis of results

Results for the various contingencies and loss reduction techniques applied are analysed in terms of established network regulations/limits and/or network constraints to ensure acceptable state of operation and to demonstrate the application and effectiveness of the developed efficiency plan.

1.4 Outline of the thesis

The thesis is divided into ten chapters:

Chapter 2 presents the theory of power in AC circuits.

Chapter 3 presents the theory on the operation of distribution networks.

Chapter 4 underpins the significance of load flow studies or analysis in distribution systems and power systems. It covers the techniques used to conduct the load flow program and methodologies or formulae for conducting load flow studies are given.

Chapter 5 gives an in-depth review of contingency analysis in power systems. Methods on how to conduct contingency analysis and some of the remedies that can be used to curb the system behaviour when subjected to such scenarios are highlighted.

Chapter 6 discusses the existing energy-efficiency techniques.

Chapter 7 proposes a developed efficiency plan for reducing power losses in an interconnected ring main network under contingency conditions.

Chapter 8 presents the application of the efficiency plan on the case studies under study.

Chapter 9 evaluates the effectiveness of the efficiency plan using the results obtained in chapter 8.

Chapter 10 presents the overall conclusions and recommendations on the main contributions of the thesis and directions for future research are offered

CHAPTER TWO

POWER IN AC CIRCUITS

This chapter presents the ground work for the study of electric systems.

2. Introduction

Power is defined as the rate at which energy is absorbed/delivered by/to an electric component at a specific time (Glover & Sarma, 2002:44). The SI unit of power is the watt (W). The power of a circuit can be obtained by multiplying the voltage (v) and the current (i) which is passing through the circuit. When v and i vary with time, their product is instantaneous power p (Glover & Sarma, 2002:44).

$$p = vi \quad (2.1)$$

Where v and i are the instantaneous voltage and instantaneous current, respectively.

Equation 2.1 refers to instantaneous power which is positive when power is consumed (load) and is negative when power is produced (source).

For AC circuit the voltage and current phasors are most of the time separated by an angle, the phase angle (El-Hawary, 1995:12). Hence the power of electrical AC circuit is dependent on the phase angle between the voltage and current.

2.1 Power in a resistive circuit

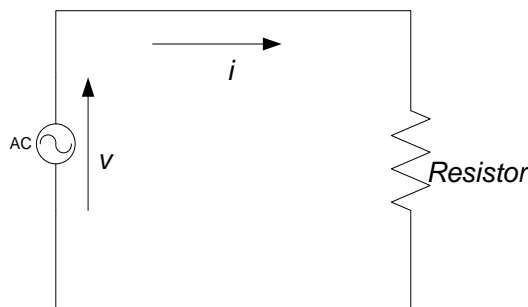


Figure 2.1: Resistive circuit

In a network consisting of only a resistor, the voltage applied to the resistance is calculated as:

$$v = V_p \sin \omega t \quad (2.2)$$

The resultant current will be:

$$i = I_p \sin \omega t \quad (2.3)$$

where, V_p and I_p are peak voltage and current, and ω is the angular velocity in radians/seconds (rad/s). The corresponding power is then:

$$p = vi = V_p I_p (\sin^2 \omega t) \quad (2.4)$$

Since $\sin^2 x = \frac{1}{2}(1 - \cos 2x)$, then:

$$p = V_p I_p \left(\frac{1 - \cos 2\omega t}{2} \right) \quad (2.5)$$

Figure 2.2 shows the voltage, current and power waves in a resistive circuit. It can be seen that the voltage and current are in phase and consequently their product is always positive. Also, when the voltage is negative, so is the current, In other words, the power dissipated is never negative (Grainger & Stevenson, 1994:5). This is because a resistor always takes power from the source and turns it into heat. Since the resistor cannot store energy it can never return power to the source.

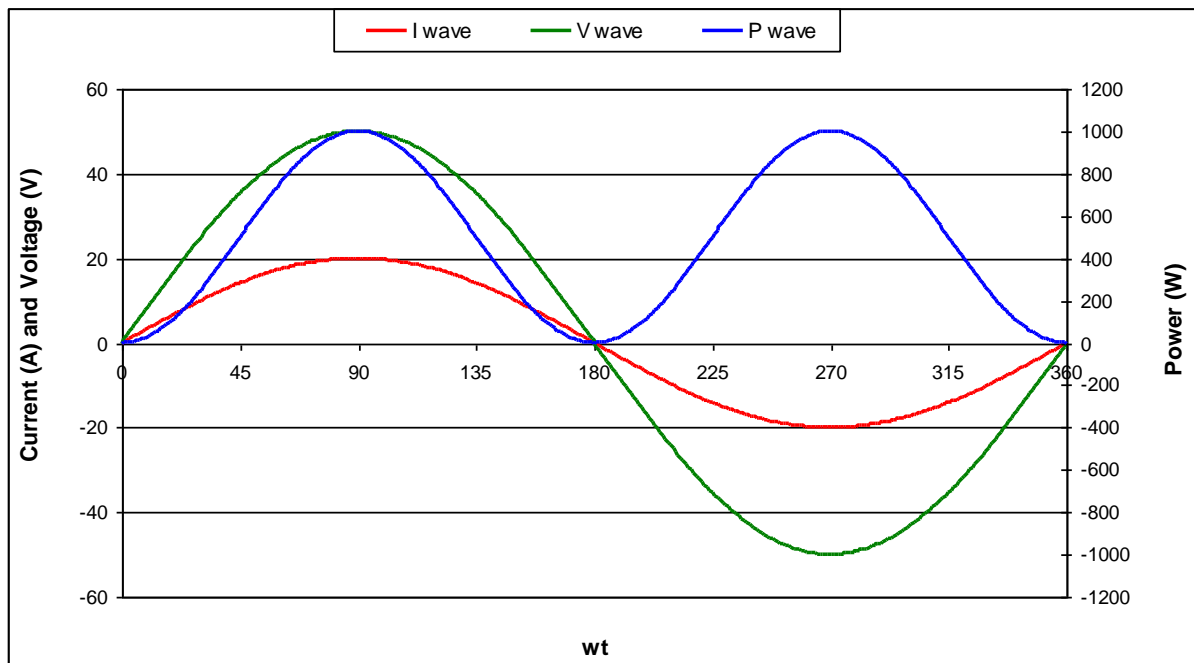


Figure 2.2: Relationship between v, i and p in a resistor

Because the power is continually fluctuating, the power in an AC circuit is taken to be the average value of the wave (El- Hawary, 1995:12).

The average value of $(1 - \cos 2\omega t)$ is 1, so

$$P_{av} = \frac{V_p I_p}{2} \quad (2.6)$$

2.1.1 Power in an Inductive circuit

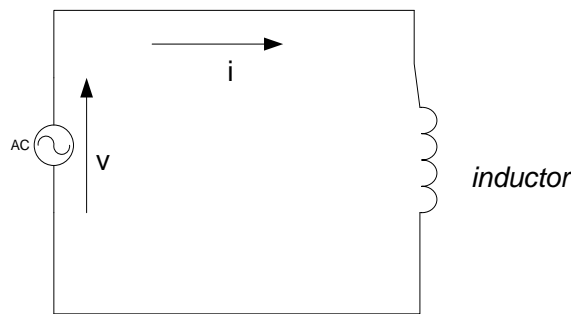


Figure 2.3: Inductive circuit

If the network in study is considered to be purely inductive, the inductive voltage and current will be:

$$v = V_p \sin \omega t \quad (2.7)$$

$$i = -I_p \cos \omega t \quad (2.8)$$

Hence the resultant instantaneous power becomes:

$$p = vi = V_p \sin \omega t \times -I_p \cos \omega t = -V_p I_p \left(\frac{\sin 2\omega t}{2} \right) \quad (2.9)$$

Figure 2.4 depicts a wave diagram from an inductive AC circuit and shows the current lagging the voltage by 90°. The power in an inductive circuit consists of negative and positive pulses. The average of these pulses over a half-cycle is zero and therefore no heating occurs (Glover et al., 2002:45). In this case the negative power is due to energy that has been stored in the magnetic field, being fed back into the circuit.

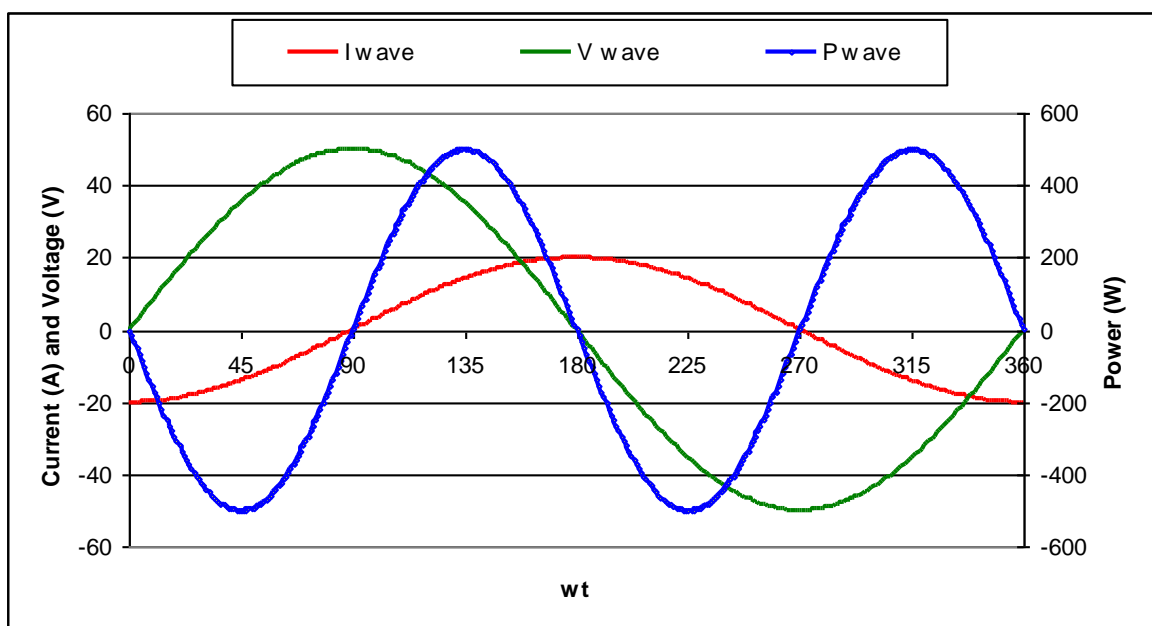


Figure 2.4: Relationship between v, i and p in an inductor

During the first and third quarter cycles, the power is negative, this means that the power is being consumed by the inductor. In the second and fourth quarter cycles, the power is positive thus, the inductor is returning back the power to the source.

2.1.2 Power in a capacitive circuit

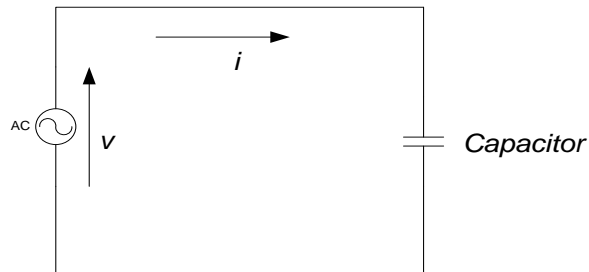


Figure 2.5: Capacitive circuit

If a voltage:

$$v(t) = V_p \sin \omega t \quad (2.10)$$

is applied across a capacitance C , the current will be given by:

$$i(t) = I_p \cos \omega t \quad (2.11)$$

Hence the resultant power will be:

$$p = v(t)i(t) = V_p \sin \omega t \times I_p \cos \omega t = V_p I_p \left(\frac{\sin 2\omega t}{2} \right) \quad (2.12)$$

Figure 2.6 depicts the waveform diagram for an AC capacitive circuit and shows the current leading the voltage by 90° . In the first-quarter cycle both v and i are positive, thus the power is also positive. In the second quarter-cycle v stays positive while i has gone negative, therefore p is negative. In the third-quadrant both i and v are negative and so p is positive. Finally, in the fourth-quadrant i is positive and v is still negative resulting in p being negative. The power wave is thus a series of identical positive and negative pulses whose average value over a half-cycle of voltage is zero.

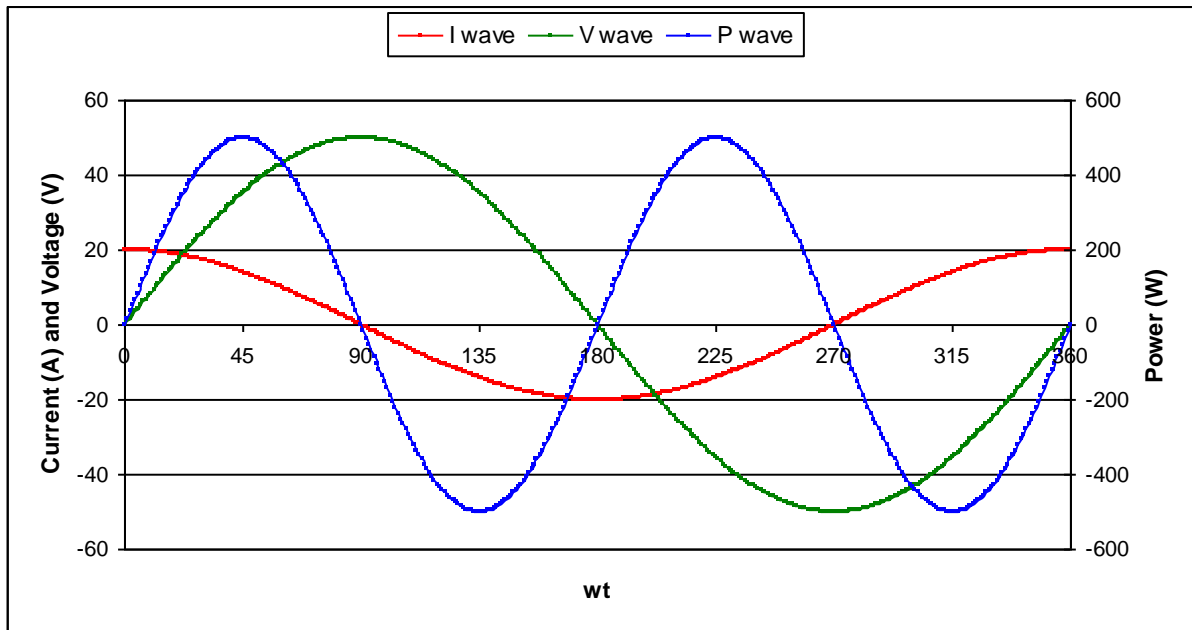


Figure 2.6: Relationship between v, i and p in a capacitor

During the first and third quarter-cycles the power is positive this means that power is supplied by the circuit to charge the capacitor. In the second and fourth quarter-cycles, p has a negative value, this means the capacitor is discharging thus, it is supplying the energy stored in it back to the circuit. Although negative power may seem like an odd concept the minus (-) or plus (+) signs simply indicates the direction in which the power is flowing. Since this interchange of energy dissipates no average power, no heating will occur and no power is lost.

In this case, the capacitor also exchanges energy with the source. In one cycle, the total energy consumed by the capacitor is zero. The average value of the instantaneous power for a capacitor is zero, which is similar to that for inductance (Glover & Sarma, 2002:45).

2.1.3 Circuit with Resistance and Reactance

When considering a general case in which the current differing in phase from the applied voltage, the current is shown lagging the voltage by an angle ϕ .

Let the instantaneous voltage be:

$$v(t) = V_p \sin \omega t \quad (2.13)$$

Then instantaneous value of current is:

$$i(t) = I_p \sin(\omega t - \phi) \quad (2.14)$$

Hence by multiplying the corresponding instantaneous values of voltage and current, resultant instantaneous power will be:

$$\begin{aligned}
p(t) &= V_p \sin \omega t \times I_p \sin(\omega t - \phi) \\
p(t) &= \frac{1}{2} V_p I_p (\cos \phi - \cos(2\omega t - \phi)) \\
p(t) &= \frac{1}{2} V_p I_p \cos \phi - \frac{1}{2} V_p I_p \cos(2\omega t - \phi)
\end{aligned} \tag{2.15}$$

This instantaneous power has two components:

- i. $\frac{1}{2} V_p I_p \cos \phi$, which remains constant irrespective of time, and
- ii. $\frac{1}{2} V_p I_p \cos(2\omega t - \phi)$, indicating the variation of this component of power at twice the supply frequency. However the average value of this component over one complete cycle is zero and hence, it does not contribute towards the average value of power drawn from the supply.

Hence, average power over one cycle is given by:

$$P_{av} = \frac{1}{2} V_p I_p \cos \phi = \frac{V_p}{\sqrt{2}} \times \frac{I_p}{\sqrt{2}} \cos \phi \tag{2.16}$$

Using the effective (rms) values of voltage and current and substituting:

$V_p = \sqrt{2}(V_{rms})$, and $I_p = \sqrt{2}(I_{rms})$, we get,

$$P_{av} = V_{rms} I_{rms} \cos \phi \tag{2.17}$$

where V_{rms} and I_{rms} are the rms values of the voltage and current respectively; this average power in the circuit is called active (real) power (Grainger & Stevenson, 1994:8). The active power is denoted by P. It is used to produce either work or heat. Its units are the watt (W), kilowatt (kW), Megawatt (MW), etc.

Since the average power in a purely inductive or capacitive circuit is zero i.e. we have a voltage and current but no power dissipated, the expression $p=vi$ (using rms values) is no longer valid. The product of current and voltage in this case is called reactive power (Grainger & Stevenson, 1994:8).

2.1.4 Reactive power

The reactive power is the power exchanged between the source and the inductive or capacitive components in the circuit (Glover et al., 2002:47). It was previously discussed that the inductive and capacitive elements have their instantaneous power in sinusoidal form, as shown in Figures 2.4 and 2.6. This means the power is drawn from the source then delivered back to the source (Grainger & Stevenson, 1994:8). It's denoted by the symbol Q, measured in a unit called *Volt-Amps-Reactive* (VAR) and its magnitude is given by:

$$Q = I_{\text{rms}} V_{\text{rms}} \sin \phi \quad (2.18)$$

where, V_{rms} and I_{rms} are rms values of the terminal voltage and current, and ϕ is the phase angle by which the current lags the voltage.

2.1.5 Complex power

We define a value referred to as complex power by the relationship:

$$S = P + jQ \quad (2.19)$$

where P and Q are the active and reactive power. The unit for S is the volt-ampere and this unit terminology is used to distinguish it from watts (for P) and vars (for Q). S may be represented in the form of a power triangle shown in Figure 2.7.

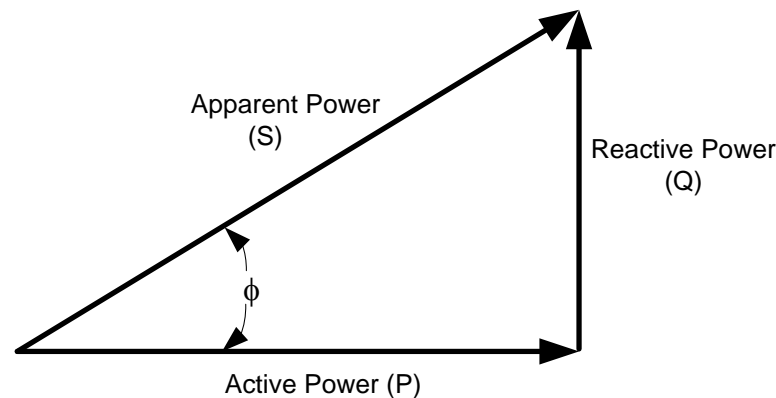


Figure 2.7: Power triangle for an inductive load

The magnitude is clearly given by:

$$|S| = \sqrt{P^2 + Q^2} \quad (2.20)$$

This magnitude of the complex power is referred to as the **apparent power** because it represents the required volt-amp capacity of a device required to supply a certain average power (El-Hawary, 1995:13). If a load is not purely resistive, this apparent power is always greater than the average power; that is, the amount of power which must be supplied to a system is always greater than what the system is able to consume ($|S| > P$).

2.1.6 Power factor (PF)

The ratio of P used in the system to S is called the power factor of the circuit (Hughes, 2005:267). Its value lies between 0 and 1. For sinusoidal voltage and current waves, the power factor is obtained as follows:

$$P = V_{\text{rms}} I_{\text{rms}} \cos \phi = S \cos \phi$$

$$\therefore \cos \phi = \frac{P}{S} \quad (2.21)$$

where ϕ is the phase angle between V_{rms} and I_{rms} .

Hence, in circuits whose waveforms follow the sine law, power factor is the cosine of the angle between the applied voltage and the resultant current flowing in the circuit (El-Hawary, 1995:12). Power factor is normally called lagging when the current lags the applied voltage (thus inductive loads dominate) and leading when the current leads the voltage (thus capacitive loads dominate). Thus, for power factor consideration, the applied voltage is always regarded as reference quantity (Hughes, 2005:267).

Power factor for the AC circuits can be written as:

$$\cos \phi = \frac{P}{S} = \frac{I_{\text{rms}} R}{I_{\text{rms}} Z} \quad (2.22)$$

Thus,

$$\cos \phi = \frac{R}{Z} \quad (2.23)$$

where R and Z are the resistance and impedance of the circuit respectively.

2.1.7 Active and reactive currents

When the inductive loads are in service, they introduce inefficiencies into the system by drawing additional currents called inductive reactive currents (I_{reactive}). If these loads have a low power factor, they require much more current than is theoretically required as discussed above. The excess current (I_{reactive}) flows through the component in the same manner as the useful current (I_{active}). Hence the total current flowing in a component will be:

$$I_{\text{total}} = I_{\text{active}} \pm jI_{\text{reactive}} \quad (2.24)$$

Figure 2.8 a and b graphically show the current in different circuits

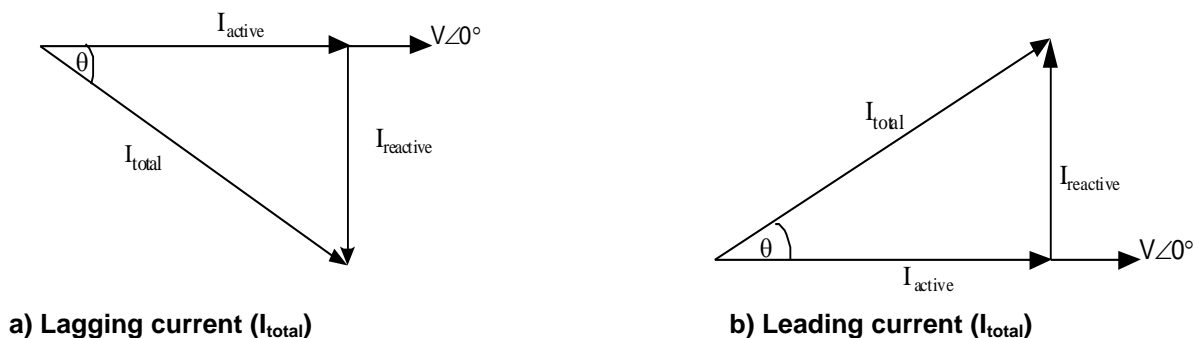


Figure 2.8: Currents in different circuits

2.2 Reactive power in distribution networks

Most of the electrical loads in distribution networks are inductive in nature. Typical examples are induction motors, transformers and fluorescent lighting. These loads absorb both reactive and active power. The active power is used by the load to perform the work, whereas reactive power is used by the load to sustain the electro-magnetic field. The reactive power is always 90° lagging with respect to active power as shown in the power triangle in Figure 2.7. The supply of reactive power from the network results in reduced network efficiency due to:

- Increased current for a given load
- Higher volt-drop in the network
- Increase in losses of transformers and cables
- Higher apparent power (S) demand from the supply system

It is therefore necessary to reduce and manage the flow of reactive power to achieve higher efficiency of the electrical network. The easiest method of reducing and managing reactive power is by power factor improvement through shunt capacitors.

2.2.1 Shunt capacitors

Typically, as discussed, for distribution loads (inductive loads), the current lags the voltage. Shunt capacitors however, draw a leading current which counteracts the lagging component of the current at the point of installation (Grainger & Stevenson, 1994:10). As a result, the power factor is improved, a voltage rise occurs at the point of capacitor installation, and more importantly, the reactive component in the distribution line is reduced and this lowers the I^2R loss (Wakileh, 2001:35).

The extent of these benefits depends on the location, size, type, and number of shunt capacitors placed in the network (Su & Lee, 2000:97). Hence an optimal solution for placement and sizing of shunt capacitors in a distribution system is a very important aspect to be considered (Su, 2006:23).

The shunt capacitors are automatically controlled by either being switched in or out of the system (Mtshaulana, 2008:11). The effect of these switchings is also important to be taken into account.

2.2.2 Benefits of shunt capacitors

The following lagging power factor circuits and phasor diagrams illustrate how addition of shunt capacitors bring change into the network, in terms of power factor correction, voltage rise and power loss reduction.

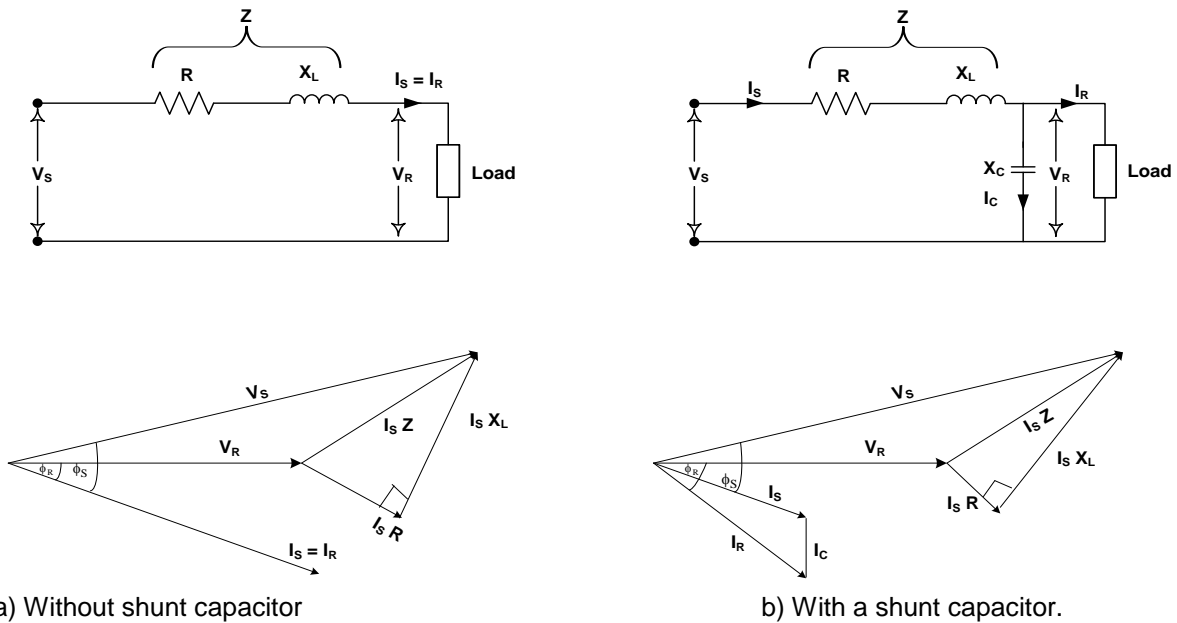


Figure 2.9: Circuit representation

Figure 2.9a is an illustration of a circuit without shunt capacitor. It shows a circuit with its corresponding phasor diagram. When there are no shunt capacitors in a network, the sending-end current (I_s) is equal to the receiving-end current (I_R) but because of the volt-drop across the line impedance (Z) the sending-end voltage (V_s) is not equal to the receiving-end voltage (V_R), in fact V_s is far bigger. V_s is the phasor sum of the volt-drop across the line impedance and V_r . The phasor diagram in Figure 2.9a shows that the angle (ϕ_R) between I_R and V_R is big and this means that the power factor is low.

Figure 2.9b is an illustration of a circuit with a shunt capacitor. It shows a circuit with its corresponding phasor diagram. From the phasor diagram of Figure 2.9b, I_R lags behind V_R by ϕ_R . The capacitive current, I_C leads V_R by 90° as shown. The phasor sum of I_C and I_R is the sending end current, I_s . The volt-drop in the line resistance ($I_s R$) is in phase with I_s , whereas the inductive volt-drop ($I_s X_L$) leads I_s by 90° . The voltage V_s is the phasor sum of V_R and $I_s Z$. Sending end current, I_s is less therefore the volt-drop is also less.

The following equations are used to calculate the correct size of the capacitor at a specified station.

- Total apparent power (S)

$$S = 3 \times V_{\text{rms}} \times I_{\text{rms}}^* = P + jQ \quad (2.25)$$

- where I_{rms}^* is the conjugate rms current.

- *Angle phi (ϕ)*

The angle phi is the angle between the phase voltage and current.

$$\phi_1 = \cos^{-1}(\text{PF}_{\text{old}}) \quad (2.26)$$

$$\phi_2 = \cos^{-1}(\text{PF}_{\text{new}}) \quad (2.27)$$

where: PF_{old} = is the PF before shunt capacitor addition,

PF_{new} = is the desired PF after shunt capacitor addition.

- *Total capacitive reactive power (Q_c)*

$$Q_c = P[\tan(\phi_1) - \tan(\phi_2)] \quad (2.28)$$

2.2.2.1 Voltage rise

The shunt capacitors provide the benefit of causing the voltage to rise back within the permissible range. The percent voltage rise ($\% \Delta V$) can be obtained by (Dugan, McGranaghan & Beaty, 1996:200):

$$\% \Delta V = \frac{100 \cdot (V_{\text{with cap}} - V_{\text{no cap}})}{V_{\text{with cap}}} \quad (2.29)$$

where,

$V_{\text{with cap}}$, is the voltage magnitude with shunt capacitor, $V_{\text{no cap}}$, is the voltage magnitude with no shunt capacitor, that is V_R at a given load value.

2.2.2.2 Reduced Power loss

The current decreases in direct proportionality to PF improvement and the losses are inversely proportional to the square of the PF (Dugan, McGranaghan & Beaty, 1996:204). Figure 2.10 graphically displays the variation of the power loss in distribution lines. The losses are expressed in percentage as a function of PF (PDH Online, 1999:6).

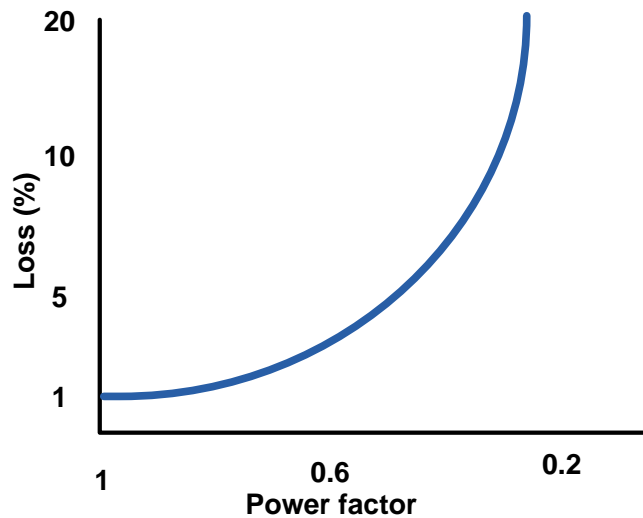


Figure 2.10: Relationship between power loss and power factor

Figure 2.10 shows that for a given load, if the PF is low, the current drawn is high. Consequently, the power loss which is proportional to the square of the current in the distribution line will be higher. The new power loss due to PF correction is obtained by:

$$\% \text{ power losses} \propto 100 \left(\frac{\text{PF}_{\text{old}}}{\text{PF}_{\text{new}}} \right)^2 \quad (2.30)$$

Therefore

$$\% \text{ loss reduction} = 100 \left[1 - \left(\frac{\text{PF}_{\text{old}}}{\text{PF}_{\text{new}}} \right)^2 \right] \quad (2.31)$$

where

% loss reduction = per cent reduction in loss

2.2.2.3 Reduction in line current

The percent line current reduction can be obtained from:

$$\% \Delta I = 100 \left[1 - \left(\frac{\cos \phi_1}{\cos \phi_2} \right) \right] \quad (2.32)$$

where %ΔI= percent current reduction

Capacitor switching is however the most common source of transient voltages and currents in the power system. This is a concern that should not be ignored.

2.3 Transients and capacitor switching

Capacitor switching offers a greater threat due to its generation of transients in distribution networks, every time it is energized (Sabin, Grebe & Sundaram, 1999:112). These

transients can be more severe than any other types of transients caused by other equipment such as energizing lines. When an uncharged capacitor is energized, the system voltage is momentarily pulled down. The voltage will then rebound and exceed the system voltage by an amount equal to the difference between the system voltage and the capacitor voltage at the instant of energizing (Dugan, McGranaghan & Beaty, 1996:85). The overshoot will generate a transient between 1.0 and 2.0 per unit depending on system damping (Kulas, 2009:1). Switching capacitors in the network is considered as a normal operation on the utility side; however it may have a negative effect on the load side (Sabin, Grebe & Sundaram, 1999:112). The frequency transients generated can be magnified on the load side (if the load has low voltage power factor capacitors) and can as well result in nuisance tripping of the power electronic devices. The primary area of concern is typically how capacitor switching transients affect power quality for nearby industrial and commercial loads. The safe range determined in the literature is that the peak transient voltage level should be less than twice the rated voltage.

This can be expressed as follows:

$$V_{\text{transient}} \leq 2V_{\text{rated}} \quad (2.33)$$

where,

$V_{\text{transient}}$ is the voltage magnitude of the transient and V_{rated} is the rated voltage at the busbar.

Figure 2.11 is a basic circuit with parameters R_c , L_c and C_c and is used to represent and explain what happens when a capacitor is being energized via capacitor switch operation. This is a line-to-neutral representation for a three-phase circuit, where the driving AC voltage is an instantaneous line-to-neutral fundamental-frequency power system voltage, and R_c and L_c are the system impedance associated quantities.

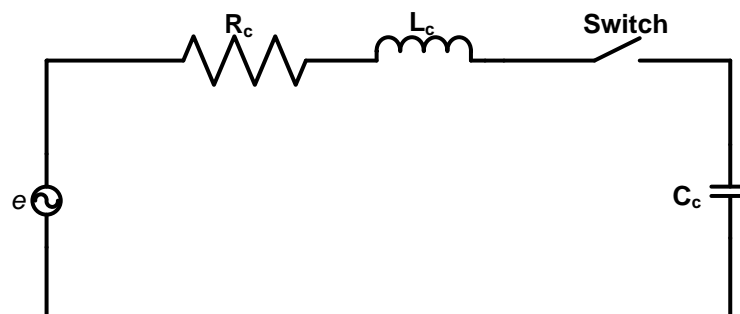


Figure 2.11: Capacitor switching equivalent circuit

When the switch in the circuit is closed, a high frequency, high-magnitude current flows in the capacitor, attempting to equalize the system voltage and the capacitor voltage. If the switch is closed at a voltage peak, the voltage on the capacitor attempts to immediately increase

from the zero-voltage, de-energized condition to the peak voltage. In the process of achieving this voltage change, an overshoot occurs, equal to the amount of the attempted voltage change. This voltage surge is also of the same high frequency as the current inrush and rapidly decays to the system voltage. The magnitude of the voltage surge theoretically reaches a peak phase-to-earth of up to 2.0 per unit (Cory, Dos-Santos & Tavares, 1998:292).

Figure 2.12 is a typical oscillogram of capacitor voltage that will result following a switch closing on an uncharged capacitor at the instant of the negative crest of the fundamental-frequency steady-state voltage.

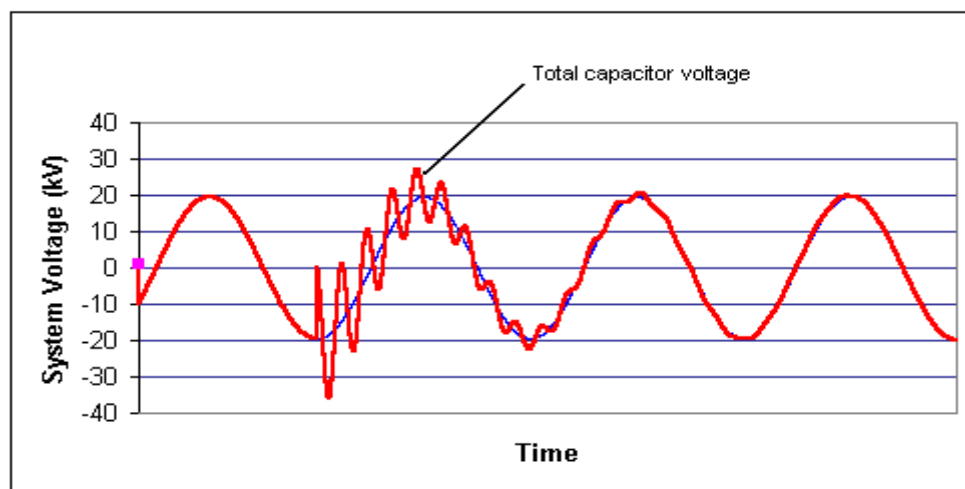


Figure 2.12: Oscillogram of total capacitor voltage transient component

It can be seen in Figure 2.12 that the transient voltage as a result of the switching, oscillates above the steady-state source voltage and reaches a positive crest value of about 28 kV. It can be seen that it returns to normal voltage after a certain time.

Figure 2.13 is the oscillogram of capacitor at the instant of crest of the fundamental-frequency voltage. The figure shows that this consists of two components

- A fundamental-frequency component
- A damped natural-frequency transient component

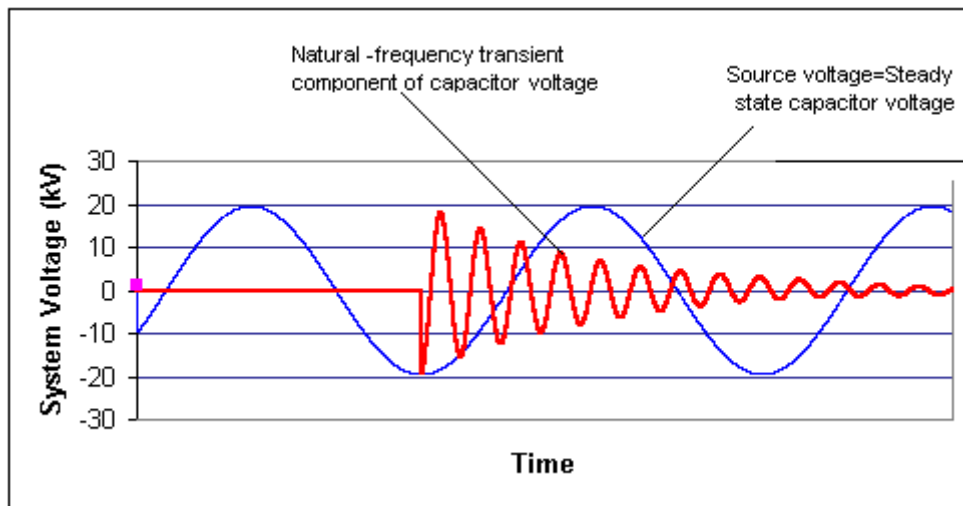


Figure 2.13: Transient and steady-state components at the oscillogram

Since voltage cannot be changed on a capacitor instantly, a transient component necessarily develops so that when added to the fundamental, the pre-switching capacitor voltage at the instant of switch closing is maintained. Thus, the initial magnitude of the transient component is the difference between the capacitor pre-switching voltage and the fundamental-frequency steady-state voltage. These are the so called “switch volts” which represent the excitation impulse that creates the transient. The greater the switch volts, the greater the transient voltage and current. A finite pre-energization capacitor voltage may increase or decrease the transient depending upon its polarity with respect to the fundamental at the instant of switching (IEEE Industry Applications Society, 1993:67). Capacitor switching and its effects are considered in this thesis.

Capacitor energizing is just one of the many switching events that can cause transients in a network. However, due to their regularity and impact on the network components, they often receive special consideration (Sabin, Grebe & Sundaram, 1999:112).

2.4 Summary

The known formulae of the average, reactive, apparent and complex AC power in the sinusoidal steady-state are presented. Pure resistor, inductor and capacitor, sinusoidal waveforms of current, voltage and power are plotted. Capacitor switching and its effects are also reviewed.

CHAPTER THREE DISTRIBUTION NETWORK THEORY AND OPERATION

In this chapter the basic concepts related to the research are defined and explained more clearly. The distribution network and its components are discussed. The operational constraints under which a distribution network must operate are defined.

3. Overview of a distribution system

Electrical energy is transferred through an extensive grid from the sources of power to the consumer points (Bakshi & Bakshi, 2007:1). Figure 3.1 shows the basic elements of a power system. A power grid generally consists of three identifiable parts, namely: generation, transmission and distribution.

Electric power is generated at **generating stations**. The generation system produces electrical power in medium or low voltage, usually between 6.6 kV to 11 kV. This voltage is stepped up to high voltage for transmission at the step-up substation.

The electrical power is transmitted from the step-up substation across long distances by the **transmission system**. The transmission system is composed mainly of transmission lines, transformers, and protective devices.

The **subtransmission system** transmits power in smaller quantities from the transmission substations to the distribution substations. Large industrial customers are commonly supplied directly from the subtransmission system.

The **distribution system** represents the final stage in the transfer of power to the individual customers. The primary distribution system is typically between 11kV and 33 kV. The primary distribution system transports the electrical power by distribution feeders which can be overhead distribution (O/H) lines or underground cables (U/G cable) to the distribution transformers that step the primary distribution voltage down to utilization voltage, to supply a secondary distribution system to which the loads such as residential, commercial, etc... are connected (Von Meier, 2006:150). These loads are normally operated at voltages ranging between 230-400 V. Big loads such as industrial loads are directly fed in the primary distribution system (Kundur, 1994:6).

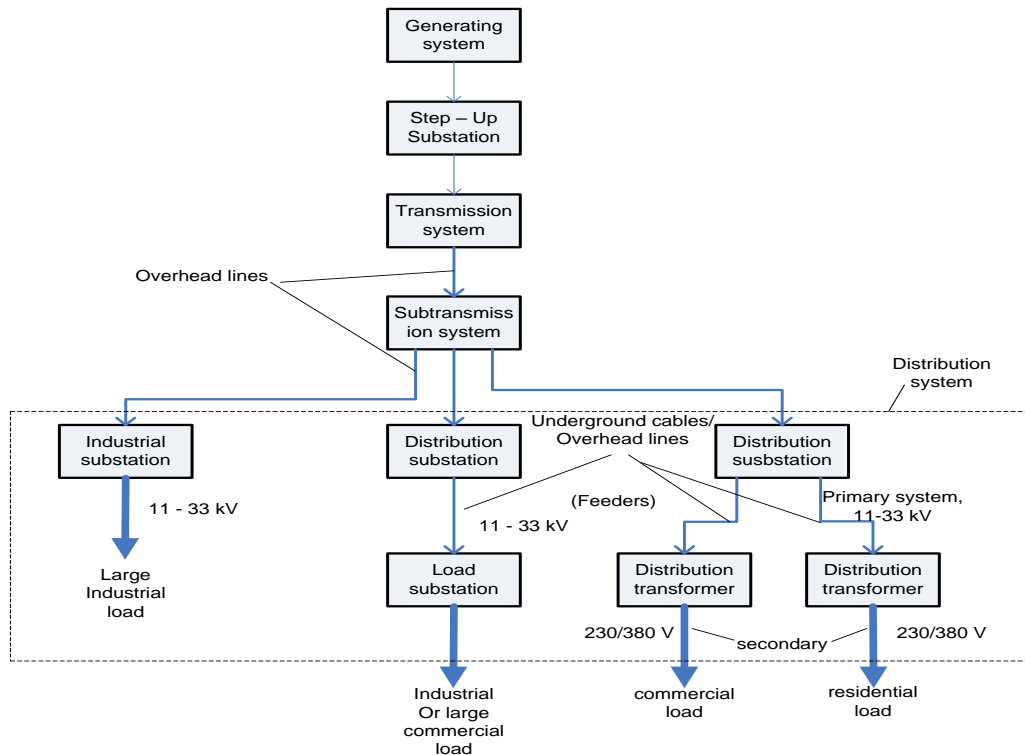


Figure 3.1: Overview of the power system from generation to load's switch

Interconnections to neighbouring power systems are usually formed at the transmission system level. The overall system thus consists of multiple generating sources and several layers on transmission networks. This provides a higher degree of structural redundancy that enables the system to withstand unusual contingencies without service disruption to the customers (Kundur, 1994:8).

3.1 Types of distribution systems

An important characteristic of distribution systems is their topology, or how their feeders are connected. There are three different distribution system layouts used by electric utilities, each of which has variation in its own design.

- Radial feeder system
- Ring main feeder system
- Interconnected feeder system

3.1.1 Radial feeder system

Figure 3.2 shows a radial feeder system. Where, feeders AB and AD supply the loads at points C and E respectively. Obviously, the loads are fed at one point only i.e. point A in this case. Each path typically includes circuit breakers for protection and /or switching. Radial feeder systems are the simplest systems to plan, construct, and maintain.

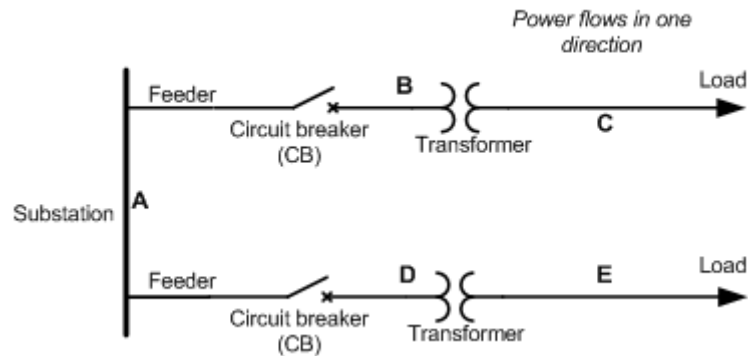


Figure 3.2: Radial feeder system

(Adapted from Von Meier, 2006:151)

The disadvantage of a radial feeder system is that if the fault occurs on the feeder, all customers connected to that feeder will be affected. There would be an interruption of supply to such customers (Bakshi & Bakshi, 2007:369).

3.1.2 Ring main feeder systems

In a ring main system, the primary side of each distribution transformer forms a loop. The loop circuit starts from the sub-station bus-bars, makes a loop through the area to be supplied, and returns to the sub-station (Pansini, 1991:140). Figure 3.3 shows the single line diagram of ring main system. The load areas are supplied by substation S through a closed loop ABCDEGH.

The ring main system has the following advantages:

- This arrangement, if properly designed and operated, comes with an advantage of being quick to recover from a single feeder fault with no continuous loss of power to the loads (IEEE Industry Applications Society, 1993:61).
- The second most important characteristic of this system is that a section of a feeder may be disconnected and isolated from the loop for maintenance or repair while the other parts of the network are still functioning (Bakshi & Bakshi, 2007:370). For example, suppose that fault occurs at point F of section AB of the feeder shown in Figure 3.3. The section of AB of the feeder can be isolated for repairs while continuity of supply is maintained to all the consumers via the feeder SHGEDCB.

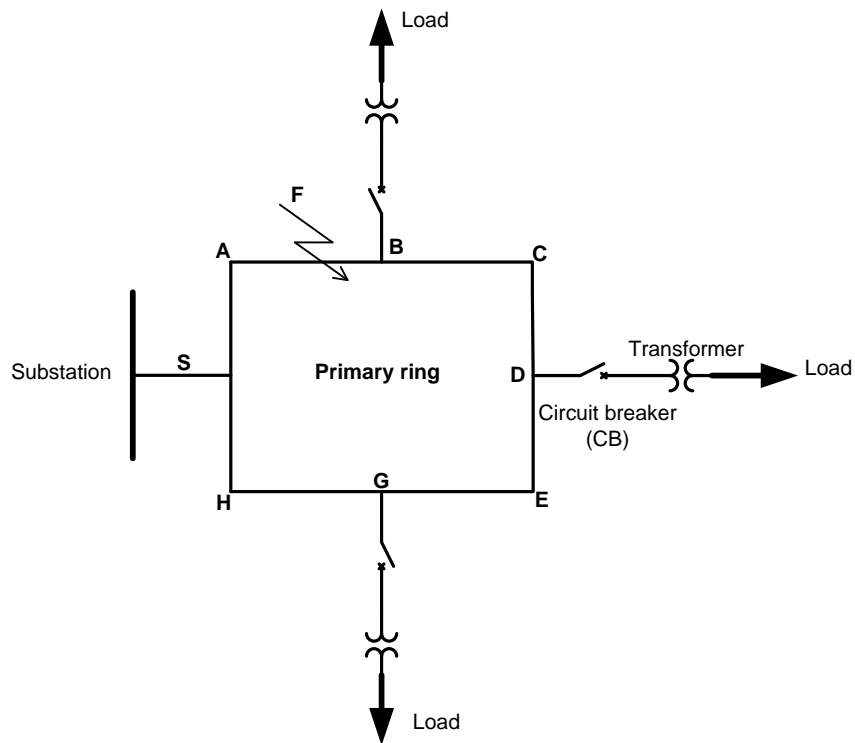


**Figure 3.3: Ring main feeder system
(Adapted from Von Meier, 2006:151)**

3.1.3 Interconnected distribution system

When a ring network is supplied by two or more than two generating stations or sub stations, it is called an inter-connected system. Figure 3.4 shows the single-line diagram of an interconnected system where the closed feeder ring ABCD is supplied by two substations SS1 and SS2 at points D and C, respectively. Loads are connected to points EFGH of the feeder ring through distribution transformers.

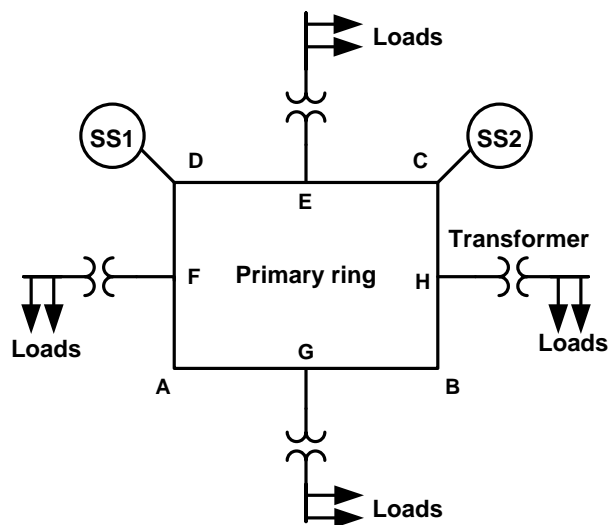


Figure 3.4: Typical interconnected ring main network

Distribution networks are normally interconnected by long transmission lines. Interconnections are very important in cases of a loss of one or more generation stations in a utility grid. This increases system reliability and helps in minimising reserve power capacity during peak demand and consequently increasing the systems efficiency.

3.2 Components of a distribution network

3.2.1 Underground cables (U/G cables)

U/G cables can be defined as insulated conductors which are put together and finally provided with a number of layers of insulation to give proper mechanical support and also for heat dissipation purposes. For U/G cables, heat dissipation is an issue. The conductors mostly used for U/G cables are usually Aluminium or Copper. Copper is more expensive, but it has a lower resistance than Aluminium. Copper's low resistance is generally desirable for power lines to minimise power loss, but also because the increase of heat in a conductor limits the conductor's ability to carry current (Von Meier, 2006:175).

Figure 3.5 represents the AC equivalent circuit of an U/G cable. Because of the close proximity of conductors in an U/G power cable, capacitance cannot be ignored hence the π -equivalent circuit is used to represent an U/G cable.

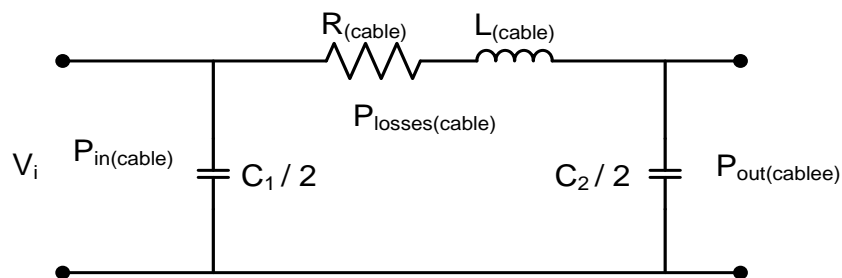


Figure 3.5: Single equivalent circuit of a power cable

where,

V_1 is the source voltage; $P_{in(cable)}$ and $P_{out(cable)}$ are the input and output power respectively; $P_{loss(cable)}$ is the power lost in the power cable; $R_{(cable)}$ and $L_{(cable)}$ are conductor resistance and inductance respectively; C_1 and C_2 are the shunt capacitances of the cable.

3.2.1.1 U/G Cable parameters

a) Resistance

The resistance of the conductor causes real power loss in an U/G cable (El-Hawary, 1995:94). The real power loss is proportional to the resistance of the cable, which depends on the length, cross sectional area and the resistivity of the material of which the cable conductor is made.

Direct current (DC) resistance of a uniform conductor at a specified temperature T is:

$$R_{DC,(T)} = \frac{\rho_T \times l}{A} \Omega \quad (3.1)$$

where,

ρ_T = the resistivity of the conductor material at temperature T (It is equal to 0.028×10^{-6} ohm meters for Aluminium and 0.018×10^{-6} ohm meters for Copper at a temperature of 20° C (Atkinson-Hope,2005:7)).

l = length of the conductor

A = cross-sectional area of the conductor

T = temperature

The longer the U/G cable the higher is its resistance and therefore the higher its power loss. Similarly, a larger cross-sectional area gives a smaller resistance and lower power loss than a smaller diameter conductor.

The resistivity of the cable depends on the material, Aluminium or Copper. Resistance is affected by temperature. A better conducting material will result in lower resistivity and lower power loss. The resistivity of the metal in the cable will be affected by the temperature. As the temperature increases, resistance increases, causing higher loss (Benedict et al., 1992:36).

The resistivity of a cable is obtained from,

$$\rho_1 = \rho_2 \frac{T_2 - T_0}{T_1 - T_0} \quad (3.2)$$

T_0 is a reference temperature; ρ_1 and ρ_2 are the resistivities at temperature T_1 and T_2 , respectively.

b) Inductance

When current flows in a conductor, a magnetic field is generated, this magnetic field will interact with the conductor and surrounding conductors. Due to these flux linkages there will be an inductance associated with each wire.

The inductance per phase in a conductor of a U/G cable is given by:

$$L_{(cable)} = \left(0.05 + 0.2 \ln \frac{d}{r} \right) \text{mH / km} \quad (3.3)$$

where,

$L_{(cable)}$ is the inductance, d is the distance between the conductors and r is the radius of the conductor.

The inductive reactance will then be:

$$X_L = 2\pi \cdot f_1 \cdot L_{(\text{cable})} \quad (3.4)$$

where;

X_L is the inductive reactance, f_1 is the power source frequency and $L_{(\text{cable})}$ is the inductance

c) Capacitance

As the conductors run in parallel for a considerable distance there will be a capacitance between any pair of conductors. The capacitance of a single conductor in an U/G cable is given by:

$$C = \frac{2\pi\epsilon_r\epsilon_0}{\ln\left(\frac{D}{d}\right)} \text{ F/m} \quad (3.5)$$

where

C is the capacitance,

ϵ_r is the relative permittivity of the insulation.

ϵ_0 is the permittivity of the free space = 8.854×10^{-12} F/m

D is the total diameter with sheath

d is the conductor diameter itself

The capacitive reactance will then be:

$$X_C = \frac{1}{2\pi f_1 C} \Omega \quad (3.6)$$

However in practice, these parameters values are usually obtained from manufacturer table and are not generally calculated.

3.2.2 Overhead lines

An overhead line consists of conductors, insulators, support structures and shield wires. Conductors of overhead distribution lines typically consist of Aluminum, which is lightweight and inexpensive, and are often reinforced with steel for strength (Prakash, 2007:60). One of the most common conductor types is Aluminum Conductor Steel-Reinforced (ACSR), which consists of layers of Aluminum strands surrounding a central core of steel strands (Glover & Sarma, 2002:146).

When working with O/H lines a distinction is usually drawn between the line lengths as short, medium and long lines. These line lengths have different equivalent circuits. The equivalent circuit in Figure 3.5 represents a medium O/H line.

3.2.2.1 Overhead line parameters

The general method to calculate the constants of U/G cables applies to O/H lines.

a) Resistance

Resistance in O/H lines can be obtained using equation 3.1

b) Inductance

The inductance per phase in a conductor is given by:

$$L_{(\text{line})} = 2 \times \ln^{-7} \frac{d}{r} \text{ mH / km} \quad (3.7)$$

$L_{(\text{cable})}$ is the inductance, d is the geometric mean distance between conductors including earth conductors and r is the radius of the conductor.

c) Capacitance

The capacitance per phase in a conductor is given by:

$$C = \frac{2\pi\epsilon_0}{\ln \frac{(d-r)}{r}} \quad (3.8)$$

where

C is the capacitance,

$\epsilon_0 = 8.85 \times 10^{-12}$ permittivity of free space

d is the geometric mean distance between conductors

r = radius of conductors

The inductive and capacitive reactances for O/H lines are determined as per U/G Cable in equations 3.4 and 3.6 respectively.

3.2.3 Power transformer

The transformer is a valuable apparatus in electrical power systems, for it enables one to utilise different voltage levels across the system for the most economical value (Hughes, 2005:670). Generation of power by synchronous machines is normally done at a relatively low voltage, which is most desirable economically. Stepping up of this generated voltage to high voltage is done through power transformers. This is done to suit the power transmission requirement, to minimise power losses and increase the transmission capacity of the lines. The transmission voltage level is then stepped down for distribution and utilisation purposes (EI-Hawary, 2000:97).

3.2.3.1 General theory of transformer operation

Figure 3.6 shows the general arrangement of a transformer. A steel core C consists of laminated sheets, insulated from one another (Shepherd, Morton & Spence, 1970:275). The

reason for laminating the core is to reduce eddy-current loss, also known as the core loss. The vertical portions of the core are referred to as limbs and the top and bottom portions are the yokes (Hughes, 2005:672). The Primary and Secondary coils or windings are wound on the limbs (Hughes, 2005:672). The Primary coil is connected to the source while the secondary coil is connected to the load.

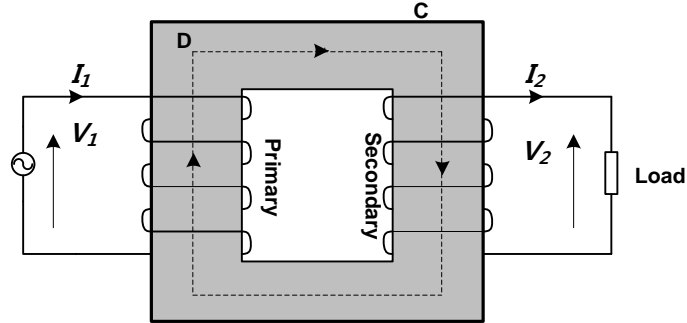


Figure 3.6: A transformer

When alternating voltage V_1 is applied to the primary coil it circulates an alternating current through the coil and this current produces an alternating flux (ϕ) in the steel core. (Hughes, 2005:672) The mean path of this flux is represented by the dotted line D. If the whole of the flux produced by the primary coil passes through the secondary coil, the e.m.f induced in each turn is the same for the primary and secondary. Thus, if N_1 and N_2 are the number of turns on primary and secondary respectively then,

$$\frac{\text{Total emf induced in Secondary}}{\text{Total emf induced in Primary}} = \frac{N_2 \times \text{emf per turn}}{N_1 \times \text{emf per turn}} = \frac{N_2}{N_1} \quad (3.9)$$

If the secondary is an open circuit, its terminal voltage is the same as the induced emf. The primary current is very small, so that the applied V_1 is practically equal and opposite to the emf induced in the primary (Shepherd, Morton & Spence, 1970:274). Hence,

$$\frac{V_1}{V_2} = \frac{N_1}{N_2} \quad (3.10)$$

where, N_1 and N_2 are the numbers of turns of the primary and secondary windings, respectively. In this case V_1 is obtained by,

$$V_1 = e_1 = N_1 \frac{d\phi}{dt} \quad (3.11)$$

where e_1 is the e.m.f induced in the primary winding. The e.m.f e_2 is induced in the secondary winding by the alternating core flux ϕ :

$$V_2 = e_2 = N_2 \frac{d\phi}{dt} \quad (3.12)$$

Under load conditions V_2 induced in the secondary winding coil drives I_2 into the load. In addition, I_2 also produces its own magnetic field which acts to oppose (in consequence reduce) the original field in the steel core laminations (Bayliss, 1999:492). This in turn reduces the field in the primary and allows more current to flow until a turns balance is

reached. The total I_1 and I_2 produce equal and opposite magnetic fields in the core so the overall effect is to leave the magnetic field unchanged from what it was before the load was applied to the secondary coil (Bayliss, 1999:492). This leads, at large load currents when the primary current, I_1 , is much greater than the no-load current, I_0 to the following expression:

$$\frac{I_1}{I_2} = \frac{N_2}{N_1} \quad (3.13)$$

It should be noted that the magnetic flux levels in the core do not rise in proportion to the load current. The magnetic field due to the secondary is always balanced by the field due to the primary current. The net magnetizing flux is due only to the magnetizing current and magnetic flux levels do not therefore reach very high levels under abnormal short circuit conditions.

Combining the two fundamental equations 3.10 and 3.13 gives:

$$\frac{I_1}{I_2} = \frac{V_2}{V_1} \quad (3.14)$$

3.2.3.2 Transformer equivalent circuit

The transformer equivalent circuit shown in Fig. 3.7 is fundamental for transformer operation calculations involving voltage drop or regulation under various load conditions (Shepherd, Morton & Spence, 1970:280). The magnetizing circuit is taken as a shunt-connected impedance (inductance to represent the setting up of the magnetic field and resistance to represent heat loss in the core) (Shepherd, Morton & Spence, 1970:280). As an approximation this equivalent circuit assumes the no-load current, I_0 , to be sinusoidal and the core flux constant at all loads.

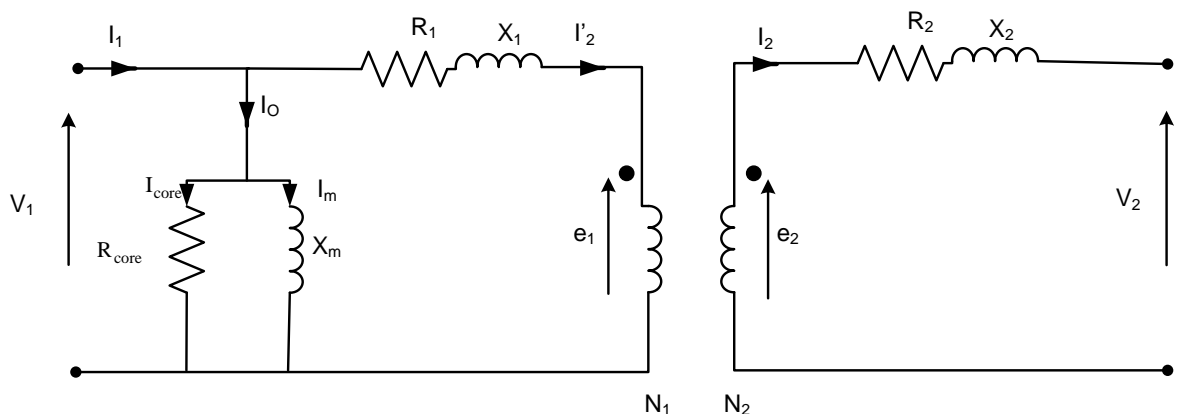


Figure 3.7: Equivalent circuit of a practical single-phase 2-winding transformer

where V_1 and V_2 are supply and secondary voltages; R_1 and X_1 are primary resistance and leakage reactance; R_2 and X_2 are secondary resistance and leakage reactance; R_{core} and I_{core} are resistance and current accounting for the core loss (no-load loss); I_m and X_m are magnetising current and reactance; N_1 and N_2 are number of turns at the primary and

secondary; I_1 , I_2 , I_0 are primary, secondary and no-load (primary) current; e_1 and e_2 are induced voltage at the primary and secondary respectively.

3.2.3.3 Transformer performance measures

Two important performance measures are of interest when choosing transformers. They are voltage regulation and efficiency of the transformer.

a) Voltage regulation

Voltage regulation of a transformer is defined as the variation of the secondary voltage between no-load and full load (F.L.) (Shepherd, Morton & Spence, 1970:285). It is expressed as either a per-unit or a percentage of the no-load voltage, the primary voltage being assumed constant. The percentage voltage regulation (P.V.R) is thus given by:

$$\% \text{V.R} = \frac{|V_{2(\text{no-load})}| - |V_{2(\text{full load})}|}{|V_{2(\text{no-load})}|} \times 100\% \quad (3.15)$$

The approximate percentage voltage regulation for a current loading of n times rated full-load current and a secondary load PF of $\cos\phi$ is given by the following expression:

$$\text{P.V.R} = n(V_R \cos\phi + V_X \sin\phi) \quad (3.16)$$

where, n is the ratio of operating power to full load power. n lies between 0 and 1; V_R is the percentage resistance voltage, and V_X is the percentage reactance voltage.

b) Loss and efficiency

The losses which occur in a transformer can be divided into two groups:

1. The Copper loss ($P_{\text{loss(copper)}}$) in primary and secondary windings
2. Core loss ($P_{\text{loss(no load)}}$) due to hysteresis and eddy currents.

The total power loss $P_{T(\text{trf loss})}$ at any load $n \times$ full-load will be:

$$P_{T(\text{trf loss})} = n^2 P_{\text{loss(copper)}} + P_{\text{loss(no load)}} \quad (3.17)$$

The efficiency of a transformer is obtained by:

$$\% \eta = \frac{\text{output power}}{\text{input power}} = \frac{\text{input power} - \text{losses}}{\text{input power}} = 1 - \frac{\text{losses}}{\text{input power}} \times 100\% \quad (3.18)$$

Thus, the corresponding efficiency for any load $n \times \text{full-load}$ is:

$$\begin{aligned} \eta &= \frac{n \times \text{full load } S \times \text{PF}}{n \times \text{full load } S \times \text{PF} + P_{\text{loss(no-load)}} + n^2 \times P_{\text{loss(copper)}}} \\ &= 1 - \frac{P_{\text{loss(no load)}} + n^2 P_{\text{loss(copper)}}}{n \times \text{full load } S \times \text{PF} + P_{\text{loss(no load)}} + n^2 \times P_{\text{loss(copper)}}} \\ \therefore \quad \eta &= 1 - \frac{1}{1 + \frac{n \times \text{full load } S \times \text{PF}}{P_{\text{loss(no load)}} + n^2 \times P_{\text{loss(copper)}}}} \end{aligned} \quad (3.19)$$

where S is the full load secondary apparent power, η is the efficiency and PF is the secondary load PF .

Figure 3.8 shows a typical efficiency curve of a transformer.

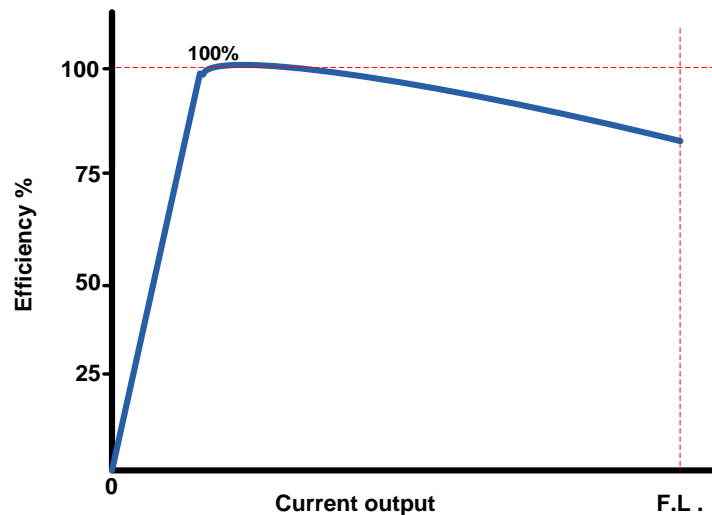


Figure 3.8: Efficiency curve

3.2.4 Circuit breakers and switches

Circuit breakers (CB) and switches are crucial components in a ring main network. The CB serves as a protective device that breaks or interrupts overloads and short-circuit currents (Deshpande, 1966:291). Switches are control devices that can be opened or closed deliberately to make or break a connection. The difference between a CB and a switch is that CBs automatically interrupt abnormally high currents, whereas switches are designed to be operable under normal currents (Rajput, 2006:868).

3.3 Operational constraints of a distribution network

South Africa utilities need to comply and adhere to the minimum standards as set out by the NRS standard document. This document was set up to ensure quality of supply from utilities to customers. It provides the following constraints:

3.3.1 Supply frequency standard

The NRS provides that a three-phase voltage shall be supplied at a nominal standard frequency of 50 Hz. The allowed deviation is $\pm 1\%$ (NRS 048-2, 2003:14).

The frequency magnitude must be maintained within the permissible limit:

$$f_{\min} \leq |f_i| \leq f_{\max} \quad (3.20)$$

3.3.2 Voltage standards

3.3.2.1 Voltage regulation

Voltage regulation is an important operational constraint in a distribution network. Voltage regulation is defined as the change in voltage at the receiving-end of the line when the load varies from no-load to a specified full-load at a specified power factor, while the sending-end voltage is held constant (Atkinson-Hope, 2005:6).

In the ideal case, the voltage level at the load buses would remain at exactly a pre-set value, but in practice this is not possible due to continuing changes in load and system configurations. The NRS 048-2:2003 states that, the voltage at the load side must conform to an acceptable value within $\pm 10\%$ of nominal voltage. Thus, if the nominal voltage is 400 V, then the highest voltage should not exceed 440 V while the lowest voltage should not be less than 360 V.

The voltage magnitude at each bus must be maintained within its permissible limit

$$V_{\min} \leq |V_i| \leq V_{\max} \quad (3.21)$$

where:

$|V_i|$ is the voltage magnitude at busbar i ;

V_{\min} , V_{\max} are the bus minimum and maximum voltage limit at bus i respectively.

The percentage voltage regulation can be expressed as:

$$\left[\% \text{VR} = \frac{|V_{\text{no min al}}| - |V_o|}{|V_{\text{no min al}}|} \times 100\% \right] \leq 10\% \quad (3.22)$$

where,

%VR is the percent voltage regulation

$|V_{\text{nominal}}|$ is the expected or rated voltage of the load

$|V_o|$ is the actual operating voltage

3.3.2.2 Voltage drop

According to South African SANS 10142-1, the maximum volt-drop constraint during full load running condition should not exceed 5% of the nominal voltage (SANS 10142-1, 2006:120).

$$\% V_{\text{drop}} \leq 5\% \quad (3.23)$$

3.3.3 Conductor current carrying capacity

The U/G cables and O/H lines are limited by their current carrying capacity. Thus,

$$|I_F| \leq I_{F,\text{max}} \quad (3.24)$$

where,

I_F and $I_{F,\text{max}}$ are the current magnitude and maximum current capacity of U/G cable or O/H line F, respectively.

3.4 Summary

A distribution system plays a major role in a power system. It transports electric power from transmission to the loads. The arrangement of feeders in a distribution system determines the operation of the system. This chapter gave an explanation of the types of distribution networks, theory and operation. It also describes the components found in the distribution system and their roles in the delivery of electric power. For a distribution system to operate efficiently it must adhere to certain operational constraints and these are defined in the chapter.

CHAPTER FOUR LOAD FLOW

4. Power flow analysis

Load flow studies are performed using computer software that simulates actual steady-state power system operating conditions (normal or emergency operating conditions), enabling the evaluation of bus voltage profiles, real and reactive power flow, and loss (Glover & Sarma, 2002:251). The power flow studies are extremely important in evaluating the operations of power systems, controlling them and planning for future expansions (Nasar, 1996:336). For example, load flow studies assist power system planners to see the effects of components and network reconfigurations, load growth and contingencies such as planned maintenance and component failures. In addition, load flow analysis forms the basis of other power systems studies namely harmonics, stability, fault and transients studies. Successful operation of electrical systems requires that:

- Generation must supply the demand (load) plus the loss.
- Generators must operate within specified real and reactive power limits.
- Bus voltage magnitudes must remain close to rated values.
- Transmission lines and transformers should not be overloaded for long periods.

Given certain known quantities, typically the amount of power generated and consumed at different locations in the power system, load flow studies allow one to determine other quantities (Von Meier, 2006:195). The most important of these quantities are the voltages at locations throughout the system which, for alternating current (AC) systems, the voltage consist of both magnitude and phase angle. Once the voltages are known, the currents flowing through every U/G cable or O/H line and power injections can be easily calculated. Analysing the solution of this problem for numerous conditions helps ensure that the power system is designed to satisfy its performance criteria while incurring the most favourable investment and operation costs.

4.1 Methods for power flow solution in a ring main network

Power flow analysis in ring distribution systems uses the principle of islanding techniques or the same techniques that are used to find power flow between two active sources. Figure 4.1 represents two sections of a power system interconnected by a transmission system, with power transfer from one section to the other. There are many factors that influence the flow of power between buses including, voltages angle, reactive and active power of the generators and impedance of the lines between them. In addition power systems are generally assumed to be lossless, hence line impedances are normally assumed to be inductive and with shunt admittances lumped at the ends for medium and long lines (Kundur,

1994:250). In practice, powers systems have loss due to imperfection in manufacturing of conductors and other system components.

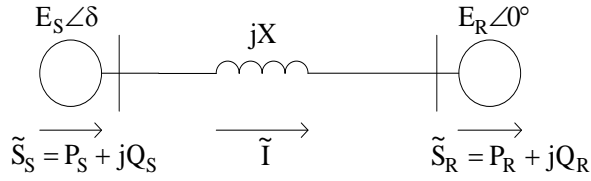


Figure 4.1: Power flow between two sources

Figure 4.2 shows the phasor diagram of above power flow systems.

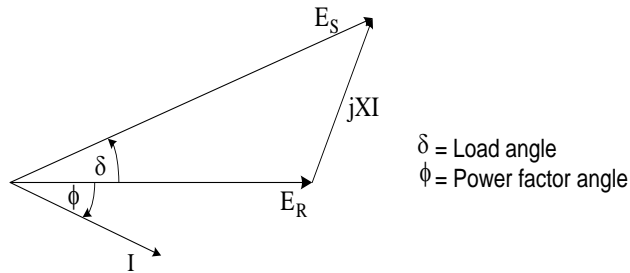


Figure 4.2: Power phasor diagram

Power equations for power transfer:

Referring to Figure 4.1, the complex power at the receiving-end is

$$\begin{aligned} \tilde{S}_R = P_R + jQ_R &= \tilde{E}_R \tilde{I}^* = \tilde{E}_R \left[\frac{\tilde{E}_S - \tilde{E}_R}{jX} \right]^* \\ &= E_R \left[\frac{E_S \cos \delta + jE_S \sin \delta - E_R}{jX} \right]^* \end{aligned} \quad (4.1)$$

where,

E_S and E_R are the sending-end and receiving-end voltages respectively. \tilde{S}_R , P_R and Q_R are the receiving-end complex, active and reactive powers respectively. X is the line reactance.

From equation 4.1, the receiving-end active and reactive powers can be obtained by:

$$P_R = \frac{E_S E_R}{X} \sin \delta \quad (4.2)$$

$$Q_R = \frac{E_S E_R \cos \delta - E_R^2}{X} \quad (4.3)$$

Similarly, the sending-end active and reactive powers can be obtained by:

$$P_S = \frac{E_S E_R}{X} \sin \delta \quad (4.4)$$

$$Q_S = \frac{E_S^2 - E_S E_R \cos \delta}{X} \quad (4.5)$$

These equations describe the way in which active power and reactive power are transferred between active parts of a power network. In addition, if the series resistance R of the network is considered, then the loss in the network will be obtained by:

$$P_{\text{loss}} = RI^2 = R \frac{P_R^2 + Q_R^2}{E_R^2} \quad (4.6)$$

$$Q_{\text{loss}} = XI^2 = X \frac{P_R^2 + Q_R^2}{E_R^2} \quad (4.7)$$

Thus S_{loss} is given by:

$$S_{\text{loss}} = Z \frac{(P_R^2 + Q_R^2)}{E_R^2} \quad (4.8)$$

It can be seen from the equations 4.6 and 4.7 that reactive power absorbed by the line impedance is $I^2 X$. This is referred to as the reactive power loss. Similarly the active power loss, $I^2 R$ is associated with resistive elements. It can also be observed from the equations that an increase in the reactive power leads to an increase in both active and reactive power losses. This has an impact on the efficiency of power transmission and voltage regulation.

The relationship among P , Q and bus voltage V , or generated voltage E , with respect to the signs of P and Q is important when the flow of power in a power system is considered. The question involves the direction of flow of power, that is, whether power is being generated or absorbed when voltage and current are specified. Figure 4.3 shows the power flow directions with respect to the signs of the powers given in equations 4.2, 4.3, 4.4 and 4.5.

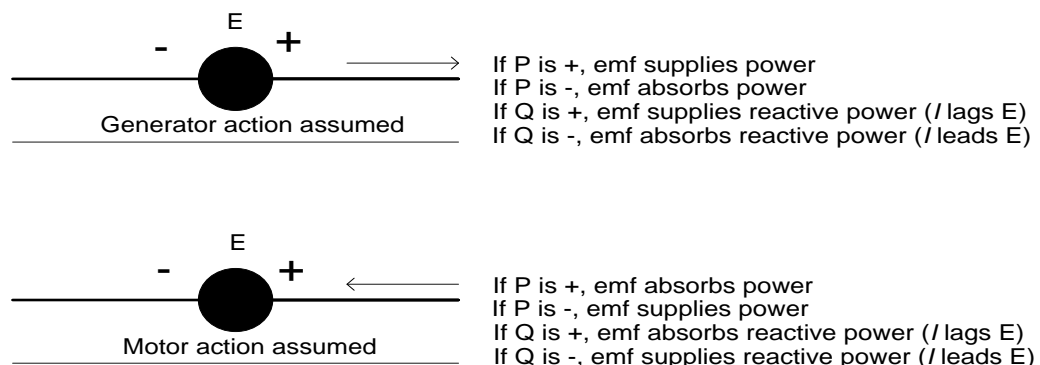


Figure 4.3: Summary of power flow directions

In large power systems and consequently ring distribution networks with multiple feeders, power flow is based on the above factors that determine power directions. Interconnected or ring networks usually consist of two or more buses, where one bus forms the sending end and other the receiving end. These buses are classified into three major buses that make modelling and simulation of power systems simpler.

4.2 Bus classification

The objective of power flow analysis is to determine the four main variables, that is, the voltage, current, active and reactive power as well as the power factor at every bus and the loss in the branches between buses. The information obtained during load flows are:

- Magnitude of voltages (V)
- Phase angle of voltages (δ)
- Active power (P)
- Reactive power (Q)

At each bus, two of these variables are specified as input data, and other two are unknowns to be computed by the power flow program. Depending upon which quantities have been specified, the buses are classified in the following three categories:

- a) Slack bus – this bus is also referred to as swing bus. This is where the magnitude and phase angle of the voltage are specified. The slack bus is a reference for which $V \angle \delta = 1.0 \angle 0^\circ$ per unit, is input data. There is only one slack bus, which is taken as reference. The power flow program computes P and Q. The slack bus will take care of the additional generation needed and transmission loss (Wadhwa, 1991:13).
- b) Load bus (PQ bus) – here P and Q are the input data. It is desired to find out V and δ through the power flow program. Voltages at the load bus are allowed to vary within the prescribed limits e.g. $\pm 10\%$. Most buses in a typical power flow program are load buses.
- c) Voltage controlled bus – here P and V are specified. It is required to find out the Q and δ . Examples are buses connected to generators, switched capacitors or static var systems. Table 4.1 summarizes the above discussion:

Table 4.1: Power flow buses and variables

<i>Bus Type</i>	<i>Quantities specified</i>	<i>Quantities to be obtained</i>
<i>Slack bus</i>	$ V , \delta$	P, Q
<i>Load bus</i>	P, Q	$ V , \delta$
<i>Voltage controlled bus</i>	$P, V $	Q, δ

4.3 Formulation methods for load flow solutions

Although the principles of power flow studies are straightforward, a realistic study relating to a power system can only be carried out with the help of a computer. In such a case, mathematical computations are carried out in a systematic manner by an iterative procedure. Two of the commonly used mathematical algorithms are the Gauss-Seidel method and the Newton-Raphson method (Nasar, 1996:336).

The Gauss-Seidel method solves the power-flow equations in rectangular (complex variable) coordinates until differences in bus voltages from one iteration to another are sufficiently small.

The Newton-Raphson load flow method begins with converting branch impedance between the buses or nodes into their equivalent admittance values, hence the formation of the Y-bus matrix (Grainger & Stevenson, 1994:160). The method uses an initial guessing technique where bus voltages and angles at the slack bus are assumed and the P and Q at the load bus are known. Values for the Jacobian matrix are entered and the “Jacobian” is inverted, the correct voltage and power flow results at every bus are then calculated. The power flow results give the real values of the unknown and guessed quantities. This solution happens after some iterations under given tolerance values (Atkinson-Hope, 2005:67).

The real and reactive powers are solved at each bus using the following formulae:

$$P_i = V_i \sum_{j=1}^{N_{bus}} Y_{ij} V_j V_i \cos(\theta_{ij} - \delta_i + \delta_j) \quad (4.9)$$

$$Q_i = V_i \sum_{j=1}^{N_{bus}} Y_{ij} V_j V_i \sin(\theta_{ij} - \delta_i + \delta_j) \quad (4.10)$$

where, P_i and Q_i are the net injected active and reactive powers at the i_{th} bus. V_i and δ_i are the amplitude and angle of the voltage at the i_{th} bus, respectively, and Y_{ij} and θ_{ij} are the amplitude and angle of the branch admittance between the i_{th} and j_{th} buses respectively.

In ring distribution networks, power flow between multiple buses depends on where and to what they are connected. Because of these multiple loops, power can go through a certain branch depending on its load-ability which is influenced primarily by line impedances. Line

impedance is proportional to distance, consequently more current tends to flow in shorter overhead lines or U/G cables. If a line is lost the power takes alternative loops to reach respective loads hence the directions of power flow are subjected to this system changes.

In this thesis, two software packages, DlgSILENT powerfactory and Power System Computer Aided Design (PSCAD), are used. The DIGSILENT software package utilises the Newton-Raphson methodology to obtain the power flow results.

4.3.1 DlgSILENT powerfactory

The calculation program DlgSILENT Powerfactory is a computer aided engineering tool for the analysis of industrial, utility, and commercial electrical power systems. It has been designed as an advanced integrated and interactive software package dedicated to electrical power system investigations in order to achieve the main objectives of planning and operation optimization (DlgSILENT GmbH, 2001:4). One of its capabilities is its ability to predict real life steady-state load flow results of complex industrial networks.

4.3.2 PSCAD

PSCAD is a general-purpose time domain simulation program for multi-phase power systems and control networks (Manitoba HVDC Research Centre, 2005:2). It has a capability to study the transients in power systems. A full library of advanced components allows a user to precisely model interactions between electrical networks and loads in various configurations. A graphical user interface and numerous control tools make PSCAD a convenient and interactive tool for both analysis and design of any power system. PSCAD is a fast, accurate, and easy-to-use power system simulator for the design and verification of all types of power systems. This software provides graphical results of the transients hence it is considered to be the ideal for generating switching effect waveforms.

4.4 Summary

In this chapter, the significance of load flow studies in distribution systems and power systems at large is emphasized. The techniques used to conduct the load flow studies were discussed. In addition an overview how to classify system buses when modelling the network and the methodologies or formulae for conducting the load flow studies were discussed.

CHAPTER FIVE CONTINGENCY ANALYSIS

5. Overview

Contingency analysis is one of the crucial power system studies. It refers to the security of the system operation under the loss of one or more of the major system components due to a failure (Deuse et al., 2003:1). In the case of a loss of one component, this corresponds to the $N - 1$ criterion, i.e. the system should be able to support the load when one of the N basic transmission system components e.g transmission line, generator etc... is out of operation (Grainger & Stevenson, 1994:591). The application of the criterion can also be extended to the case of loss of a combination of these basic components. When applied to the loss of two components, it leads to the $N - 2$ criterion (Grainger & Stevenson, 1994:593). Contingency analysis helps to look at the system's vulnerable points and helps in obtaining through simulations, standard solutions which will enable the operator to react in real time situation to resolve the problem in a short time. Operator reaction time is very much limited in real time.

Since a contingency can take place at any instant of operation, the system design should be such that the system is able to deal with different operating conditions such as peak or off-peak load of the system (Papaefthymiou et al., 2006:1). The application of the criteria is based on deterministic measures, i.e. determining the change of line/cable connections and bus voltages in the new steady state after loss of a component. The results of this analysis correspond to the system operation under the chosen conditions and are used for the realization of a planning or operational decision.

Ring main networks are not immune to the contingency scenarios. It is therefore very important that networks be studied under these conditions to note any overloads or voltage violations in excess of constraints and to implement preventative and corrective actions required to ensure continuity of supply. Unlike radial networks, ring main networks are advantageous when subjected to contingencies i.e. if a U/G cable or transformer fails, power is delivered to the loads through alternative paths to ensure continuity and security of supply. The directions of power flow might thus change when subjected to contingencies as a result of the loss of a cable or component, while in radial distribution networks if an O/H line is lost, all customers down the line lose power, and power can only be restored when the line is restored.

If the system operating point stays within operating boundaries, the system is then declared "N-1" secure, and if two elements are disconnected the system is declared "N-2" secure if still no violations are noted. Corrective actions include:

- Shunt capacitors

- Switching in/out lines
- Load shedding
- Generator rescheduling

5.1 Contingency analysis methodology

Figure 5.1 shows a proposed method of carrying out a contingency analysis developed by Hawtrey & Atkinson-Hope, (1998:34). The developed methodology gives steps that should be followed when conducting a contingency analysis.

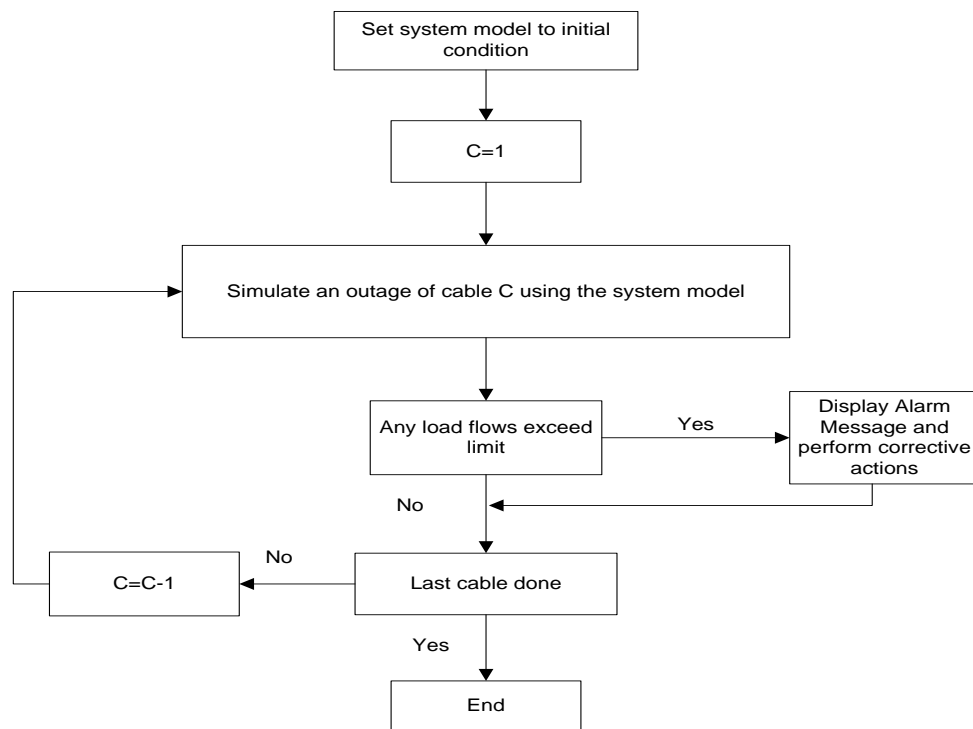


Figure 5.1: Contingency analysis methodology

5.1.1 Contingency case

To illustrate the operation of the flow chart given in Figure 5.1, consider the one-line diagram displayed in Figure 5.2. The one-line diagram has three 66 kV/11kV infeed substations X, Y and Z. The network consists of 21 U/G cables, plus 6 N/O switches. The loads in the system will be supplied from any of the three substation infeeds depending on the state of the switches, N/O1, N/O2, N/O5, and N/O6.

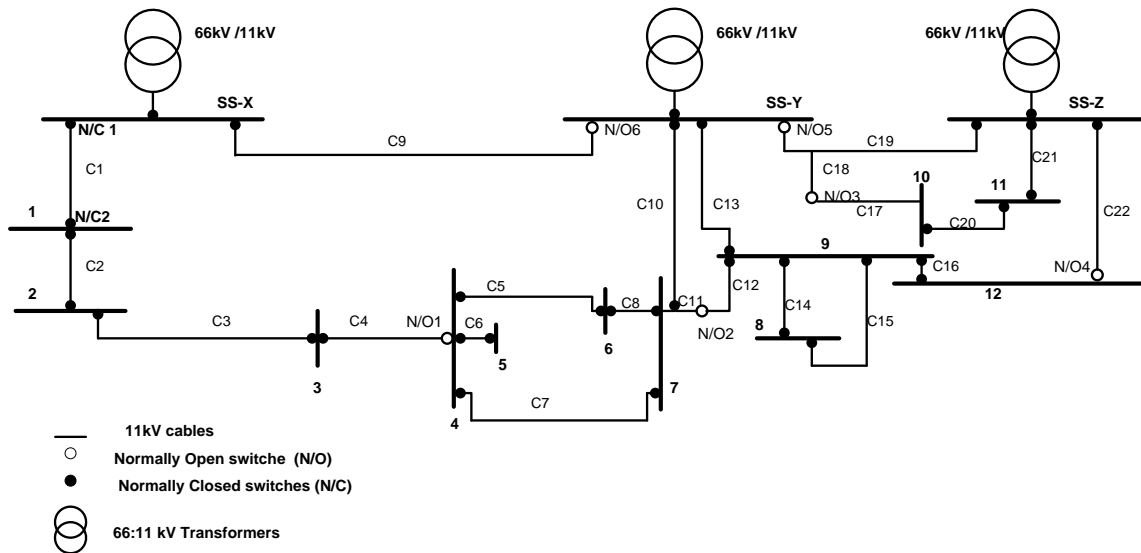


Figure 5.2: One-line diagram of a typical interconnected network

For illustration, the contingency case is assuming a fault on C1 (Cable 1). The configuration of the system is in its initial condition with all its N cables operating correctly. C1 is then removed from service (N-1), and the following steps are used to analyse the contingency:

- a) Open the switches N/C1 and N/C2 on the simulated system to isolate the fault.
- b) Simulate a load flow for this contingency case. The contingency case caused a supply power loss at stations 1, 2 and 3. In this case the N/O switches have to be reconfigured so that optimal voltage levels and power flows are achieved.
- c) For this contingency case the optimum solution will be to :
 - Close N/O1
 - Close N/O2

Closing N/O1 will allow substation infeed Y to supply power to the affected stations 1, 2 and 3, provided that SS-Y has sufficient capacity to do so. Closing Switch N/O2 will allow C10 to share the load with C13 to avoid cable overloading.

- d) Simulate a load flow for this new configuration and extract the new voltage levels and power flows and verify such values against appropriate violation limits.
- e) Select the next cable C to be taken out of service.
- f) Continue this way until all contingencies have been analysed.

If it happens that Substation infeed Y does not have sufficient capacity to provide the affected stations, one can consider closing N/O 4. This will allow SS-Z to take on some of the loads.

Under extreme overload conditions where there is either no available distribution capacity to reroute, or if there is a shortfall in power generation, due to contingency, some loads may be shed or selectively disconnected.

5.1.2 Reserve margin

As discussed in the previous section, a power system in a secure operating state can sustain one or several contingencies, and still continue to function without interruption, by transitioning into a new configuration in which the burden is shifted to other components. Transitioning to a new configuration can be effected by transferring of some loads to other U/G cables, by changing the status of the switches or by increasing the supply. If a power system is serving an ever increasing load, the number of alternative operating configurations diminishes, and the system becomes increasingly vulnerable to disturbances. In extreme cases, with all generators fully loaded, if one generator fails because of a low reserve margin (2% to 3%), some service to customers will be inevitably interrupted. To avoid this type of situation, utilities have traditionally retained a high reserve margin ($\pm 15\%$) of generation.

5.2 Summary

It is important for one to know how to handle major outages when they occur in the system. Contingency analysis, one of the most important studies of abnormal conditions that need to be considered is explained. The purpose of this chapter is to provide a platform, foundation for what is to come in the following chapters of this thesis.

CHAPTER SIX ENERGY EFFICIENCY TECHNIQUES

6. Overview

It is estimated that the average power transmission loss from power utilities amounts to around 5%-6% of total power demand, whereas 60%-70% of these losses are estimated to be lost in distribution networks (Thakur & Jaswanti, 2006:1). Electrical energy efficiency is one of the measures of saving energy used to provide goods and services while maintaining the desired benefits (Mthiyane, 2008:8). Electrical energy efficiency includes efforts to reduce energy usage in a particular area with the goal of reducing energy usage and peak-load demand in the network. In contrast to supply options, energy efficiency puts downward pressure on reducing demand instead of increasing supply (Pansini, 1991:291). This means that energy efficiency provides additional economic value by preserving the resource base and reducing the pressure on the environment (Mthiyane, 2008:8).

6.1 Techniques used for power loss reduction

There are energy-efficient techniques available that can reduce or keep distribution power loss down to acceptable levels. These energy-efficient techniques have the additional benefit of improving the reliability and quality of supply of the power network (Thakur & Jaswanti, 2006:2). This will also have a dramatic impact on the total amount of generation capacity needed.

The following energy-efficient techniques are used for power loss reduction:

- re-conductoring
- load balancing
- new interconnection
- addition of new feeders in the network
- replacement of old and obsolete equipment
- Energy Management Systems (EMS)
- reconfiguring the network
- capacitor placement

The following subsections describe some of the above techniques and offer some insights into their effectiveness.

6.1.1 Re-conductoring

Re-conductoring allows the capacity of an existing conductor to be increased by replacing the existing conductors with larger conductors (Prakash, 2007:29). The size of the U/G cable is an important element as it determines the current density and the resistance of the U/G

cable. A lower U/G cable size can cause high power loss and high volt-drop in the U/G cable. Hence, increasing the size of the U/G cable will result in power loss reduction.

However, larger-sized cables are expensive and the installation costs of these U/G cables also are likely to forbid re-conductoring as a feasible means of power loss reduction (Ng, 1999:8). U/G cable upgrade can only be economically justified for older networks that are operating close to their capacity and / or nearing their life span, where life span is the period of time a cable can operate safely.

6.1.2 Load balancing

When the loads connected to the three phases of a U/G cable are not balanced, as it is always the case in many distribution networks, it results in increased current flow causing the U/G cables to overload, and resulting in high power loss in the system. In this case, the loads should be shifted to the less loaded U/G cables, to reduce the overloading and hence the imbalance in the system.

6.1.3 Capacitor Addition

As discussed in section 2.2., low PF causes an increase of power loss. The increase in PF is done by adding shunt capacitors in the network, as discussed.

To reduce the power loss in the distribution network effectively, shunt capacitors should be connected in any of the following parts of the distribution network:

- Across individual customers;
- At vantage points on 11 kV feeders;
- At distribution transformers; or
- At 11 kV stations.

6.1.4 Replacement of old and obsolete equipment

This process involves the replacement of old equipment such as transformers, with more efficient ones. The replacement of old high loss devices with new high efficient devices will improve the efficiency of the whole system. However, higher efficiency transformers are considered to be very costly.

6.1.5 Reconfiguring the network

One of the most effective power loss reduction techniques in distribution networks is to include in them N/O switches and N/C switches. Network reconfiguration is achieved by changing the open/closed status of the switches, circuit breakers (CBs) and other equipment in the network (Civanlar et al., 1989:1217 & Kalinowski et al., 2007:104). The reconfiguration

process physically alters the topology of the network to achieve certain objectives. Under normal operating conditions, the network is reconfigured to transfer away loads from heavily loaded feeders and to reduce the system loss (Aoki et al., 1988:1865; Su & Lee, 2001:97 & Bueno, Lyra & Callevuci, 2004:1). Thus, if a network experiences an outage, the network is reconfigured to restore services, and minimise areas without power, whilst keeping the voltage levels and voltage drops within the desired percentage limits (Thakur & Jaswanti, 2006:1; Shirmohammadi & Hong, 1989:1492). Power utilities commonly use network reconfiguration to reduce power loss because it does not require new equipment. This is the greatest advantage of this method. Figure 6.1 is used to illustrate how reconfiguration is conducted.

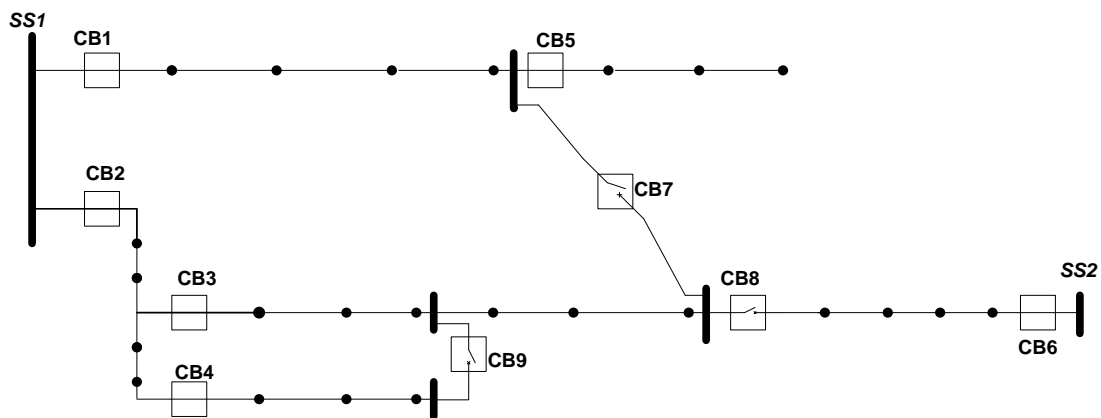


**Figure 6.1: Schematic diagram of a primary circuit of a distribution system
(Adapted from Baran and Wu, 1989:1401)**

The dots ● in Figure 6.1 represent the load centres where the transformers are tapped off from the primary distribution system. There are N/C switches connecting the U/G cable sections, these are CB1, CB2, CB3, CB4, CB5 and CB6. There are three N/O switches on the tie-lines connecting two primary feeders (CB7), two substations (CB8) and ring-type laterals (CB9). Most distribution networks are operated as radial networks; however the configuration can be changed during operation by changing the state of some switches. For example, in Figure 6.1, switches CB7 and CB8 can be closed and CB3 and CB6 can be opened to transfer loads from one feeder to another (Baran & Wu, 1989:1401).

6.1.6 Energy Management Systems (EMS)

An energy management system (EMS) is a system of computer aided tools used by operators of electric utility grids to monitor, control and optimise the performance of the distribution system. The EMS monitoring and control functions are referred to as the supervisory control and data acquisition (SCADA). This intelligent energy management system is designed to reduce energy consumption, improve the utilization of the system,

increase reliability, and predict electrical system performance as well as optimise energy usage to reduce costs.

6.2 Practical choices for power loss reduction

Given that the majority of power losses are found in the distribution level of the power system, many utilities can achieve significant savings from the implementation of one or a combination of the energy efficiency techniques outlined in section 6.1. Studies conducted to determine which energy-efficient techniques are more suitable and beneficial for application, Ng (1999:10) showed that network reconfiguration and capacitor placement are ranked the highest. Network reconfiguration and transformer load management have greater benefits in systems that are more or mostly heavily loaded. Individually, literature revealed that network reconfiguration is the most preferred method (Lo & Gers, 1994:1). This is because it does not require extra costs and equipment. The second preferred method is capacitor placement, because it does not require much capital expenditure as other techniques such as re-conductoring. Furthermore, distribution networks always have inductive components and proper capacitor placement will always result in power loss reduction.

6.3 Benefits of improving efficiency

Electricity generation accounts for a huge portion of unwanted carbon emissions into the atmosphere. Greater energy efficiency in the distribution system means lower emissions from generation to deliver the same amount of energy to the consumer. Reducing energy losses in a distribution network will also reduce the overall system demand and provide additional network capacity for utilisation and growth. Since energy losses costs are passed onto all loads, improvements in this area will benefit all loads. Efficiency improvement also reduces the risks of load shedding during contingency conditions.

6.4 Summary

Transfer of electric energy from the source of generation to the load via the transmission and distribution networks is accompanied by losses. The majority of these losses occur on the distribution system. These losses can be minimised by various measures discussed in the chapter. It is widely recognized that placement of shunt capacitors and network reconfiguration on the distribution system can lead to a reduction in power loss and are the preferred power loss reduction techniques applied. Reduction of power loss in distribution systems is essential to improve the overall efficiency of power delivery.

CHAPTER SEVEN

EFFICIENCY PLAN OF INTERCONNECTED RING MAIN NETWORK

This chapter presents an efficiency plan to minimise the power loss in a ring main network. The efficiency plan proposes an empirical approach of minimising the losses associated with the reactive component of network currents by placing capacitors at proper locations and by minimising the power losses associated with the active component of the network currents through network reconfiguration.

7. Overview

Due to low voltage on the distribution side of the power system, high currents and power losses are experienced. The pressure on utilities to improve the overall efficiency in the power system has forced them to concentrate on reducing the power loss on the distribution level, since it contributes most power losses in the power system.

Researchers have discussed and developed different algorithms to solve the power loss reduction problem in distribution networks. However, these methods were developed for radial network operations. However, most large urban distribution networks are operated as ring networks.

Furthermore, although ring main networks are believed to have less power losses compared to radial networks, loss of an important component in a ring main network can cause an increase in power losses leading to power shortage in the network. To improve the state of a network is the task of optimal load flow studies. There is thus a need for network engineers to identify efficient ways to deliver power to loads efficiently in ring networks. This is a great shortcoming in the literature.

This thesis focuses on developing an efficiency plan that can be used by network operators in response to a failure of a major component such as a substation infeed or a primary U/G cable. The developed efficiency plan is using the capacitor addition and network reconfiguration techniques to give the optimal configuration for power loss reduction.

7.1 Development of the efficiency plan work flow diagram

Figure 7.1 shows the one-line diagram of the large urban interconnected ring main distribution network that was used to evaluate and develop the efficiency plan (methodology). Such a network is typical in industry and consists of multiple ring main networks.

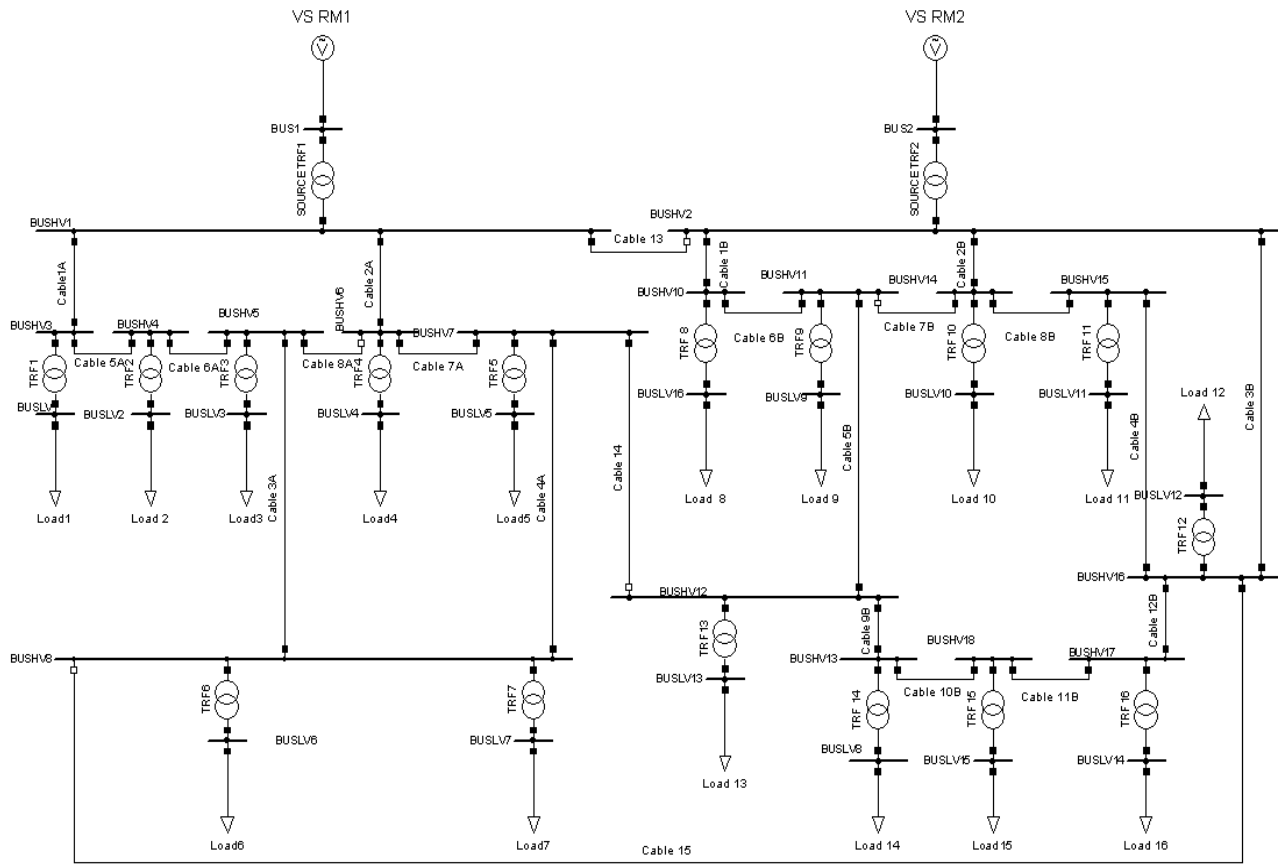


Figure 7.1: Large urban interconnected ring main networks RM1 and RM2

- ■ — N/C Switch/ Circuit breaker
- □ — N/O Switch/ Circuit breaker
- ▲ — Direction of Power flow

The network shows two interconnected ring main networks namely Ring main Network 1 (RM1) and Ring main Network 2 (RM2). Both ring main networks, RM1 and RM2, have a voltage source of $66\angle 0^\circ$ kV and a frequency of 50 Hz. The two networks are interconnected via U/G Cables 13, 14 and 15. RM1 has a step down transformer rated at 7 MVA, 66/11 kV with two primary U/G Cables, 1A and 2A. U/G Cables, 3A, 4A, 5A, 6A, 7A and 8A complete the ring main system of RM1. RM2 has a source step down transformer rated at 10 MVA, 66/11kV with three primary U/G Cables 1B, 2B and 3B and secondary U/G Cables 4B, 5B, 6B, 7B, 8B, 9B, 10B, 11B and 12B. The load ratings, transformer ratings and U/G cable ratings for both networks are shown in Tables A.1, A.2 and A.3, in Appendix A.

The studies will mainly be focused on the RM1 network. The RM2 network will however be considered in the case of network configuration when extra power is needed at RM1.

7.2 Efficiency plan Methodology

Figure 7.2 shows an efficiency plan work-flow diagram. The work-flow diagram depicts an empirical approach for finding the optimal configuration that will minimise the power losses in a ring main network that is under a contingency condition, while satisfying the given constraints. The flow diagram was evaluated using the ring main network in Figure 7.1. The load flow procedures find a series of configurations with different status of switches and addition of capacitors such that the power losses are successively reduced. The network was analyzed using DIgSILENT powerfactory and Power Systems Computer Aided Design (PSCAD) software to obtain steady-state and time domain results, respectively. The parameter models for DIgSILENT and PSCAD are shown in Appendices A and B respectively. The load flow procedures of the proposed method are mainly composed of power loss and efficiency calculations, busbar voltages and cable/feeder loading determination and empirical approach application.

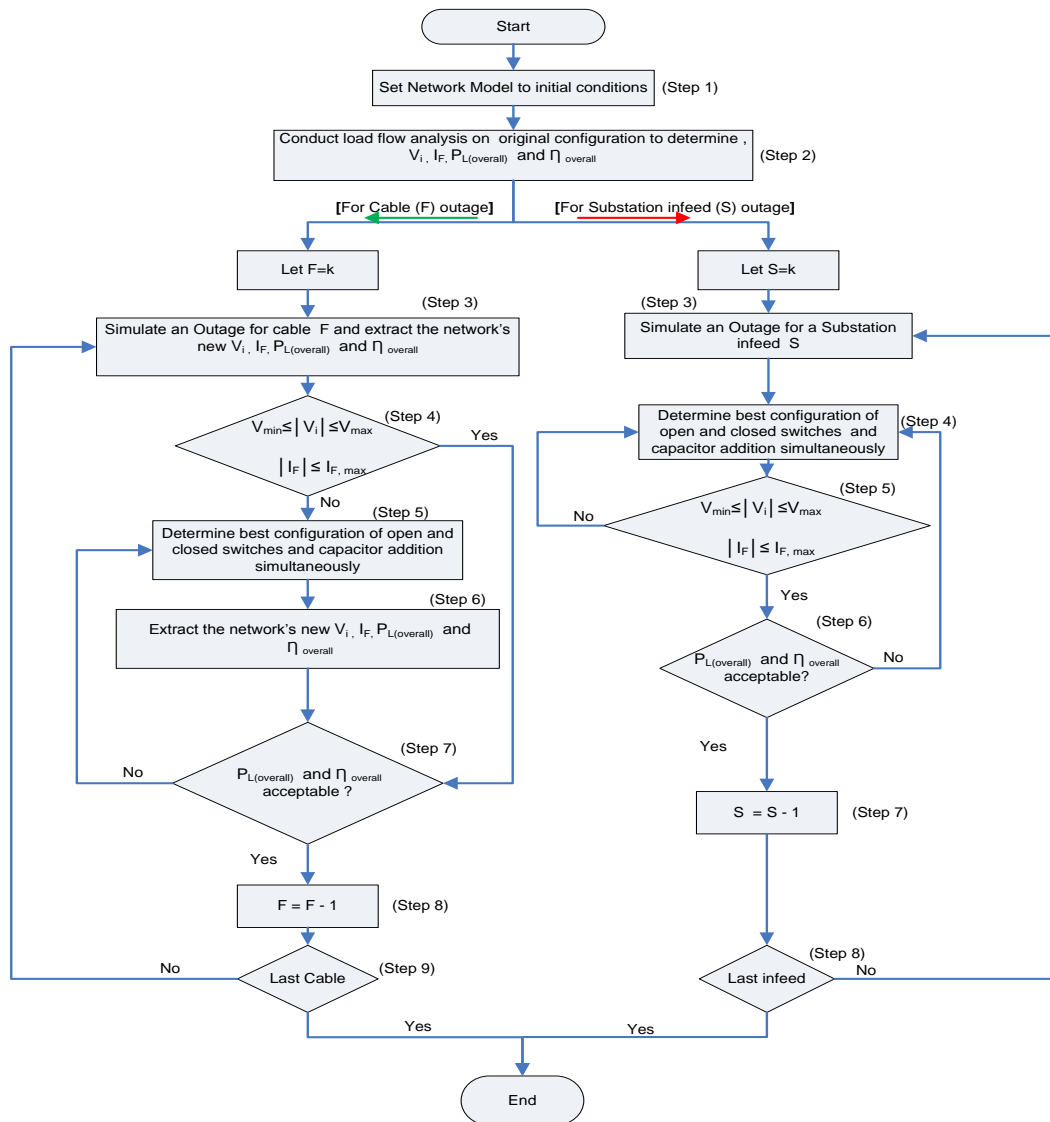


Figure 7.2: Efficiency plan: work flow diagram

In Figure 7.2, k is the number of U/G cables / O/H lines or substation infeed to be considered, its value can be any positive number; V_i is the busbar voltage level measured in Kilo-Volts (kV); V_{min} and V_{max} are the minimum and maximum permissible voltage levels of a busbar respectively; I_F and $I_{F,max}$ are the current magnitude and maximum current capacity of a U/G cable F or O/H line F , respectively; $P_{loss(overall)}$ is the overall power losses of the network; $\eta_{overall}$ is the overall efficiency of the network.

7.2.1 U/G cable outage

Step 1. Create a steady-state computer model of the network in its normal operating state.

Step 2. Simulate a load flow and obtain the normal operation (original configuration) voltage levels (V_i) of the load busbars (LV), the U/G cable /O/H Line current loadings (I_F) and hand calculate the overall power losses ($P_{loss(overall)}$) and the overall efficiency ($\eta_{overall}$). This will help the operator to know the normal operating conditions of the network.

The $P_{loss(overall)}$ is obtained by:

$$P_{loss(overall)} = \sum P_{loss(Cables)} + \sum P_{loss(TRFR)} \quad (7.1)$$

where,

$\sum P_{loss(Cables)}$ are the total losses contributed by the cables and $\sum P_{loss(TRFR)}$ are the total losses contributed by the transformers.

The $\eta_{overall}$ is obtained by:

$$\eta_{overall} = \frac{\sum P_{out(X)}}{\sum P_{in(X)}} \times 100\% \quad (7.2)$$

where,

$\sum P_{in(X)}$ and $\sum P_{out(X)}$ are the total input and output power of network X respectively.

Step 3. Select a cable, F , to be out of service, perform a load flow for this contingency condition and extract the network's new V_i , I_F , $P_{loss(overall)}$ and $\eta_{overall}$. These results will help in measuring the severity of the contingency condition under study.

Step 4. Observe if there are any busbar voltage violations or overloaded cables; If yes, continue to step 5, if no, Jump to step 7. The following constraints are taken into consideration:

- Voltage constraints (limits)

The South African National regulation standard body NRS 084-2003:2 requires a utility to supply voltage to loads within $\pm 10\%$ of the busbar nominal voltage during both normal and

abnormal operating conditions in the network (South Africa. Technology Standardization Department, 2003:11). This is to ensure efficient operation of various electrical components in the network. Table 7.1 shows the busbar voltage limits as stipulated by the NRS.

Table 7.1: South African National Voltage Limits LV busbar

South African National Regulation NRS 048-2004:2	Nominal Voltage (V)	Minimum Voltage (V)	Maximum Voltage (V)
±10%	400 V	360.00	440.00

- Current loading constraints

It is important to ensure that the primary cables are not overloaded more than their rated capacity. Table 7.2 provides the current carrying capacity of the cables used in the study as prescribed by SANS 97 for cables (ABERDARE Cables, 2008:14).

Table 7.2: Limits for cables

Cable	Maximum Current carrying capacity (Amps)		
	Ground	Ducts	Air
PILC 25	100	90	100
PILC 50	150	130	150
PILC 185	320	275	335

Step 5. Determine the best configuration of open and closed switches (network reconfiguration) and capacitor addition simultaneously.

The simultaneous solution of the optimal reconfiguration and capacitor placement problem determines which network switches should be open and which closed as well as capacitor sizes and locations in order to reduce losses, to improve voltage profile and, in a more limited way, satisfying equipment and operational constraints.

Step 6. Extract the new V_i , I_F , $P_{\text{loss}_{(\text{overall})}}$ and η_{overall} . These results will show you the effectiveness of the efficiency plan

Step 7. Check if $P_{\text{loss}_{(\text{overall})}}$ and η_{overall} has improved. The configuration that results in maximum power loss reduction should be considered as the optimal configuration.

Step 8. Continue to the next cable ($F-1$).

Step 9. Check if all cables are considered, if not go to step 3.

7.2.2 Substation infeed outage

Step 1. Create a computer model of the network in its normal operating state.

Step 2. Perform a load flow and obtain the V_i , I_F , and hand calculate the $P_{\text{loss(overall)}}$ and η_{overall} .

Step 3. Select a substation infeed S , to be out of service, and simulate a load flow study for this contingency case.

Step 4. Consider network reconfiguration and capacitor addition to the network.

Step 5. See if there are any overloaded cables or busbar voltage violations; if there is go back to step 4, if there is none, continue to step 6.

Step 6. Obtain the $P_{\text{loss(overall)}}$ and hand calculate the η_{overall} see if there is any improvement

Step 7. Continue to the next substation infeed ($S-1$) and repeat all the steps.

Step 8. Check if all substation infeeds are considered, if not go to step 3.

By utilising this plan, the optimised network reconfiguration and capacitor placement is established for the given network. Although this plan is for the specific network described its approach can be followed for other interconnected urban ring main networks or other types of contingencies.

7.3 Capacitor switching voltage transients measurements

Once the capacitor placement that gives the optimal loss reduction and improved efficiency has been selected, a transient study on the capacitor needs to be conducted to ensure that over voltages resulting from capacitor switching are not exorbitant.

The network in Figure 7.1 was built in PSCAD to determine the generated voltage transients due to capacitor switching. These voltage transients will be measured at the load buses.

The approach of capturing and evaluating the peak voltage transients was as follows:

- Set the capacitor circuit breaker's time logic to close at 0.16 seconds
- Perform the load flow study
- Record the highest peak voltage transient at each load bus
- Determine whether the peak voltage transients at each load bus are within the safe range. The safe range discussed in literature is that the peak transient voltage level should be less than twice the rated voltage (equation 2.29).

In this study, the rated voltage of the load buses is 0.4 kV, therefore:

$$V_{\text{transient}} \leq 0.8 \text{ kV}$$

- If the peak transient voltages are within the safe range, end the study, however if the voltage transients are out of the safe range, look into mitigation measures.

7.4 Summary

An interconnected urban ring main network was presented. The developed efficiency plan and transient analysis was discussed and all its steps were discussed in more details.

CHAPTER EIGHT APPLICATION OF EFFICIENCY PLAN

8. Overview

In order to underpin the network behaviour and to clearly demonstrate the significance of the efficiency plan developed, the developed efficiency plan is applied to the urban interconnected ring main network in Figure 7.1 using three different case studies.

The Efficiency plan steps developed to bring about improved power flow in the network were incorporated in the network and their impact was assessed. The objective was to conduct procedures that will result in a better, reliable and improved network that can operate optimally even when subjected to contingencies. The emphasis was placed on the voltage profile in order to keep them in the acceptable ranges as prescribed by the NRS 048, and also to minimise power losses in the network. Another aspect that was considered is the effect of power flow directional changes as a result of contingency simulation and system reconfiguration. This is vital because cable current ratings should not be exceeded even when additional power flows into the cable. As previously stated, the studies will be more focused on the RM1 network. The DIgSILENT software package was used to obtain steady-state results and PSCAD was used to measure the generated voltage transients due to capacitor switching (see modelling in Appendices A and B).

8.1 Case study 1

The first case study assumes a fault on Cable 1A in RM1. The steps of the efficiency plan in Figure 7.2 when considering a cable outage are used to analyse this contingency case.

- a) **Step 1:** set the network to its initial condition operations in the DIgSILENT window as shown in Figure 7.1.
- b) **Step 2:** conduct a load flow study on the network. The steady-state results obtained from the load flow studies conducted are as follows:

- **RM1 Load bus voltage level results (V_i)**

Table 8.1 shows the load bus voltage level results for the normal operation configuration.

Table 8.1:RM1 load bus voltage levels

Load Bus	Voltage magnitude(kV)	% Deviation
LV1	0.372	7.00%
LV 2	0.369	7.75%
LV 3	0.366	8.50%
LV 4	0.372	7.00%
LV 5	0.371	7.25%
LV 6	0.369	7.75%
LV 7	0.372	7.00%

Table 8.1 shows that the voltage levels at all load buses are within the 10% permissible limit as indicated in Table 7.1.

- RM1 Cable loading results (I_F)

Table 8.2 shows the loading of U/G cables. The maximum carrying capacities of the cables are shown in Table 7.2.

Table 8.2: RM1 Cable loading of RM1

Cable	Current magnitude (kA)	% Loading
Cable 1A	0.099	66.0%
Cable 2A	0.108	72.0%
Cable 3A	0.003	3.00%
Cable 4A	0.052	52.0%
Cable 5A	0.079	79.0%
Cable 6A	0.048	48.0%
Cable 7A	0.079	79.0%
Cable 8A	0.000	0.00%

The results presented in Table 8.2 show that all the cables are within their current carrying capacities.

The results obtained in Tables 8.1 and 8.2 show that during normal operations, the network is in a healthy state.

- RM1 Overall power loss

The calculated overall power losses of the original configuration are:

$$\begin{aligned}
 P_{\text{loss(overall)}} &= \sum P_{\text{loss (Cables)}} + \sum P_{\text{loss (TRFR)}} \\
 &= 109 \text{ kW}
 \end{aligned}$$

- RM1 Overall efficiency

To calculate the overall efficiency of RM1, the total input power ($\sum P_{\text{in(RM 1)}}$) and total output power ($\sum P_{\text{out(RM 1)}}$) must be known.

The $\sum P_{\text{in(RM 1)}}$ obtained is 3.036 MW, and the $\sum P_{\text{out(RM 1)}}$ obtained is 2.927 MW. These values were obtained from DigSILENT simulations.

Hence the overall efficiency of RM1 is:

$$\eta_{\text{overall}} = \frac{\sum P_{\text{out(RM1)}}}{\sum P_{\text{in(RM1)}}} \times 100\% = \frac{2.927}{3.036} \times 100\% = 96.42\%$$

c) Step 3: Switch cable 1A out of the RM1 network and conduct a load flow study of the network and obtain the new steady-state V_i , I_F , $P_{L(\text{overall})}$ and η_{overall} .

Cable 1A is removed from service by opening the N/C switches of cable 1A at stations BUSHV1 and BUSHV3. Figure 8.1 shows the one-line-diagram for a DigSILENT study after cable 1A was removed. The colours in Figure 8.1 represent the following:

- “Blue” represents undervoltage of load bus, busbar/station;
- “Red” represents overloading of cable or transformer;
- “Grey” represents component out of service, and
- “Black” represents components operating in a healthy state.

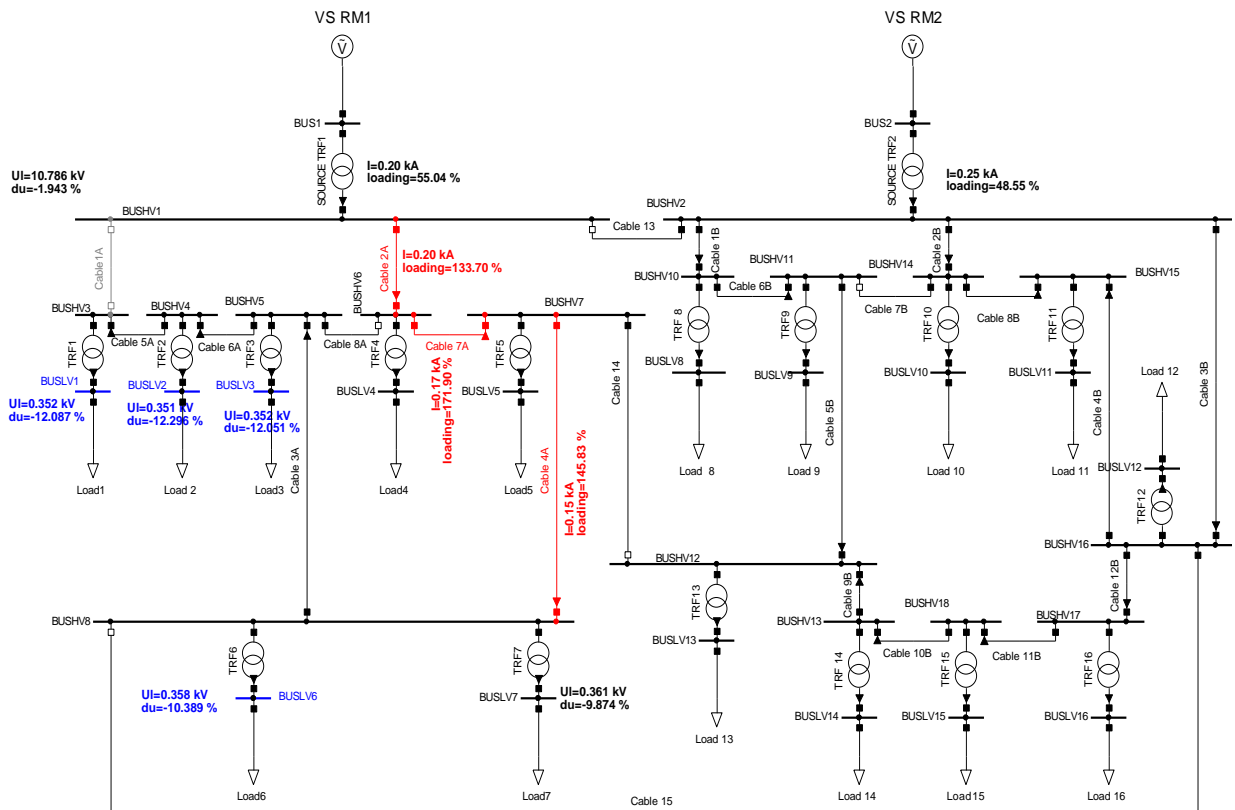


Figure 8.1: Case study 1 Single line diagram after the removal of Cable 1A

In Figure 8.1, UI is the operating voltage, du is the % voltage deviation; I is the operating current and loading is the percentage loading of the cable.

The results shown in Figure 8.1 are summarized in Tables 8.3 and 8.4.

Table 8.3:RM1 Load bus voltage levels due to removal of Cable 1A

Load Bus	Voltage magnitude(kV)	%Deviation
LV1	0.352	12.00%
LV 2	0.351	12.25%
LV 3	0.352	12.00%
LV 4	0.366	8.50%
LV 5	0.364	9.00%
LV 6	0.358	10.50%
LV 7	0.360	10.00%

The results depicted in Table 8.3, shows that the voltage level of the bus loads, LV1, LV2, LV3 and LV6 are below the permissible 10% limit, with load bus LV2 dropping the highest by 12.25%.

The loading of the U/G cables are depicted in Table 8.4.

Table 8.4: RM1 Cable loading due to removal of Cable 1A

Cable	Current magnitude (kA)	% Loading
Cable 1A	0.000	0.000%
Cable 2A	0.200	133.3%
Cable 3A	0.093	93.00%
Cable 4A	0.146	146.0%
Cable 5A	0.020	20.00%
Cable 6A	0.049	49.00%
Cable 7A	0.172	172.0%
Cable 8A	0.000	0.000%

Table 8.4 shows that the U/G cables 2A, 4A and 7A are overloaded, with cable 7A having the highest overload percentage.

- RM1 Overall power loss

The new RM1 overall power loss obtained is:

$$P_{\text{loss (overall)}} = \sum P_{\text{loss (Cables)}} + \sum P_{\text{loss (TRFR)}}$$

$$= 185 \text{ kW}$$

- RM1 Overall efficiency

The new input power supplied by VS RM1 through the remaining primary cable, cable 2A is,

$\sum P_{\text{in(RM 1)}} = 2.919 \text{ MW}$, and $\sum P_{\text{out(RM 1)}}$ is 2.732 MW. Hence the overall efficiency is:

$$\eta_{\text{overall}} = \frac{\sum P_{\text{out(RM1)}}}{\sum P_{\text{in(RM1)}}} \times 100\% = \frac{2.732}{2.919} \times 100\% = 93.67\%$$

d) Step 4: Observe if there are any busbar voltage violations or overloaded cables; If yes, continue to step 5,

- **Voltage constraints violation**

Figure 8.1 shows that load buses LV1, LV2, LV3 and LV6 have experienced undervoltage. This can be confirmed in Table 8.3.

- **Cable loading**

Table 8.4 shows that cables 2A, 4A, and 7A are overloaded.

The answer at step 4 is therefore yes, hence this takes us to step 5 of the developed efficiency plan.

e) Step 5: configure the open and closed switches and add capacitors simultaneously so that optimum voltage levels, cable loadings, overall power loss and overall efficiency is achieved.

Using empirical investigations it is found that for this contingency case the optimum solution will be to:

- Close N/O switch of Cable 8A at station BUSHV6
- Open N/C switches of Cable 3A at station BUSHV8
- Add 1.2 Mvar capacitor at station BUSHV5
- Add 1.5 Mvar capacitor at station BUSHV8
- Close N/O switch of Cable 15 at station BUSHV8
- Open N/C switch of Cable 4A at station BUSHV8

f) Step 6: Simulate the new configuration and extract the new steady-state V_i , I_F ,

$$P_{\text{loss (overall)}} \text{ and } \eta_{\text{overall}}.$$

The optimum configuration of the network obtained is shown in Figure 8.2.

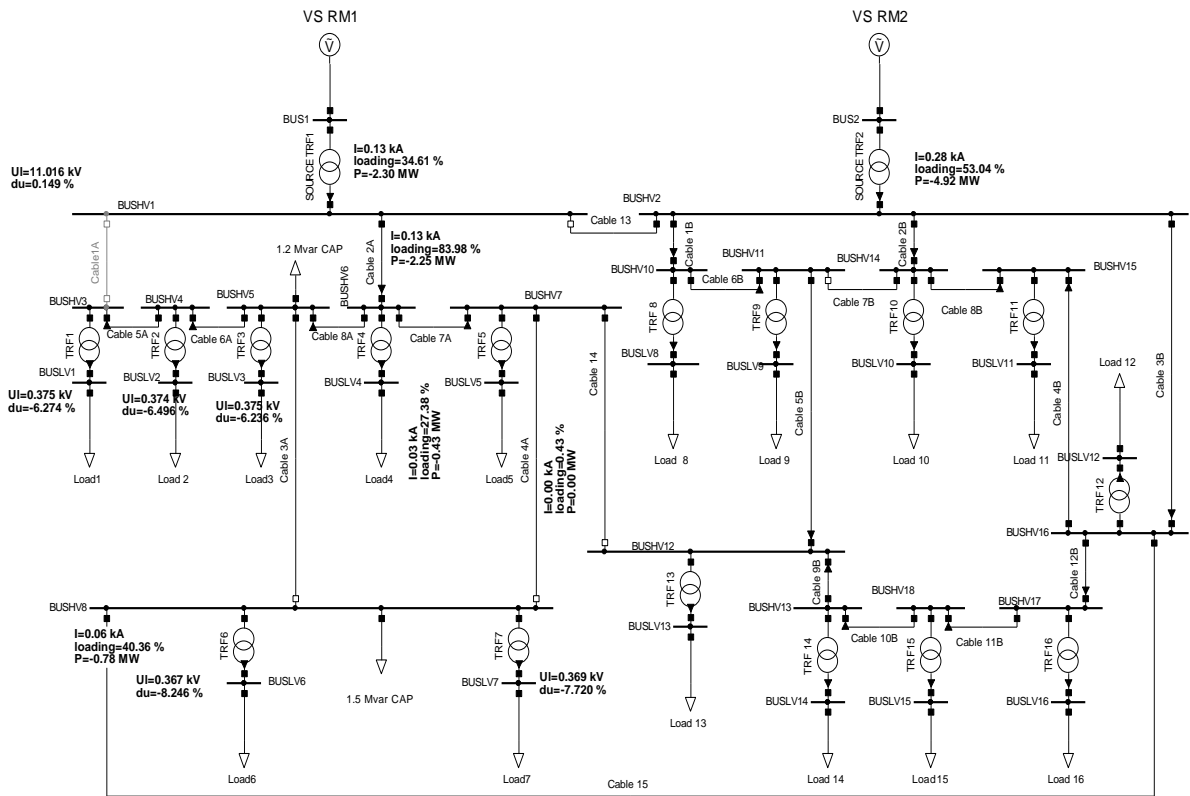


Figure 8.2: Case study 1 optimal configuration

The new steady-state load bus voltage levels and cable loadings obtained after modelling and simulating the new configuration are summarized in Tables 8.5 and 8.6.

Table 8.5: Load bus voltage levels for the optimal configuration

Load Bus	Voltage magnitude(kV)	%Deviation
LV1	0.374	6.38%
LV 2	0.374	6.60%
LV 3	0.375	6.34%
LV 4	0.378	5.55%
LV 5	0.378	5.38%
LV 6	0.375	6.37%
LV 7	0.377	5.83%

Table 8.5 shows that all the load bus voltage levels are within the permissible limit, with the lowest being LV1 and LV2 with 0.374 kV, and the highest LV4 and LV5 with 0.378 kV.

Table 8.6: Cable loadings for the optimal configuration

Cable	Current magnitude (kA)	% Loading
Cable 1A	0.000	0.00%
Cable 2A	0.126	83.73%
Cable 3A	0.000	0.00%
Cable 4A	0.000	0.00%
Cable 5A	0.022	21.62%
Cable 6A	0.052	52.31%
Cable 7A	0.027	27.38%
Cable 8A	0.074	73.88%

Table 8.6 shows that all the U/G cables are within their current carrying capacities.

- Overall power losses

The new overall power losses obtained for RM1:

$$\begin{aligned}
 P_{\text{loss (overall)}} &= \sum P_{\text{loss (Cables)}} + \sum P_{\text{loss (TRFR)}} \\
 &= 80.00 \text{ kW}
 \end{aligned}$$

- Overall efficiency

In Figure 8.2, the optimum configuration obtained shows that load 6 and load 7 were transferred to RM2. Thus, the new total $\sum P_{\text{out (RM 1)}}$ is 2.223 MW. The new input power supplied by VS RM1 through the remaining primary cable 2A is $P_{\text{in (Cable 2A)}} = 2.303 \text{ MW}$.

Thus, the overall efficiency is:

$$\eta_{\text{overall}} = \frac{\sum P_{\text{out (RM1)}}}{\sum P_{\text{in (RM1)}}} \times 100\% = \frac{2.223}{2.303} \times 100\% = 96.53\%$$

This shows an improvement in the efficiency from 93.67% to 96.53%.

Steady-state results obtained in RM2 after Load 6 and Load 7 were transferred to RM2 are shown in Apendix C.

- Capacitor switching transients

It is discussed in literature that capacitor switching causes overvoltage and high frequency current inrush (Sabin, Grebe & Sundaram, 1999:112). These transients can be very harmful to the customer's equipments. The optimal configuration for the contingency case under study was modelled and simulated using the PSCAD software in order to evaluate the capacitor energisation intensity. The optimum solution has two capacitors which were switched into the network. The two capacitors were connected at:

- 1.2 Mvar capacitor at station BUSHV5

- 1.5 Mvar capacitor at station BUSHV8

In Table 8.7, the peak voltage level at the load buses of RM1 due to the switching of capacitors is presented. The two capacitors were switched into the network at 16 ms. The results in Table 8.7 were obtained on the blue-phase.

Table 8.7: Peak voltage levels at the RM1 load buses during capacitor switching

Location	Peak value (kV)
Load bus LV1	0.468
Load bus LV2	0.459
Load bus LV3	0.447
Load bus LV4	0.435
Load bus LV5	0.443
Load bus LV6	0.419

8.2 Case study 2

Case study 2 considered the loss of substation infeed, VS RM1. The steps of the developed efficiency plan in Figure 7.2 when considering a substation infeed outage are used to evaluate this contingency case.

a) Step 1 and 2:

The results are shown in Step 1 and Step 2 of Case study 1.

b) Step 3:

When VS RM1 is removed from service, all the loads of RM1 will be without power as shown in Figure 8.3.

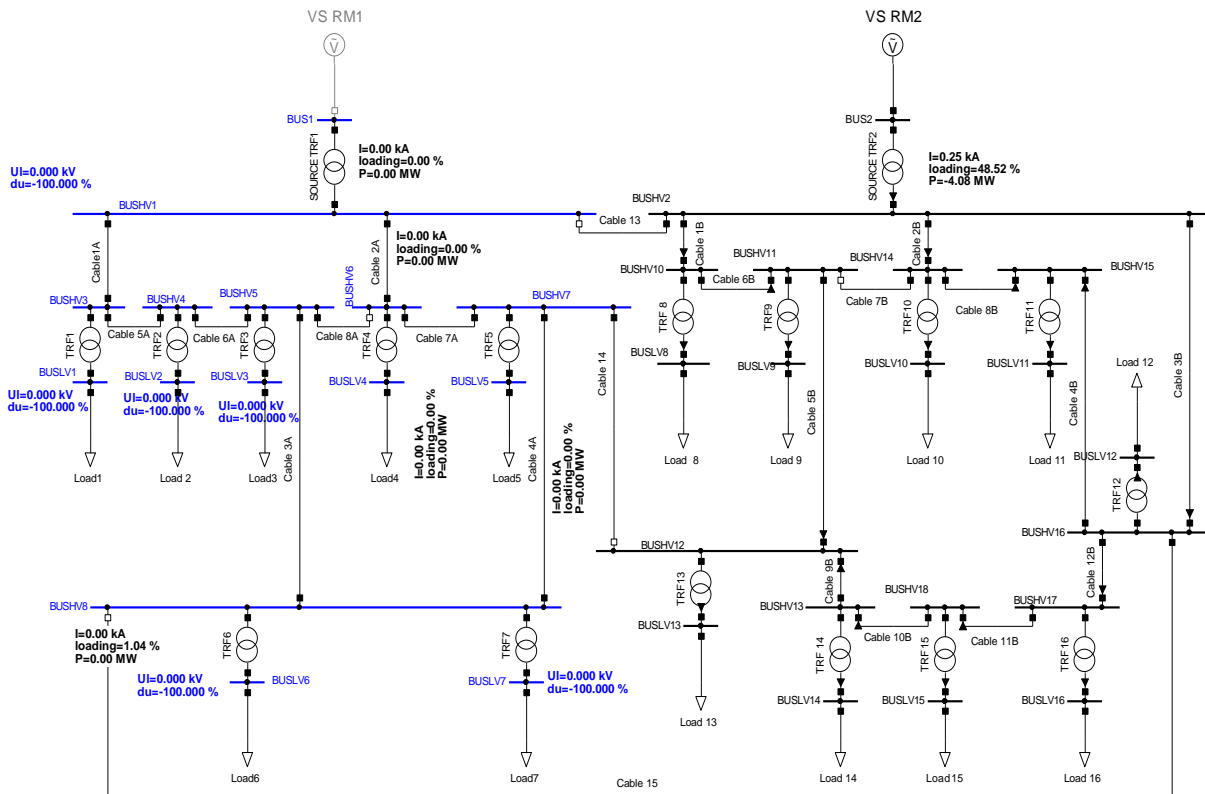


Figure 8.3: Case study 2 single line diagram after VS1 is removed

c) Step 4

Loss of VS RM1 means zero input power to RM1. Hence, in step 4 the interconnecting cables 13, 14 and 15 between RM1 and RM2 are considered to transfer power from RM2 to RM1.

Using empirical investigations, it is found for this contingency case that the optimum solution was to:

- Close the N/O switch of Cable 13 at station BUSHV1
- Add 1.2 Mvar capacitor at station BUSHV5

The load flow study with the suggested changes was conducted. The results obtained are shown in Figure 8.4.

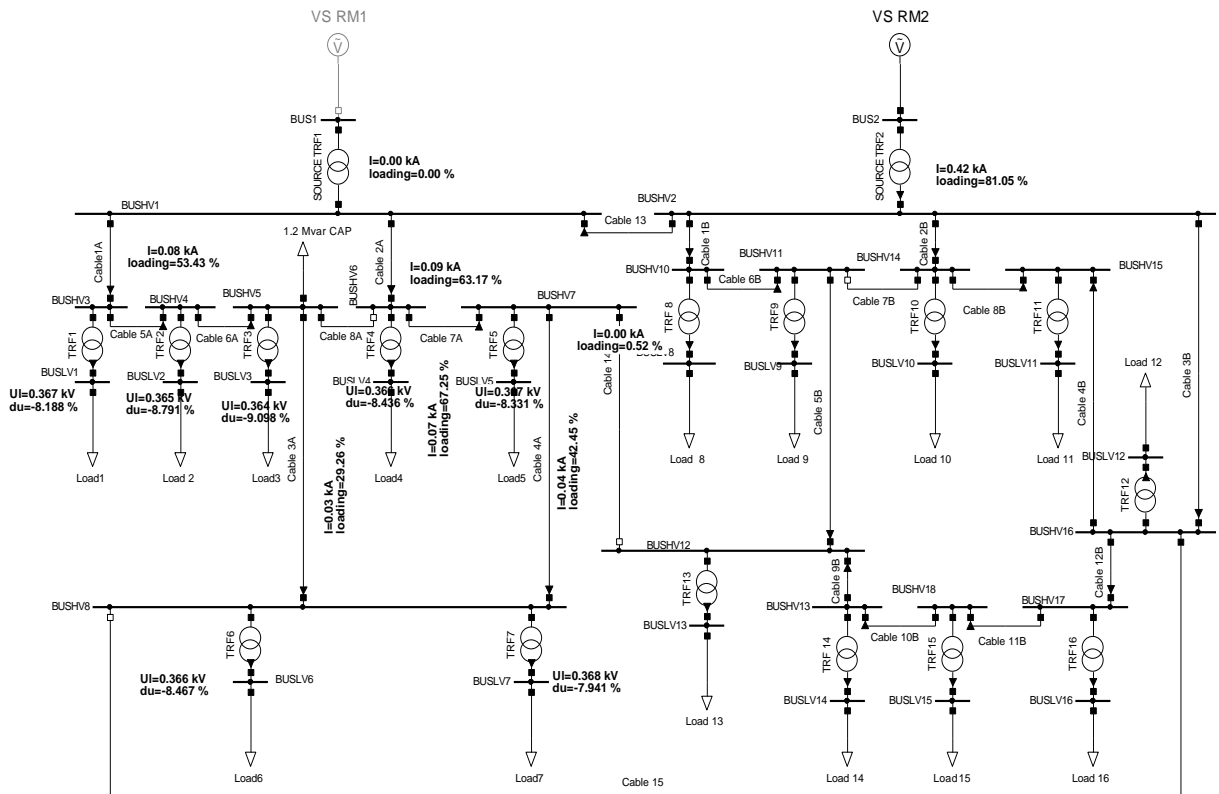


Figure 8.4: Case study 2 optimal configuration

The results in Figure 8.4 are summarized in Tables 8.8 and 8.9.

Table 8.8: RM1 load bus voltage levels for the optimal configuration

Load Bus	Voltage magnitude(kv)	%Deviation
LV1	0.367	8.21%
LV2	0.365	8.81%
LV3	0.364	9.12%
LV4	0.366	8.46%
LV5	0.367	8.35%
LV6	0.366	8.49%
LV7	0.368	7.96%

The results presented in Table 8.8 show that all the voltage levels for the load buses are within the 10 % limit.

Table 8.9: RM1 cable loadings for the optimal configuration

Cable	Current magnitude (kA)	% Loading
Cable 1A	0.080	53.11%
Cable 2A	0.094	62.78%
Cable 3A	0.029	28.76%
Cable 4A	0.042	42.37%
Cable 5A	0.060	60.10%
Cable 6A	0.035	34.94%
Cable 7A	0.067	67.23%
Cable 8A	0.000	0.00%

Table 8.9 shows that all the U/G cables are within their maximum carrying capacity.

- Overall power loss for RM1

The overall power losses obtained are:

$$\begin{aligned}
 P_{\text{loss (overall)}} &= \sum P_{\text{loss (Cables)}} + \sum P_{\text{loss (TRFR)}} \\
 &= 86.0 \text{ kW}
 \end{aligned}$$

- Overall efficiency for RM1

The total input power supplied to RM1 from VS RM2 via cable 13 is $P_{\text{in (Cable 13)}} = 2.952 \text{ MW}$, and $\sum P_{\text{out (RM 1)}}$ is 2.866 MW.

Thus, the total input power to RM1 is:

$$\sum P_{\text{in (RM1)}} = P_{\text{in (cable13)}} = 2.952 \text{ MW}$$

Hence the overall efficiency of RM1 is:

$$\eta_{\text{overall}} = \frac{\sum P_{\text{out (RM1)}}}{\sum P_{\text{in (RM1)}}} \times 100\% = \frac{2.866}{2.952} \times 100\% = 97.10\%$$

- Capacitor switching transients

In this case study, one capacitor was switched into the network to obtain an optimum configuration.

- 1.2 Mvar capacitor at station BUSHV5

In Table 8.10 the peak voltage levels at the load buses of RM1 due to capacitor switching are presented. The capacitor was switched into the network at 16 ms.

Table 8.10: Peak voltage levels of the RM1 load buses during capacitor switching

Location	Peak value (kV)
Load bus LV1	0.375
Load bus LV2	0.376
Load bus LV3	0.424
Load bus LV4	0.372
Load bus LV5	0.377
Load bus LV6	0.407

The bus load peak voltage levels presented in Table 8.10 were obtained on the blue-phase.

8.3 Case study 3

Case study 3 was conducted to determine whether the efficiency plan developed can be used in the case where an interconnected network has experienced two major outages.

This case study considered the outage of VS RM1 and an outage of Cable 3B on RM2 simultaneously. The steady-state results for both networks are considered.

This case study will follow the steps of the efficiency plan in Figure 7.2 and see if an optimal configuration can be reached.

a) Steps 1 and 2

The normal operation steady-state results for RM1 and RM2 are depicted in case study 1 (step 2) and Appendix C, respectively.

b) Step 3.

Figure 8.5 shows the load flow steady-state results obtained after VS RM1 and cable 3B were removed from service. Since $\sum P_{in(RM\ 1)} = 0$, no results were recorded for RM1.

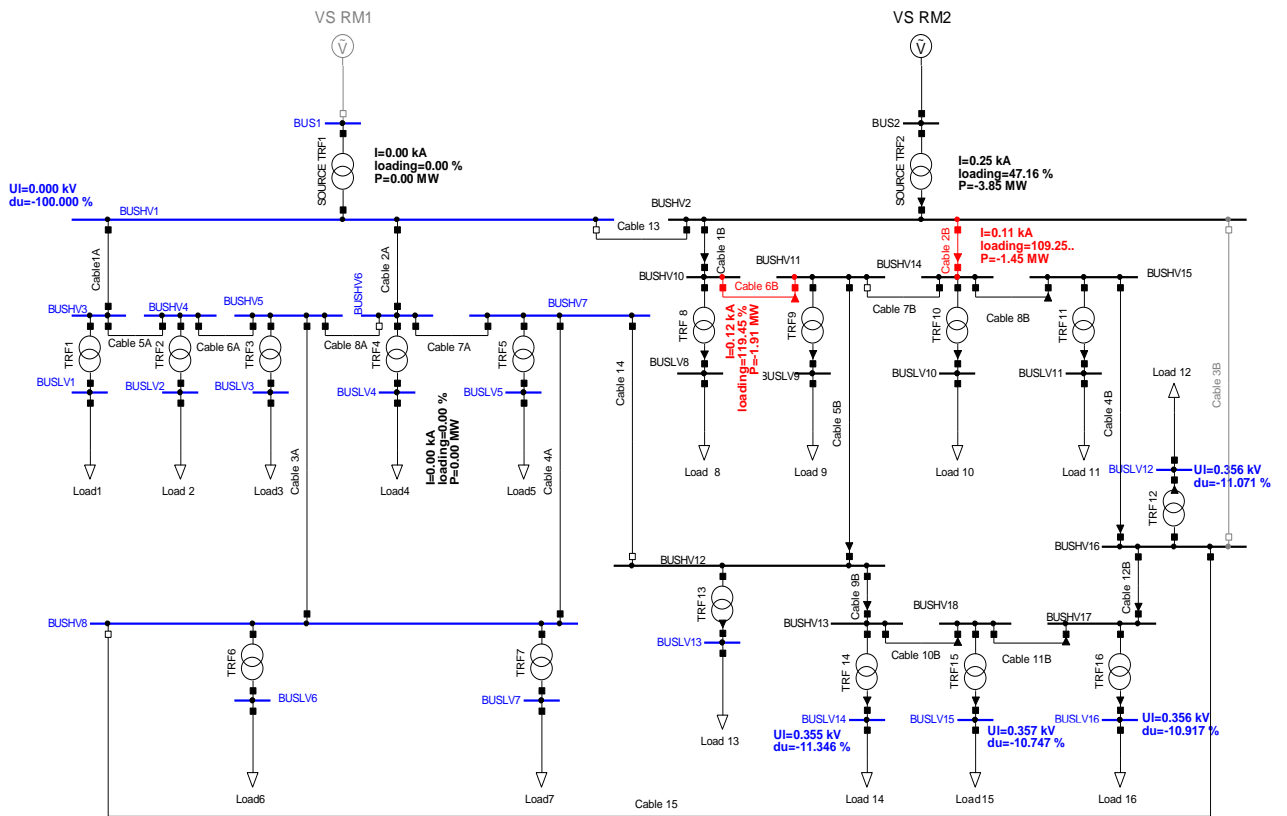


Figure 8.5: Case study 3 Single line diagram after the removal of VS RM1 and cable 3B

The steady-state results depicted in Figure 8.5 are summarised in Tables 8.11 and 8.12.

Table 8.11: RM2 Load bus voltage levels due to removal of Cable 3B

Load Bus	Voltage magnitude(kV)	%Deviation
LV8	0.354	11.50%
LV9	0.364	9.000%
LV10	0.367	8.250%
LV11	0.363	9.250%
LV12	0.355	11.25%
LV13	0.357	10.75%
LV14	0.356	11.00%
LV15	0.356	11.00%
LV16	0.372	7.000%

Table 8.11 shows that the voltage level of the load buses LV 8, LV12, LV13, LV14 and LV15 exceed 10 % limit, with LV 8 having deviated the most by 1.50%.

Table 8.12: RM2 Cable loadings due to the removal of Cable 3B

Cable	Current magnitude(kA)	% Loading
Cable 1B	0.142	94.67%
Cable 2B	0.109	109.00%
Cable 3B	0.000	0.000%
Cable 4B	0.048	48.00%
Cable 5B	0.089	89.00%
Cable 6B	0.120	120.00%
Cable 7B	0.000	0.000%
Cable 8B	0.079	79.00%
Cable 9B	0.058	58.00%
Cable 10B	0.029	29.00%
Cable 11B	0.015	15.00%
Cable 12B	0.025	16.67%

It can be seen that only Cable 2B and 6B are overloaded by 109.00% and 120%, respectively.

- RM2 Overall power losses

The overall power losses obtained for RM2 are:

$$\begin{aligned}
 P_{\text{loss (overall)}} &= \sum P_{\text{loss (Cables)}} + \sum P_{\text{loss (TRFR)}} \\
 &= 183 \text{ kW}
 \end{aligned}$$

- RM 2 Overall efficiency

The new input power for RM2 is $\sum P_{\text{in(RM2)}} = 3.84 \text{ MW}$, and $\sum P_{\text{out(RM2)}}$ is 3.657 MW. Hence the overall efficiency is:

$$\eta_{\text{overall}} = \frac{\sum P_{\text{out (RM2)}}}{\sum P_{\text{in (RM2)}}} \times 100\% = \frac{3.657}{3.84} \times 100\% = 95.23\%$$

c) Step 4

There is no power supplied to RM1 and Tables 8.11 and 8.12 clearly show that there are some constraint violations. Therefore, the next step is to find the optimal configuration for this contingency case.

d) Step 5

The optimal configuration empirically found for this contingency case was:

- Close the N/O switch of Cable 13 at station BUSHV1
- Add 1.2 Mvar capacitor at station BUSHV5

- Close the N/O switch of Cable 14 at station BUSHV12
- Close the N/O switch of Cable 8A at station BUSHV6
- Add 1.5 Mvar capacitor at station BUSHV8

e) Step 6

Figure 8.6 shows the optimal configuration and the steady-state results obtained for this contingency case.

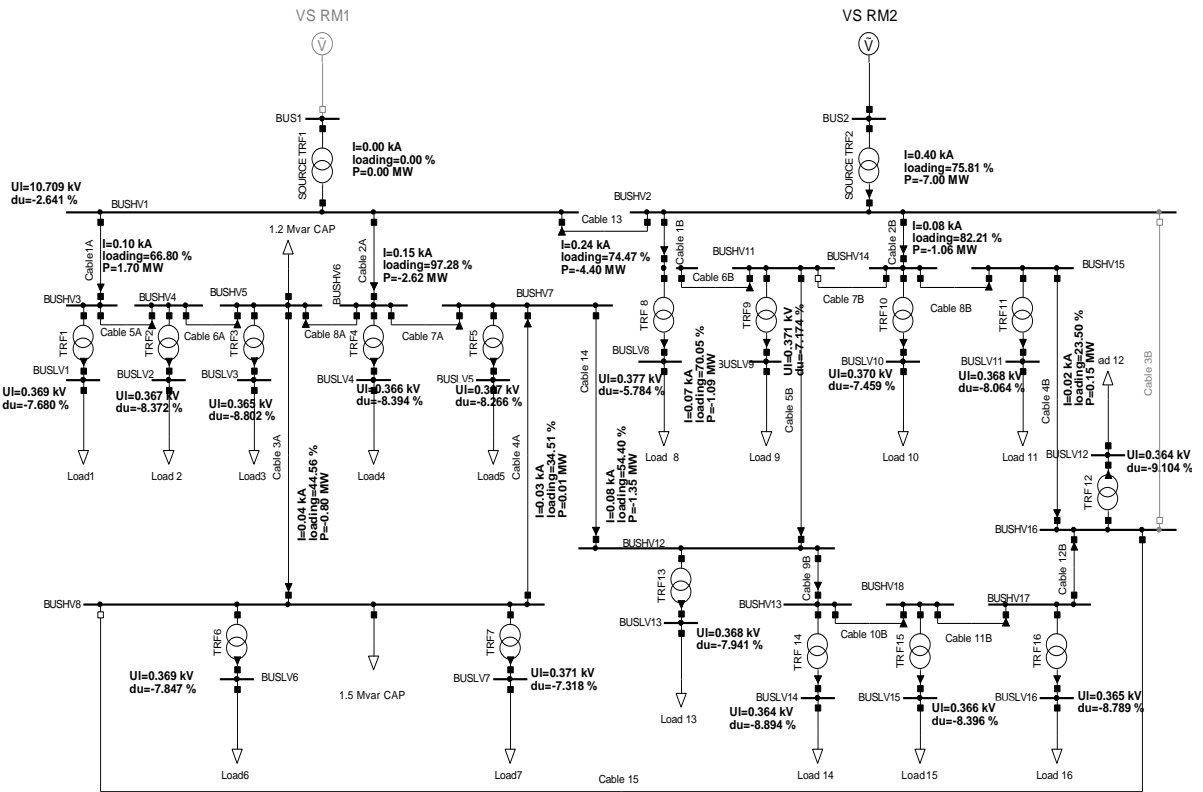


Figure 8.6: case study 3 optimal configuration

The results depicted in figure 8.6 are summarised in Tables 13, 14, 15 and 16.

i) RM1 steady-state results

- Load bus voltage level results for RM1

Table 8.13: RM1 Load bus voltage levels for the optimum configuration

Load Bus	Voltage magnitude(kV)	%Deviation
LV1	0.369	7.68%
LV2	0.367	8.37%
LV3	0.365	8.80%
LV4	0.366	8.39%
LV5	0.367	8.27%
LV6	0.369	7.84%
LV7	0.371	7.31%

Table 8.13 shows that all the load buses are within their permissible limits.

- Cable loadings for RM1

Table 8.14: RM1 Cable loadings for the optimum configuration

Cable	Current magnitude(kA)	% Loading
Cable 1A	0.100	66.45%
Cable 2A	0.146	97.32%
Cable 3A	0.045	44.70%
Cable 4A	0.035	35.41%
Cable 5A	0.080	80.00%
Cable 6A	0.054	53.82%
Cable 7A	0.098	98.18%
Cable 8A	0.098	98.18%

The results depicted in Table 8.14 show that all cables are within their current carrying capacities.

- RM1 overall power losses

The new power losses for RM1 are:

$$\begin{aligned}
 P_{\text{loss (overall)}} &= \sum P_{\text{loss (Cables)}} + \sum P_{\text{loss (TRFR)}} \\
 &= 145.0 \text{ kW}
 \end{aligned}$$

- RM1 overall efficiency

The new input power supplied from RM2 to RM1 is supplied through cable 13 and is $P_{\text{in (Cable 13)}} = 4.398 \text{ MW}$. However, Cable 14 transfers a portion of power back to RM2. The

Input power supplied back to RM2 through U/G cable 14 is $P_{\text{out(Cable 14)}}=1.364$ MW and $\sum P_{\text{out(RM 1)}}$ is 2.889 MW.

Thus total input power delivered to RM1 is:

$$\begin{aligned}\sum P_{\text{in(RM1)}} &= P_{\text{in(Cable 13)}} - P_{\text{out(Cable 14)}} \\ &= 4.398 - 1.364 \\ &= 3.034 \text{ MW}\end{aligned}$$

Hence the overall efficiency of RM1 is :

$$\eta_{\text{overall}} = \frac{\sum P_{\text{out(RM1)}}}{\sum P_{\text{in(RM1)}}} \times 100\% = \frac{2.889}{3.034} \times 100\% = 95.22\%$$

ii) Steady-state results for RM2

- Load bus voltage level results for RM2

Table 8.15: RM2 load bus voltage levels for the optimum configuration

Load Bus	Voltage magnitude(kV)	%Deviation
LV8	0.377	5.78%
LV9	0.371	7.17%
LV10	0.370	7.47%
LV11	0.368	8.08%
LV12	0.363	9.14%
LV13	0.368	7.94%
LV14	0.364	8.91%
LV15	0.366	8.42%
LV16	0.365	8.82%

All the load buses in Table 8.15 are operating within their operating limits.

- RM2 cable loadings

Table 8.16 shows the new cable loadings for the U/G cables in RM2

Table 8.16: RM2 Cable loadings for the optimum configuration

Cable	Current magnitude(kA)	% Loading
Cable 1B	0.092	61.50%
Cable 2B	0.081	81.23%
Cable 3B	0.000	0.00%
Cable 4B	0.022	22.37%
Cable 5B	0.038	38.04%
Cable 6B	0.070	69.74%
Cable 7B	0.000	0.00%
Cable 8B	0.052	51.60%
Cable 9B	0.088	87.94%
Cable 10B	0.057	56.74%
Cable 11B	0.037	36.78%
Cable 12B	0.016	10.63%

Table 8.16 shows that all cables are within their current carrying capacities.

- **RM2 overall power losses**

The overall power losses calculated were:

$$\begin{aligned}
 P_{\text{loss (overall)}} &= \sum P_{\text{loss (Cables)}} + \sum P_{\text{loss (TRFR)}} \\
 &= 100.57 \text{ kW}
 \end{aligned}$$

- **RM2 overall Efficiency**

The new total input power supplied to RM2 is:

$$\begin{aligned}
 \sum P_{\text{in (RM2)}} &= P_{\text{in (RM2)}} - P_{\text{in (Cable13)}} + P_{\text{in (Cable14)}} \\
 &= 6.996 - 4.431 + 1.35 \\
 &= 3.915 \text{ MW}
 \end{aligned}$$

Therefore the overall efficiency is:

$$\eta_{\text{overall}} = \frac{\sum P_{\text{out (RM2)}}}{\sum P_{\text{in (RM2)}}} \times 100\% = \frac{3.814}{3.915} \times 100\% = 97.44\%$$

8.4 Summary

The methodology developed in Figure 7.2 was applied to the three case studies presented. The results will be analysed and further discussed in the next chapter.

CHAPTER NINE

ANALYSIS OF RESULTS AND EVALUATION OF EFFICIENCY WORK PLAN

9. Introduction

In this chapter the effectiveness of the efficiency plan developed is evaluated in more detail. This is done by analysing the results obtained from the case studies carried out in the previous chapter. The efficiency plan can be considered to be effective if the following are achieved in the optimal configuration:

- Minimum power losses
- Minimum voltage deviation at the load buses
- No cable loading constraints are violated

9.1 Case study 1

9.1.1 Analysis of RM1 voltage profile

The load bus voltage levels obtained in Tables 8.1 (normal operations), Table 8.3 (when cable 1A is removed) and Table 8.5 (optimal configuration) are shown in Figure 9.1.

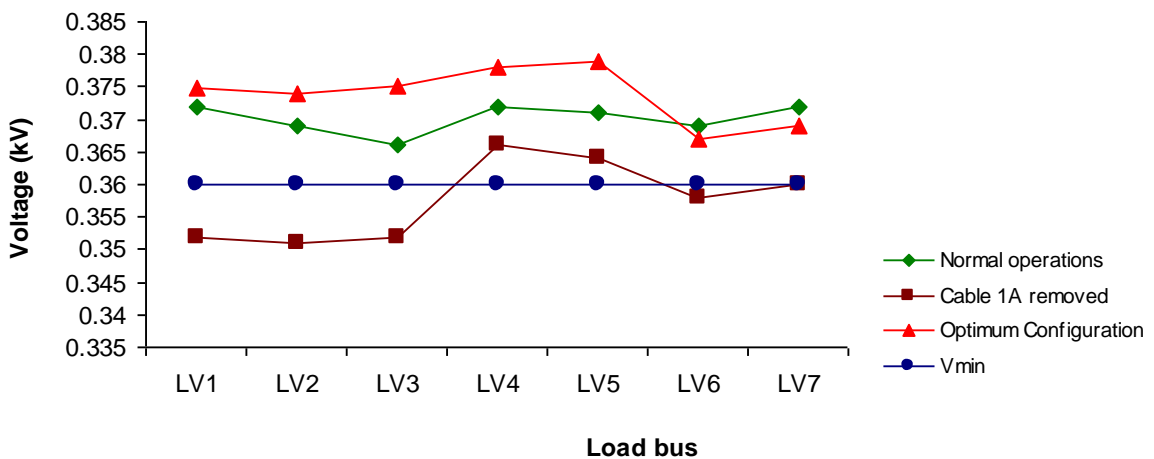


Figure 9.1: RM1 voltage profiles for case study 1

V_{\min} represents the lower allowable limit, which is 0.360kV. Figure 9.1 shows that for normal operations all the load bus voltage levels are within the standard limit. It can also be seen that at load buses LV1, LV2 and LV3 when cable 1A is removed the voltage levels are below the 0.360kV limit. As can be seen from the voltage profile of the optimum configuration in Figure 9.1, the shunt capacitors that were added at BUSHV 5 and BUSHV 8 and the reconfiguration of the network improved the voltage profile.

9.1.2 Analysis of RM1 cable loadings

Figure 9.2 shows the cable loadings recorded in Tables 8.2, 8.4, and 8.6.

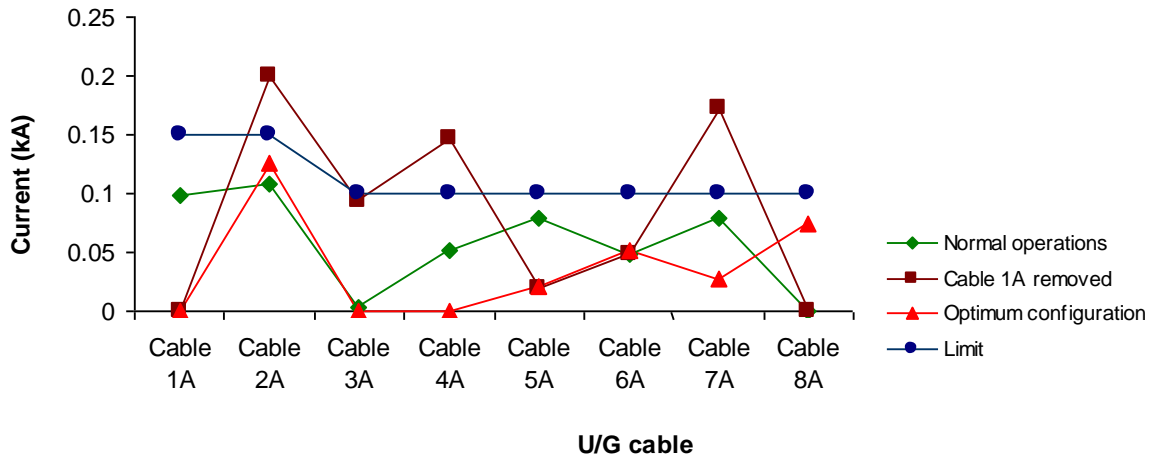


Figure 9.2: RM1 cable loadings for case study 1

It can be seen in Figure 9.2 that during normal operating conditions, RM1 operates in a very healthy state, with Cables 5A and 7A being loaded the highest, by 79%. Considering the contingency case, Cables 2A, 4A and 7A became heavily overloaded with Cable 7A affected the most with 172%.

The cable loadings obtained in the optimal configuration show that all cables are within their current carrying capacities with the highest loading being Cable 2A with 83.73%.

9.1.3 RM1 Volt-drop calculations

It is discussed in the literature review that South African SANS 10142-1 stipulates that the distribution voltage drop should be within 5%. Therefore it is important to calculate the volt-drops in the cables to see if they are within the specified limit. The highest volt-drop for each configuration is depicted in Table 9.1. The volt drops were obtained from the DlgSILENT software.

Table 9.1: Highest volt-drop for the different configurations of RM1

	Normal operations	Cable 1A removed	Optimal configuration
Volt-drop (%)	2.02% (Cable 2A)	3.74% (Cable 2A)	2.36% (Cable 2A)

The volt-drops depicted in Table 9.1 are all within the permissible limit.

9.1.4 Analysis of RM1 overall power loss

The power losses obtained in step 2 (normal operations), step 3 (cable 1A removed) and step 6 (optimal configuration) of case study 1 in chapter 8 are presented in Figure 9.3. The

figure visibly shows the distinction in the power losses obtained in the different configurations of the network.

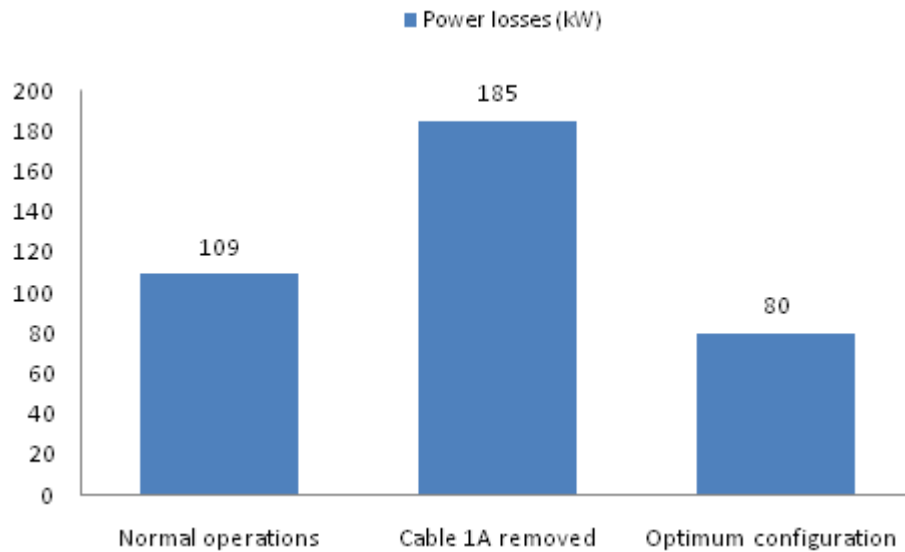


Figure 9.3: RM1 Power losses for case study 1

The power losses obtained from normal operations, are $P_{\text{loss (Normal)}} = 109.0$ kW. Due to the removal of Cable 1A at step 3, the overall power losses of RM1 are increased to $P_{\text{loss (Cable 1A removed)}} = 185.0$ kW. The losses are thus, increased by:

$$\begin{aligned} \% P_{\text{loss(increase)}} &= \frac{P_{\text{loss (Normal)}} - P_{\text{loss (Cable 1A removed)}}}{P_{\text{loss (Normal)}}} \times 100\% \\ &= \frac{109 - 185}{109} \times 100\% = 69.72\% \end{aligned}$$

The power losses were increased by 69.72%, which is a huge increment for a distribution network.

Power losses obtained in the optimal configuration, (step 6) are $P_{\text{loss (Optimum)}} = 80$ kW.

Comparing the optimum power losses to the power losses obtained after cable 1A was removed (185.0 kW), it was calculated that the overall power losses have reduced significantly by:

$$\begin{aligned} \% P_{\text{loss(decrease)}} &= \frac{P_{\text{loss (Cable 1A removed)}} - P_{\text{loss (Optimum)}}}{P_{\text{loss (Cable 1A removed)}}} \times 100\% \\ &= \frac{185 - 80}{185} \times 100\% = 56.76\% \end{aligned}$$

This shows that a huge reduction in real power loss has been achieved.

9.1.5 Analysis of RM1 overall efficiency

Figure 9.4 shows the efficiency of RM1 obtained for the different configurations of case study1.

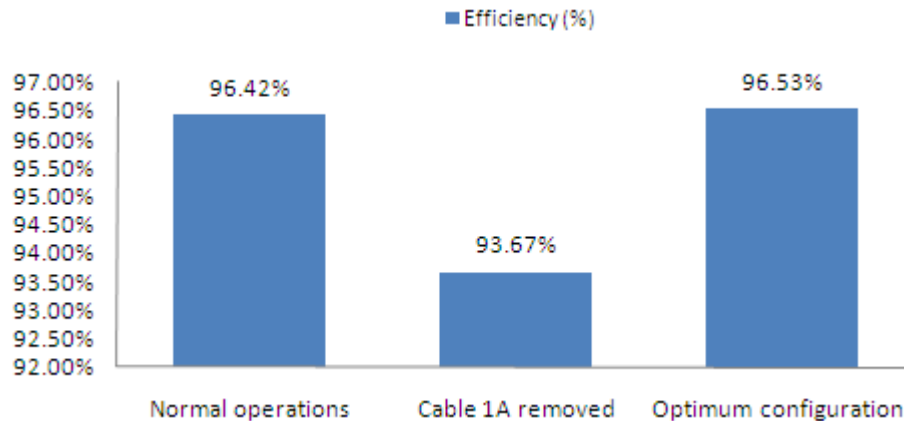


Figure 9.4: RM1 Overall efficiency for case study 1

Comparing the efficiency obtained after Cable 1A was removed to the efficiency obtained from the optimal configuration, it can be seen that the efficiency of the network has improved noticeably, exceeding the efficiency during normal operation by 0.11%.

9.1.6 Transient studies

The peak voltage transient results for different load buses were shown in Table 8.7. The peak magnitudes of these transients are not considered to be harmful. The highest voltage peak transient magnitude observed from the graphs is 0.468 kV at load bus LV1, as shown in Figure 9.5. The low transient magnitude may be caused by the power loss present in the network. According to literature, the power losses in the network dampen the transients that occur in the network (Kulas, 2009:1).

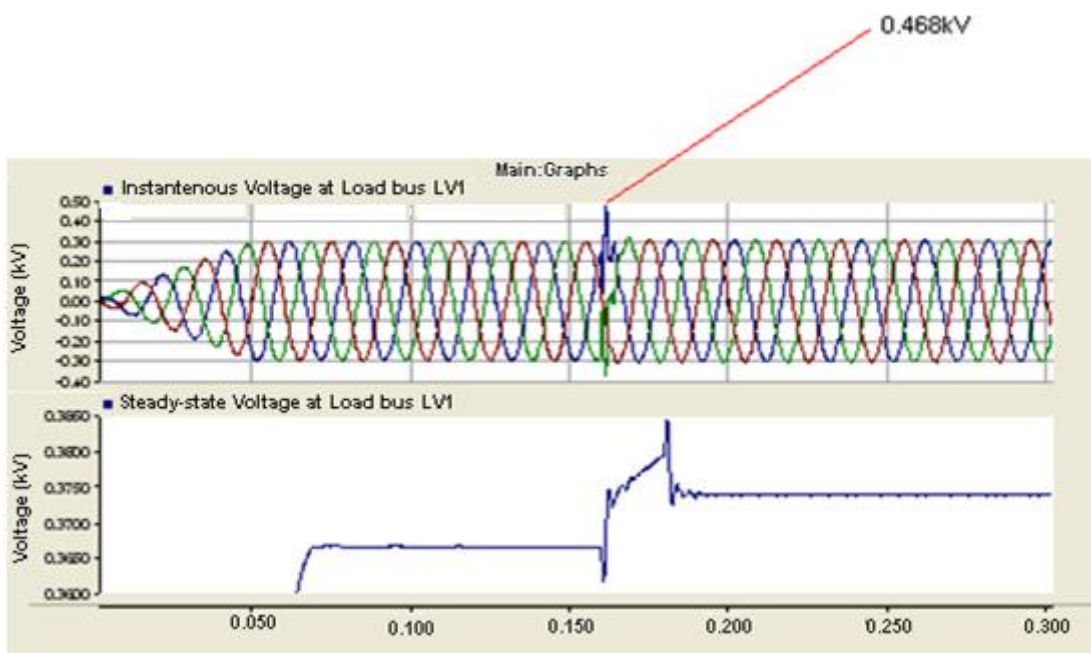


Figure 9.5: Voltage waveforms at bus LV1 during capacitor switching at station BUSHV5

Although the results in this case study were considered to be satisfactory, and no alterations were required, transients studies are considered important when conducting capacitor switching and should always be done.

9.2 Case study 2

When VS RM1 is removed from service, it resulted in zero power to RM1, hence no results were recorded when the outage was simulated. The normal operations results were compared to the optimum configuration results.

9.2.1 RM1 Voltage profile

Figure 9.6 shows the voltage profiles of the normal operations configuration and the optimum configuration.

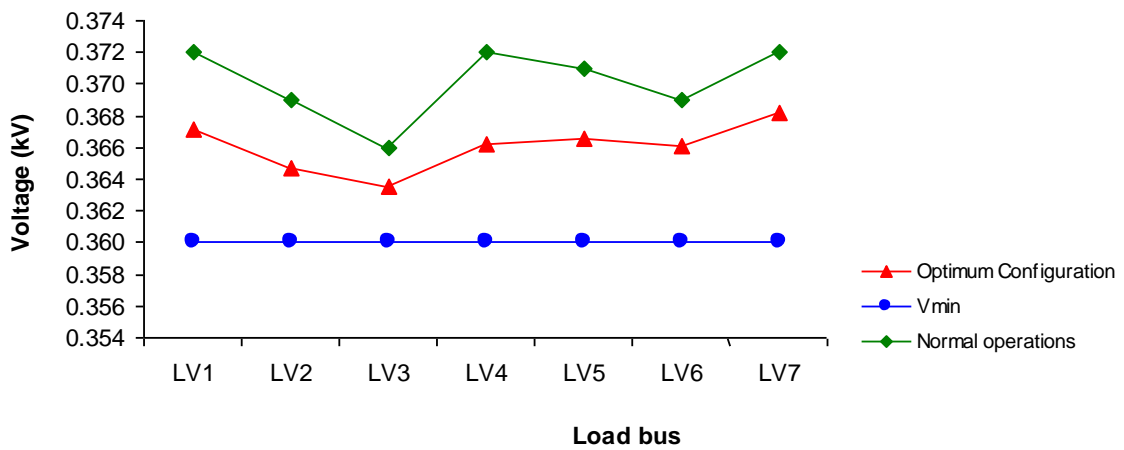


Figure 9.6: RM1 voltage profiles for case study 2

It is observed from Figure 9.6 that the minimum voltage obtained during the normal operations configuration is 0.366 kV and for optimum configuration is 0.364 kV. This is an acceptable voltage profile, especially considering that RM1 is entirely fed by RM2.

Since RM1 totally depends on RM2, the voltage profile of RM2 was also noted and shown in Figure D.1 (Appendix D). This was done to determine whether the additional load to RM2 caused any voltage violations in RM2. Figure D.1 shows that the voltage levels of RM2 are still within the permissible limit of 10%.

9.2.2 RM1 Cable loading

Figure 9.7 shows the current profile for the normal operations configuration and the optimum configuration of case study 2.

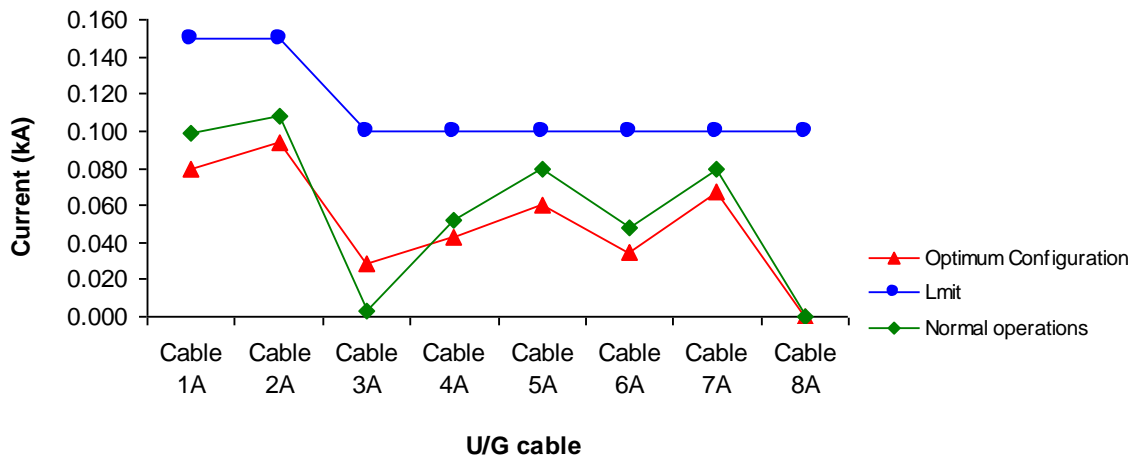


Figure 9.7: RM1 cable loadings for case study 2

The cable loading profile obtained from the optimum configuration load flow analysis is lower than that of the normal operations current loading. This means that the current flow in the cables was successfully reduced.

The cable loading for RM2 is shown in Figure D.2 (Appendix D). The figure shows that no overload conditions were encountered due to the load transfer.

9.2.3 RM1 volt-drop calculations

The highest volt-drop for each configuration is depicted in Table 9.2. The volt drops were obtained from the DIgSILENT software.

Table 9.2: Highest volt-drop for the different configurations of RM1

	Normal operations	Optimal configuration
Volt-drop(%)	2.02% (Cable 2A)	1.76% (Cable 2A)

The highest voltage drops obtained in all the networks are within the permissible limit of 5%.

The highest volt-drop for each configuration of RM2 is depicted in Table D.1 (Appendix D). The table shows that no volt-drop violation was also encountered due to the load transfer.

9.2.4 RM1 Power loss analysis

The power losses obtained from the optimum configuration load flow analysis are compared to the load flow analysis of the normal operation configuration.

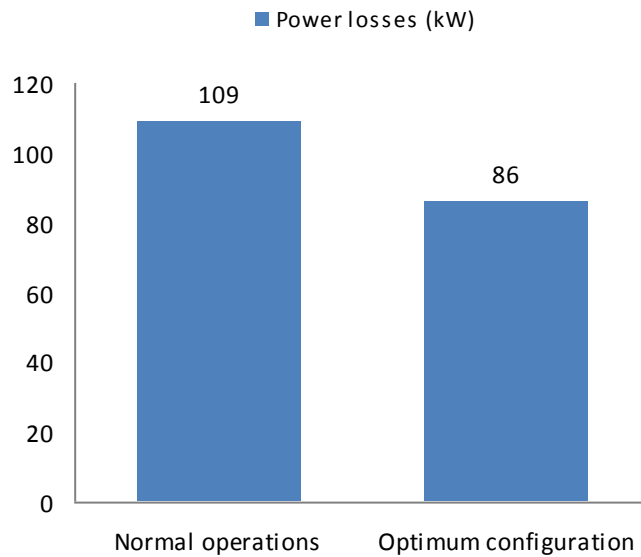


Figure 9.8: RM1 Power losses for case study 2

Figure 9.8 shows that the power losses for normal operation are 109 kW and for optimum configuration the power losses are 86 kW. It is calculated that the overall power losses have decreased by:

$$\begin{aligned} \%P_{\text{loss(decrease)}} &= \frac{P_{\text{loss (Normal)}} - P_{\text{loss (Optimum)}}}{P_{\text{loss (Normal)}}} \times 100\% \\ &= \frac{109 - 86}{109} \times 100\% = 21.10\% \end{aligned}$$

A percentage decrease of 21.10% is considered as a significant change in the power losses studies.

The load transferred to RM2 did not cause any power loss increase on the RM2 network as it would be expected; instead it has caused a decrease in the power losses of the network. The power losses of RM2 have decreased by 4.71%. The calculations are shown in Appendix D whilst the distinction between the power losses is depicted in Figure D.3 (Appendix D).

9.2.5 RM1 Overall Efficiency

Figure 9.9 depicts the efficiency obtained in the original configuration of RM1 as well as in the optimum configuration of RM1.

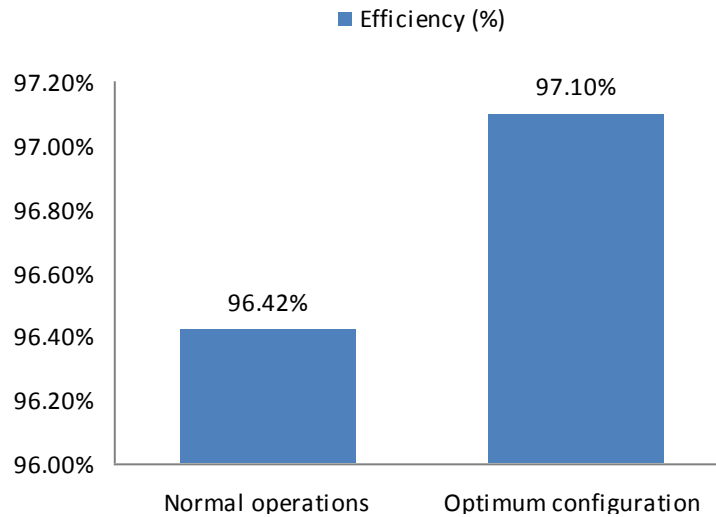


Figure 9.9: RM1 Overall efficiency for case study 2

Figure 9.9 shows that RM1 is operating at a high efficiency during the optimal configuration compared to the normal operation efficiency. The efficiency has increased by 0.71%.

After the RM1 load was transferred to RM2, the RM2 overall efficiency increased from 95.89% to 95.91%. This is shown in Figure D.4 (Appendix D).

9.2.6 Transient studies

The peak voltage transient values recorded in case study 2 were given in Table 8.10. It is discussed in section 7.3 that the peak voltage transients are considered safe if they are less than 0.8 kV. From Table 8.10, the highest peak voltage transient recorded was 0.424 kV at load bus LV 3. Figure 9.10 shows the graph recorded at LV3 during capacitor switching.

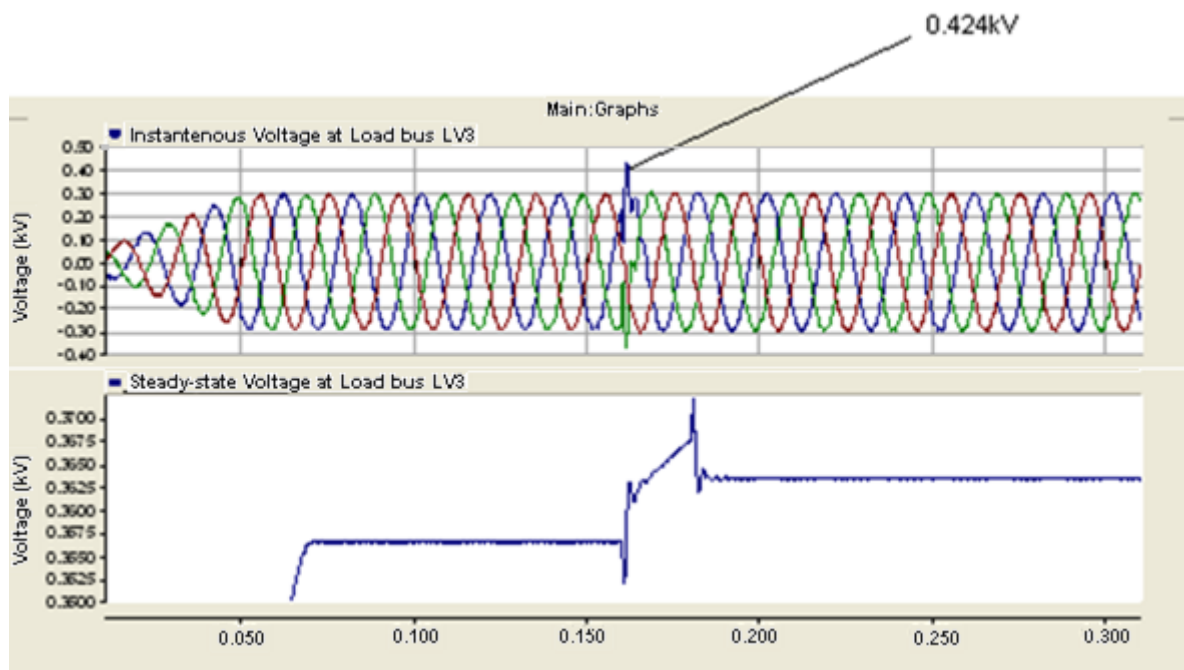


Figure 9.10: Voltage waveforms at bus LV3 during capacitor switching at station BUSHV5

9.3 Case study 3

It is discussed in case study 2 that when the substation infeed VS RM1 is removed from service, RM1 will have no power. The same applies for case study 3, therefore the only results obtained for RM1 in this case study were the normal operation results and the optimum configuration results. Since both RM1 and RM2 networks have experienced an outage, their results were all recorded and analysed.

9.3.1 RM1 Voltage profile

The voltage profiles for the different configurations obtained in case study 3 are shown in Figure 9.11.

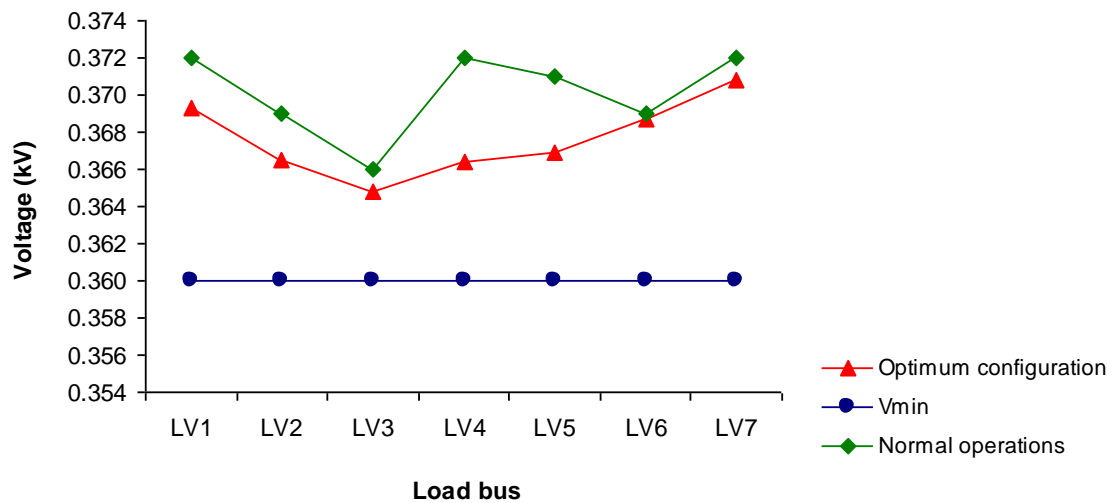


Figure 9.11: Voltage profiles of Case study 3 for RM1

Figure 9.11 shows that the voltage profile obtained from the optimum configuration is within acceptable limits.

9.3.2 RM2 Voltage profile

The voltage profiles of RM2 for the different configurations are shown in Figure 9.12.

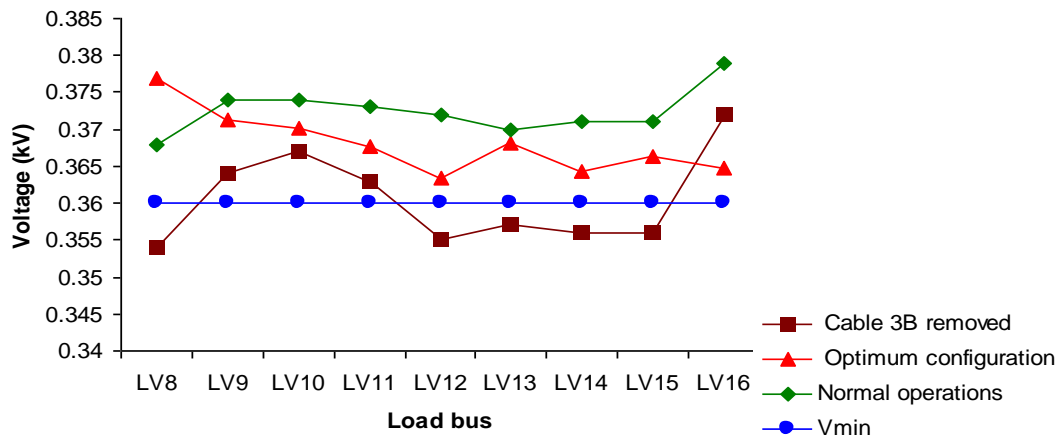


Figure 9.12: Voltage profiles of case study 3 for RM2

Figure 9.12 clearly shows that when Cable 3B was removed, load buses LV8, LV12, LV13, LV14 and LV15, experienced undervoltage. It can also be seen that for the optimum configuration, all the load bus voltage levels are within their 10% limit.

9.3.3 Cable loading for RM1

Figure 9.13 shows the cable loadings of RM1 for case study 3 configurations .

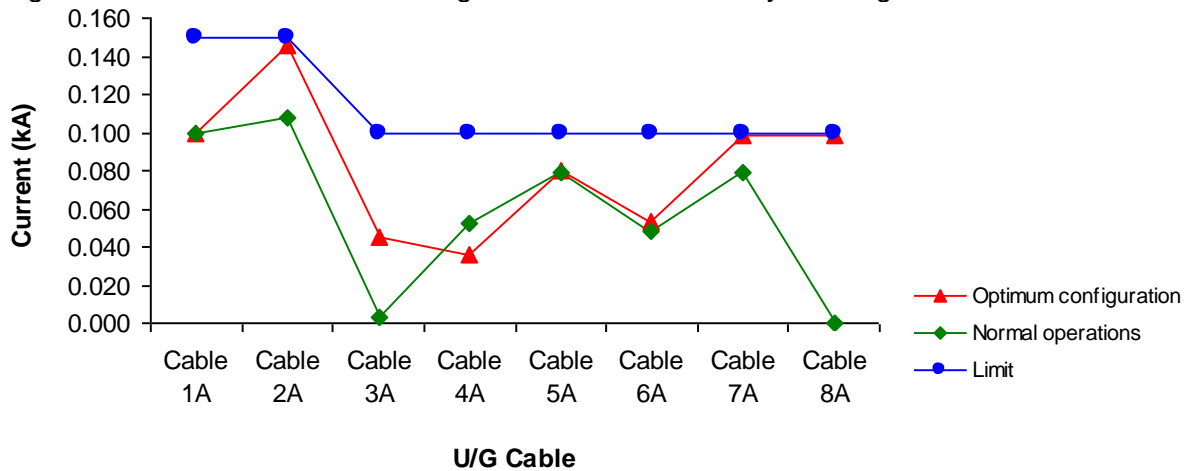


Figure 9.13: Cable loadings of case study 3 for RM1

All the U/G cables of RM1 are within their current carrying capacities.

9.3.4 Cable loading for RM2

Figure 9.14 displays the cable loadings obtained in RM2 for case study 3.

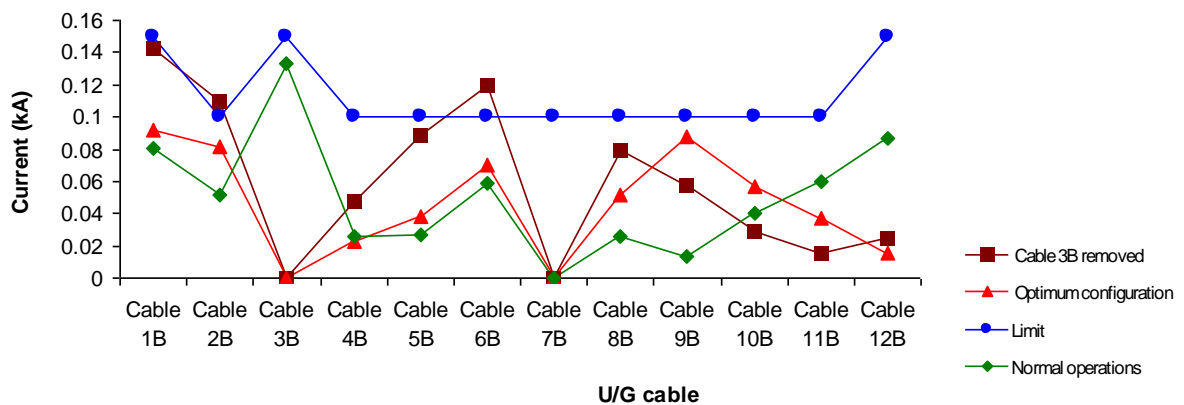


Figure 9.14: Cable loadings of case study 3 for RM2

Cable loadings obtained when Cable 3B was removed, show that Cables 2B and 6B became overloaded to 109% and 120%, respectively. However, no cable was overloaded in the optimum configuration.

9.3.5 RM1 and RM2 volt-drop calculations

The highest volt-drop for each configuration in both networks is depicted in Tables 9.3 and 9.4 respectively. The volt drops were obtained from the DigSILENT software.

a) RM1

Table 9.3: Highest volt-drop for the different configurations of RM1

	Normal operations	Optimal configuration
Volt-drop(%)	2.02% (Cable 2A)	2.59% (Cable 2A)

b) RM2

Table 9.4: Highest volt-drop for the different configurations of RM2

	Normal operations	Optimal configuration
Volt-drop(%)	3.18% (Cable 3B)	3.23% (Cable 2B)

It can be seen that the highest voltage drops obtained in all the configurations are within the permissible limit.

9.3.6 Analysis of Power loss of RM1

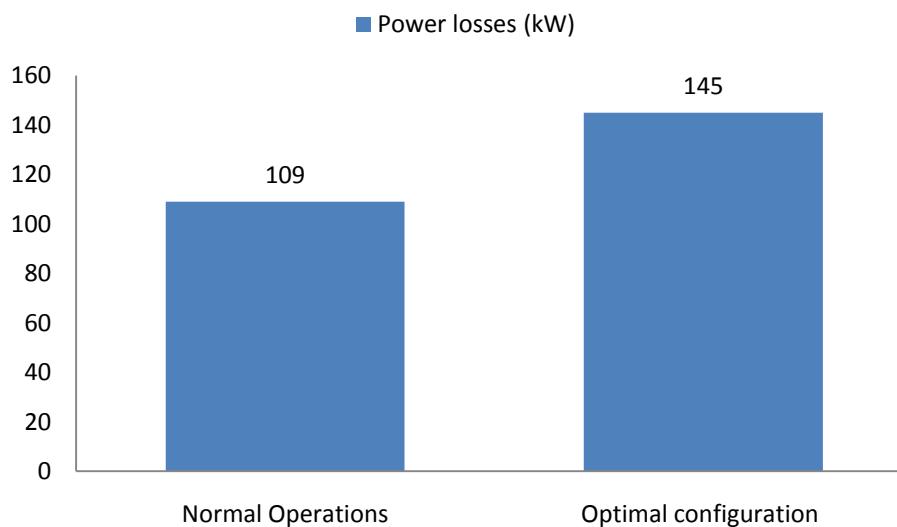


Figure 9.15: RM1 Power losses for case study 3

The overall power losses obtained from the optimum configuration are 145 kW. The power losses are very high compared to the original power losses of the network. However these losses can be considered to be acceptable since RM1 is wholly fed from RM2 which is also operating under contingency conditions.

9.3.7 Analysis of RM2 Power losses

Figure 9.16 shows a comparison of the power loss obtained in RM2 from different configurations.

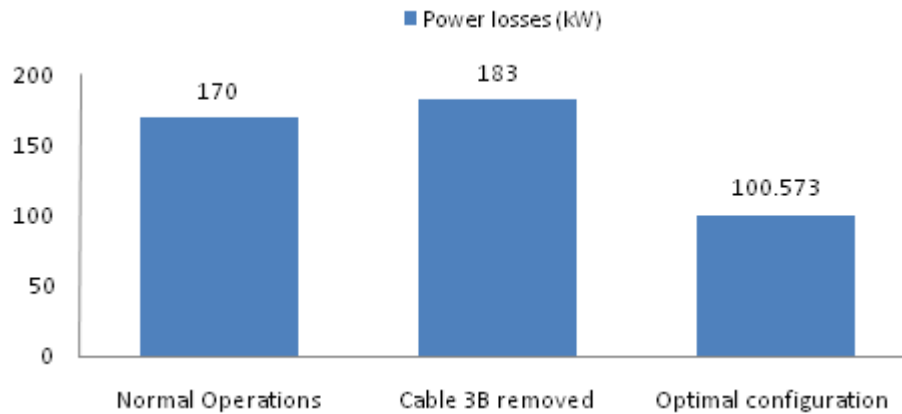


Figure 9.16: RM2 Power losses for case study 3

Figure 9.16 shows that due to the optimum configuration the power losses have decreased noticeably by:

$$\begin{aligned} \%P_{\text{loss(decrease)}} &= \frac{P_{\text{loss (Cable 3B removed)}} - P_{\text{loss (Optimum)}}}{P_{\text{loss (Cable 3B removed)}}} \times 100\% \\ &= \frac{183 - 100.573}{183} \times 100\% = 45.042\% \end{aligned}$$

Thus, we have been able to find a new ring operating structure that minimises the system power losses while satisfying operating constraints.

9.3.8 RM1 Overall efficiency

Figure 9.17 depicts the efficiency obtained in the original configuration of RM1 as well as in the optimum configuration of RM1.

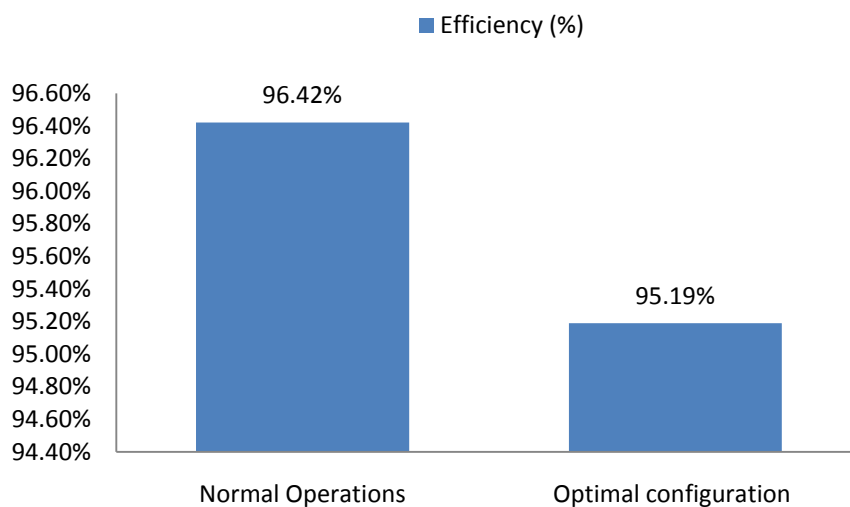


Figure 9.17: RM1 Overall efficiency for case study 3

The efficiency obtained in the optimal configuration of RM1 was 95.19% which was considered to be acceptable since both networks were operating under contingency conditions.

9.3.9 RM2 Overall efficiency

Figure 9.18 shows the change in efficiency when Cable 3B was removed and the optimum configuration load flow was conducted.

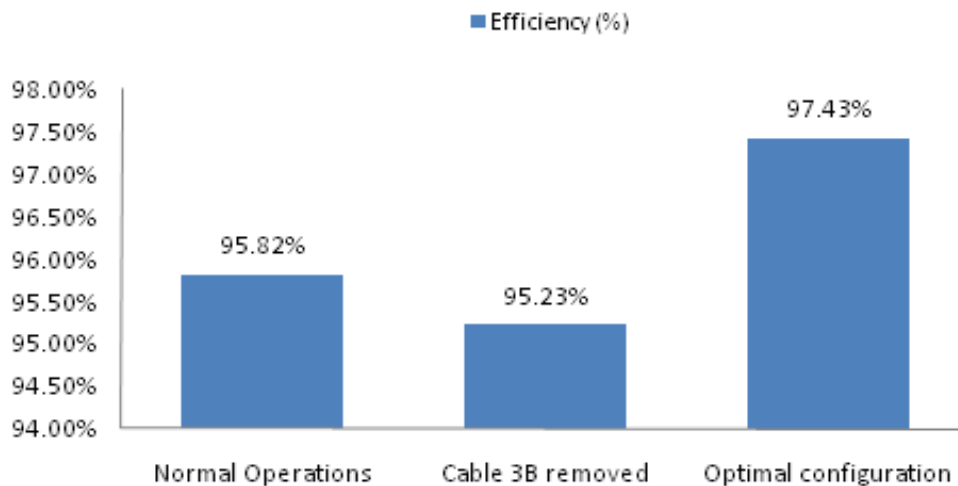


Figure 9.18: RM2 Overall efficiency for case study 3

The results show that the efficiency for RM2 has increased by 2.2% compared to the efficiency during the contingency and by 1.61% compared to the efficiency during normal operation.

9.4 Discussion of significant findings arising from the existing and proposed optimal configurations in this research

a) Power losses in the network

The power losses recorded in the optimal configurations obtained in the case studies represented an improvement in loss reduction.

b) Voltage profiles of the networks

All the load bus voltages in the proposed optimum configurations are within the acceptable limits of $\pm 10\%$ as shown in the figures.

c) Contingency Analysis

The contingency cases considered showed numerous voltage violations outside the statutory limits of $\pm 10\%$ compared to the proposed optimum configuration whose voltages were within acceptable limits.

d) Cable loading

Due to the contingency conditions applied on the networks, some cables were overloaded with the highest overload recorded at 172%. However no cable was overloaded in the proposed optimum configurations.

e) Ring systems

In the optimal solutions, more ring systems were provided to enhance better efficiency and reliability of the network, thus creating alternative routes in the cases of outages. The alternative routes were provided and the shunt capacitors were added for the load buses that experienced low voltages and high power losses in the network to help improve the voltage profiles and minimise the power losses.

9.5 Summary

The results for the case studies were evaluated and analysed. From the optimised networks obtained, it is observed that the loading on the individual cables and the load bus voltages are all within their operational limits.

CHAPTER TEN CONCLUSIONS, RECOMMENDATIONS AND FUTURE WORK

With the present electrical energy crises, saving power has become a major challenge worldwide. Therefore the urgency to reduce high power loss is well justified. This highlights the importance of this study. A better understanding of the effectiveness of the usage of power in networks is demonstrated. The research also shows how to utilise available resources.

Power losses in networks are caused by the physical properties of the components in the networks. These losses are inevitable, but can be reduced to an optimal level. The losses that occur in distribution networks are large enough to make efforts to reduce them worthwhile. Hence one should try to find ways of minimising these power losses under normal or abnormal conditions.

Ring main networks are considered to be efficient and believed to have low power losses but this is a general assumption since how they operate under contingency conditions, in terms of efficiency is found not to be well known. Thus, the loss of a major component in ring main network tends to increase the power losses causing power shortage to the network. However, networks can be improved more to work efficiently by using specific techniques to lower the power losses within them and in so doing decrease the input power drawn, easing any strain on power stations that may be running with a low reserve margin.

An empirical approach is used to develop an efficiency plan that can be used by network operators as a guideline to bring about improved network performance and ensure network quality of supply when the system is subjected to contingencies. It was found that by using opening/closing of switches (network reconfiguration) and capacitor addition, power loss reduction techniques in networks ensure that network constraints are maintained under contingency conditions.

The developed efficiency plan, in the form of a flow chart, which is a novel contribution to the studying of power loss reduction under contingency conditions has been shown to be effective and is recommended for use and/or application by industry. The plan can be easily adapted so that it can be applied to any large urban ring main network and even to multiple ring networks.

Three case studies were conducted to apply and evaluate the effectiveness of the efficiency plan; Case study 1 considered a contingency case (N-1) of Cable 1A; case study 2 considered a loss of substation infeed VS RM1 (N-1); and the third case study considered

two contingency cases (N-2) at once which were the loss of substation infeed VS RM1 and Loss of Cable 3B in RM2. The developed steps of the efficiency plan were applied to all the case studies. All studies including contingency cases were firstly modelled for simulation studies, the load bus voltage levels, cable current loadings, power losses and the overall efficiencies were obtained from each load flow simulation. The optimal configurations were obtained for each case study. All case studies were simulated using the DlgSILENT package. Additional studies were conducted for case studies 1 and 2 in which the voltage transients caused by capacitor switching were measured and evaluated using PSCAD, a time domain software package. Models for these studies were developed and serve also as a contribution to this field of research, the details of which can be found in Appendices A and B.

It was found that higher power loss reduction was achieved in all the case studies. Also found for transient studies was that for the cases studied, the peak voltage transients obtained were in the safe range of less than 2p.u. Thus, the addition of capacitors to a network as a loss reduction technique is an important finding as their use has proved to be very effective.

From the studies, several important observations can be concluded as follows:

1. The power loss of distribution systems can be effectively reduced by proper network reconfiguration and capacitor addition.
2. The efficiency plan developed has shown to be an effective tool for corrective switching, especially when considering loss reduction.

Work that still needs to be done in the future is to develop an efficiency plan for a large urban ring main network under contingency conditions but extend the investigation to networks that contain harmonic sources causing voltages and currents to become distorted as well as looking at efficiency under network resonance conditions and the role of harmonic filters under contingency states.

REFERENCES

- ABERDARE CABLES. 2008. Paper Insulated Cables Brochure. Johannesburg, South Africa
- Aoki, K., Satoh, T. Itoh, M., Kuwabara, H. & Kanezashi, M. 1988. Voltage drop constrained restoration of supply by switch operation in distribution systems. *IEEE Transactions on Power Delivery*, 3(3):1267-1274, July.
- Atkinson-Hope, G. 2005. *Power Systems 4*. Cape Town: Cape Peninsula University of Technology. [Course notes]
- Benedict, E., Collins, T., Gotham, D., Hoffman, S., Karipides, D., Pekarek, S., and Ramabhadran, R. 1992. Losses in electric power system. *ECE Technical Reports*. Paper 266, December 1992.
- Bakshi, U.A & Bakshi, M.V. 2007. *Electrical Power Transmission and Distribution*. 1st ed. Pune: Technical Publications.
- Baran, E.M. & Wu, F.F. 1989. Network reconfiguration in distribution systems for loss reduction and load balancing. *IEEE Transactions on Power Delivery*, 4(2): 1401-1407, April.
- Bayliss, C.R. 1999. *Transmission and Distribution Electrical Engineering*. 2nd ed. Burlington: Newness-Elsevier
- Bueno, E. A, Lyra, C. & Cavellucci, C. 2004. Distribution Network Reconfiguration for Loss Reduction with Variable Demands. *IEEE/PES Transmission & Distribution Conference and Exposition, Latin America*.
- Civanlar, S., Grainger, J.J., Yin, H. & Lee, S.S. 1989. Distribution feeder reconfiguration for loss reduction. *IEEE Transactions on Power Delivery*, 3(3):1217-1223, July.
- Coury, D.V., Dos- Santos., J. & Tavares, M.C. 1998. Transient analysis resulting from shunt capacitor switching in an actual electrical distribution system. Paper presented at the 8th International Conference on Harmonics and Quality of Power, Athens, 14-16 October 1998.
- Deshpande, M.V. 1966. *Elements of electrical power station design*, London.: Pitman
- Deuse, J., Karoui, K., Bihain, A. & Dubois, J. 2003. Comprehensive approach of power system contingency analysis. Paper presented at IEEE Bologna Power Tech Conference, Bologna, 23-26 June 2003
- DlgSILENT GmbH. 2001. *Basic user's Manual Version 12.1*. Gormaringen, Germany.
- Dugan, R.C., McGranaghan, M. F & Beaty, H.W. 1996. *Electrical Power Systems Quality*. New York: McGraw-Hill, Inc.
- El-Hawary, M. E. 1995. *Electric power systems: Design and Analysis*. Revised Edition. New York: IEEE Press.
- El-Hawary, M. E. 2000. *Electric power systems*: CRC Press LLC: Florida
- Fourie, J.W. 2004. *A strategy for the management of energy loss in a local electricity distribution network*, Pretoria, University of Pretoria [Unpublished Masters thesis]
- Fredericks, M. 2005. *Capacitor Control of Reactive Power, Voltage and Harmonic Distortion in a Network*, Cape Town, Cape Peninsula University of Technology [Unpublished BTech. Thesis]

- Glover, J.D. & Sarma, M.S. 2002. *Power Systems Analysis and Design*. 3rd ed. Pacific Grove: Brooks/Cole.
- Grainger, J.J. & Stevenson, W.D. 1994. *Power Systems Analysis*. New York.: McGraw-Hill, Inc.
- Haque, M.N. 1996. Load flow solution of distribution systems with voltage dependent load models. *Electrical Power System Research*, 36(3):151-156, March.
- Hawtrey P. & Atkinson-Hope, G. 1998. *Contingency Analysis of an 11kV Distribution Network*, Cape Town, Cape Peninsula University of Technology [Unpublished BTech Thesis]
- Hughes, E. 2005. *Hughes electrical and electronic technology*, 9th ed. London: Pearson Prentice Hall.
- IEEE Industry Applications Society.1993. IEEE Std 141–1993-IEEE Recommended Practice for Electric Power Distribution for Industrial Power Plants. *IEEE Industry Applications Society*. New York: 2 December
- Kalinowski, E.M., Steiner, M.T.A., Carneiri, C., Mussi, N.H. & Gullin, C. 2007. The problem of restoration of distribution networks: a heuristic method. *International journal of computer science and network security*, 3(7):104-111, March.
- Kulas, S.J. 2009. Capacitor Switching Techniques. Paper presented at the International Conference on Renewable Energies and Power Quality, Valencia, 15-17 April 2009.
- Kundur, P. 1994. *Power system stability and control*. New York :McGraw-Hill Inc.
- Lo, K.L. & Gers, J.M. 1994. Feeder reconfiguration for loss reduction in distribution systems. *Proceedings of the 1994 UPEC Conference*, University College Galway, September.
- Lupescu, M. & Leca, A. 2008. Improving the energy efficiency in power distribution networks through loss reduction. Paper presented at the WEC regional energy forum-FOREN, Neptun, 15-19 June.
- Manitoba HVDC Research Centre. 2005. *PSCAD Users Guide v.4.21*. Winnipeg Canada.
- Mohamed, A. R. & Lee, K. T. 2006. Energy for sustainable development in Malaysia: Energy policy and alternative energy. *Energy policy*, 34(15): 2388-2397, October.
- Mtshaulana, N. 2008. *Optimal capacitor placement using empirical optimisation*, Cape Town, Cape Peninsula University of Technology [Unpublished BTech. Thesis]
- Mthiyane, F.S. 2008. *Electrical energy efficiency awareness by poor communities in South Africa and its impact on their energy needs*, Cape Town, University of Stellenbosch [Unpublished Masters Thesis]
- Nasar, S.D. 1996. *Electric Energy systems*. New Jersey: Prentice-Hall Inc.
- Ng, H. 1999. *A novel and practical approach to distribution system performance enhancement using a fuzzy capacitor allocation method*, Ontario, University of Waterloo [Unpublished PhD thesis]
- Pansini, A.J. 1991. *Power Transmission and Distribution*. Lilburn: Fairmont Press Inc.
- Papaefthymiou, G., Verboomen, J., Schavemaker, P.H. and Van der Sluis, L. 2006. Impact

of Stochastic Generation in Power Systems Contingency Analysis. Paper presented at the 9th International Conference on Probabilistic Methods Applied to Power Systems, Stockholm, 11-15 June 2006.

PDH Online. 1999. Power Factor in Electrical Energy Management.
<http://www.pdhonline.org/courses/e144/e144content.pdf> [13 August 2010].

Prakash, P. 2007. BEE-001 Power Distribution Sector. New Delhi: Indira Gandhi National Open University School of Engineering and Technology.

Rajput, R.K. 2006. *Power system engineering*. New Delhi: Laxmi publications (Pty) Ltd.

Sabin, D.D., Grebe, T.E. & Sundaram, A. 1999. Assessing distribution system transient overvoltages due to capacitor switching. Paper presented at the International Conference on Power Systems Transients, Budapest, 20-24 June 1999.

Shepherd, J., Morton, A.H. & Spence, L.F. 1970. *Higher Electrical Engineering*. London: PITMAN.

Shirmohammadi, D. & Hong, H.W. 1989. Reconfiguration of electric distribution networks for resistive line loss reduction. *IEEE Transactions on Power Delivery*, 2(4):1492-1498, April.

South Africa. Technology Standardization Department (TSD). 2003. *NRS 048-2:2003: Electricity supply-Quality supply: Part 2: Voltage characteristics, compatibility levels, limits and assessment methods*. Pretoria: Standards South Africa.

South Africa. National Standard. 2006. *SANS 10142-1:2006. The wiring of premises Part 1: Low-voltage installations*. Pretoria. SABS Standards Division.

Su, C-T. & Lee, C-S. 2001. Feeder reconfiguration and capacitor setting for loss reduction of distribution systems. *Electric power systems research*, 58(2):97-102, December.

Thakur, T. & Jaswanti, T. 2006. Study and characterization of power distribution network reconfiguration. *Transmission & Distribution Conference and Exposition IEEE/PES, Latin America*, 15 -18 August 2006.

Von Meier, A. 2006. *Electric Power Systems: A Conceptual Introduction*, New York: IEEE Press-John Wiley & Sons Ltd.

Wadhwa, C.L. 1991. *Electrical Power Systems*. 2nd ed., New Delhi: Wiley Eastern.

Wakileh, G.J. 2001. *Power Systems Harmonics fundamental analysis and filter design*, New York: Springer

APPENDIX A

DigSILENT Modelling

A. Distribution network parameters

The loads, transformers and U/G cable ratings for both networks are shown in Tables A.1, A.2 and A.3, respectively.

A.1.1 Load modelling

The loads (Loads1-16) in RM1 and RM2 are considered to be general linear loads. They represent residential and commercial loads and are modelled as static loads. By default a general load has 100% static behaviour. Table A.1 shows the specifications of the loads.

Table A.1: Load Specifications

Element	Voltage (kV)	MVA	Power factor (lag)
Load 1	0.4	0.44	0.78
Load 2	0.4	0.63	0.75
Load 3	0.4	0.95	0.77
Load 4	0.4	0.6	0.82
Load 5	0.4	0.565	0.84
Load 6	0.4	0.563	0.81
Load 7	0.4	0.563	0.8.1
Load 8	0.4	0.47	0.86
Load 9	0.4	0.65	0.86
Load 10	0.4	0.65	0.79
Load 11	0.4	0.65	0.83
Load 12	0.4	0.55	0.86
Load 13	0.4	0.67	0.91
Load 14	0.4	0.67	0.83
Load 15	0.4	0.43	0.88
Load 16	0.4	0.55	0.86

Most of the conventional load flow methods, for distribution systems, use the constant-power load model which assumes that active and reactive powers are independent of voltage changes. In reality, constant power load models are highly questionable in distribution systems, as most nodes are not voltage controlled. It is suspected that the simple constant-impedance load model is better and can provide more accurate results than the constant-power load model (Haque, 1996:151). A constant impedance load model is a static load model where the power varies with the square of the voltage magnitude. Hence the loads in both RM1 and RM2 are modeled as constant impedance loads in both DigSILENT and PSCAD software packages.

General loads are modelled by the following two formulae:

$$P_r = P_o \cdot \left(\frac{V_r}{V_o} \right)^{kpu} \quad (A.1)$$

$$Q_r = Q_o \cdot \left(\frac{V_r}{V_o} \right)^{kqu} \quad (A.2)$$

where:

P_r = Rated real power

P_o = Operating real power

Q_r = Rated reactive power

Q_o = Operating reactive power

V_r = Rated voltage

V_o = Operating voltage

kpu = Voltage dependency index for P

kqu = Voltage dependency index for Q

Because the loads are modelled as constant impedance loads, the kpu and kqu must be equal to 2 as required in DIgSILENT modelling.

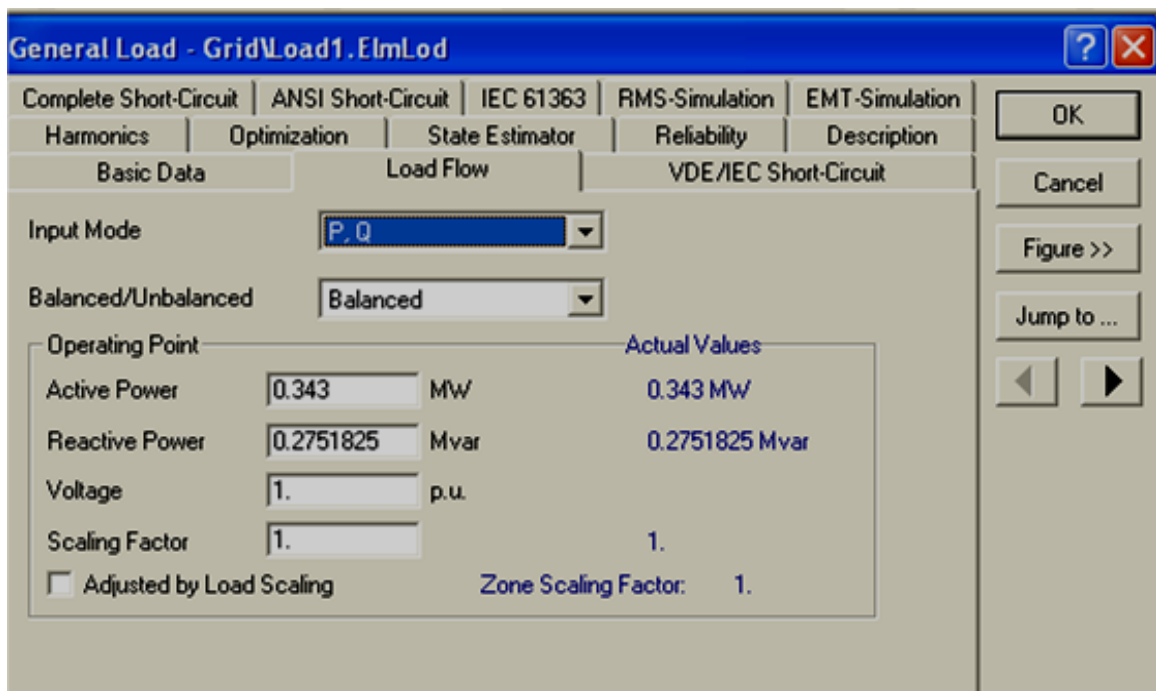


Figure A.1: Linear load modelling

A.1.2 Transformer modelling

The two winding distribution transformers were modelled as type bus net elements with the following input parameters:

- Voltage rating
- percentage impedance

Table A.2 shows the ratings of the distribution transformers

Table A.2: Transformers Specifications

Element	Voltage (kV)	MVA	Z%	X/R (%)
Source TRF RM1	66/11	7.0	8.0	9.0
Source TRF RM2	66/11	10	8.0	15.5
TRF 1	11/0.4	0.53	5.57	5.79
TRF 2	11/0.4	0.73	5.57	5.79
TRF 3	11/0.4	1.0	5.57	5.79
TRF 4	11/0.4	0.715	5.57	5.79
TRF 5	11/0.4	0.715	5.57	5.79
TRF 6	11/0.4	0.63	5.57	5.79
TRF 7	11/0.4	0.63	5.57	5.79
TRF 8	11/0.4	0.6	5.57	5.79
TRF 9	11/0.4	0.75	5.57	5.79
TRF 10	11/0.4	0.75	5.57	5.79
TRF 11	11/0.4	0.75	5.57	5.79
TRF 12	11/0.4	0.6	5.57	5.79
TRF 13	11/0.4	0.75	5.57	5.79
TRF 14	11/0.4	0.75	5.57	5.79
TRF 15	11/0.4	0.5	5.2	5.1
TRF 16	11/0.4	0.63	5.57	5.79

The screenshot displays a software window titled "2-Winding Transformer Type - Library\SOURCE TRFR 1. TypTr2". The interface includes several tabs at the top: "RMS-Simulation", "EMT-Simulation", "Harmonics", "Optimization", "State Estimator", "Reliability", and "Description". Below these are sub-tabs for "Basic Data", "Load Flow", "VDE/IEC Short-Circuit", "Complete Short-Circuit", "ANSI Short-Circuit", and "IEC 61363". The "Basic Data" tab is active, showing the following parameters:

- Name:** SOURCE TRFR 1
- Technology:** Three Phase Transformer
- Rated Power:** 7 MVA
- Nominal Frequency:** 50 Hz
- Rated Voltage:**
 - HV-Side: 66 kV
 - LV-Side: 11 kV
- Vector Group:**
 - HV-Side: D
 - LV-Side: Y
- Phase Shift:** 0 *30deg
- Positive Sequence Impedance:**
 - Short-Circuit Voltage uk: 8 %
 - Ratio X/R: 9.000001
- Zero Sequ. Impedance, Short-Circuit Voltage:**
 - Absolute uk0: 3 %
 - Resistive Part ukr0: 0 %

Figure A.2:Transformer modelling

A.1.3 U/G cable modelling

The U/G cables-conductor type, Paper-Insulated Lead-Covered (PILC) specifications are used. The 11kV PILC cables are widely used in 11kV distribution networks. All these cables are of different lengths. Table A.3 shows the cable specifications used.

Table A.3: U/G cable Specifications

Element	Length (km)	Size of Cable(mm) and Conductor Type	+/- Sequence		Capacitance nF/km	Current Carrying Capacity (kA)
			Resistance ohm/km	Inductive Reactance ohm/km		
Cable 1A	2.45	PILC 50	0.463	0.105	242	0.15
Cable 2A	2.50	PILC 50	0.463	0.105	242	0.15
Cable 3A	0.80	PILC 25	0.117	0.87	204	0.1
Cable 4A	0.94	PILC 25	0.117	0.87	204	0.1
Cable 5A	0.68	PILC 25	0.117	0.87	204	0.1
Cable 6A	1.00	PILC 25	0.117	0.87	204	0.1
Cable 7A	0.49	PILC 25	0.117	0.87	204	0.1
Cable 8A	0.50	PILC 25	0.117	0.87	204	0.1
Cable 1B	3.79	PILC 50	0.463	0.105	242	0.15
Cable 2B	3.60	PILC 25	0.117	0.87	204	0.1
Cable 3B	3.20	PILC50	0.463	0.105	242	0.15
Cable 4B	3.50	PILC 25	0.117	0.87	204	0.1
Cable 5B	3.45	PILC 25	0.117	0.87	204	0.1
Cable 6B	1.40	PILC 25	0.117	0.87	204	0.1
Cable 7B	2.98	PILC 25	0.117	0.87	204	0.1
Cable 8B	1.40	PILC 25	0.117	0.87	204	0.1
Cable 9B	0.62	PILC 25	0.117	0.87	204	0.1
Cable 10B	0.45	PILC 25	0.117	0.87	204	0.1
Cable 11B	0.85	PILC 25	0.117	0.87	204	0.1
Cable 12B	0.78	PILC 50	0.463	0.105	242	0.15
Cable 13	1.60	PILC185	0.120	0.087	347	0.32
Cable 14	1.50	PILC 50	0.463	0.105	242	0.15
Cable 15	3.00	PILC 50	0.463	0.105	242	0.15

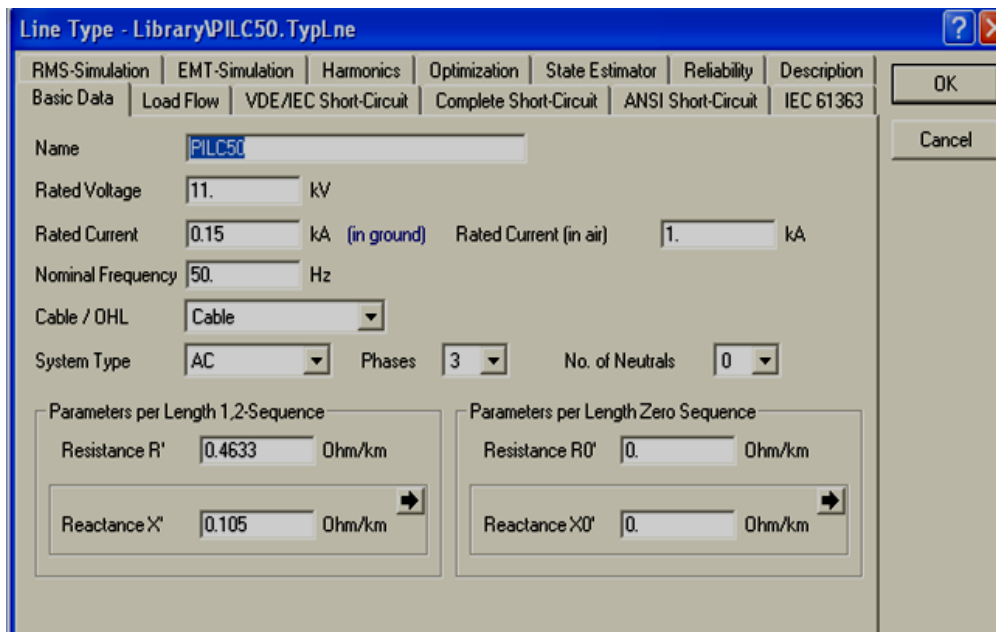


Figure A.3: Cable modelling

A.1.4 AC Voltage source modelling

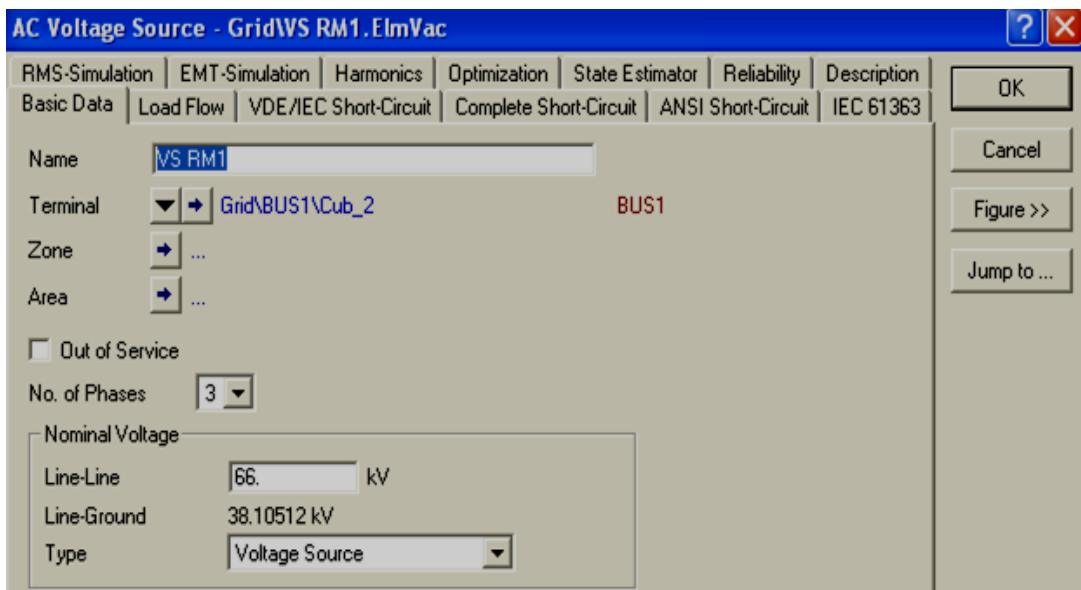


Figure A.4: Voltage source modelling

A.1.4 Busbar modelling

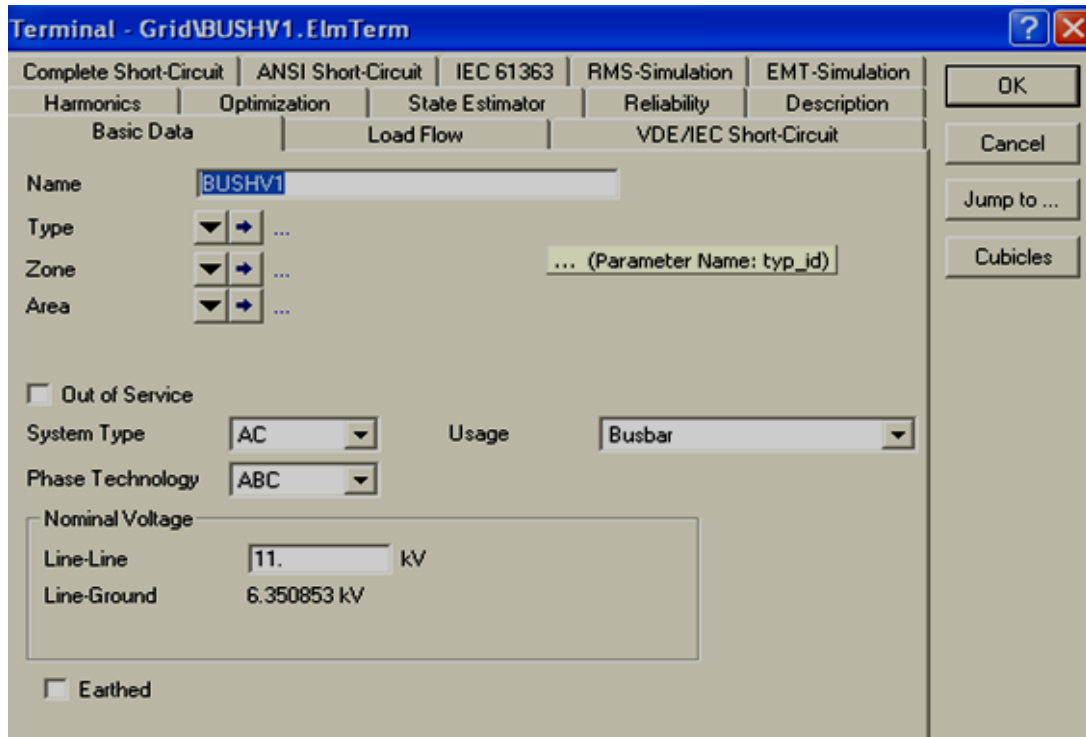


Figure A.5: Busbar modelling

A.1.4 Capacitor Modelling

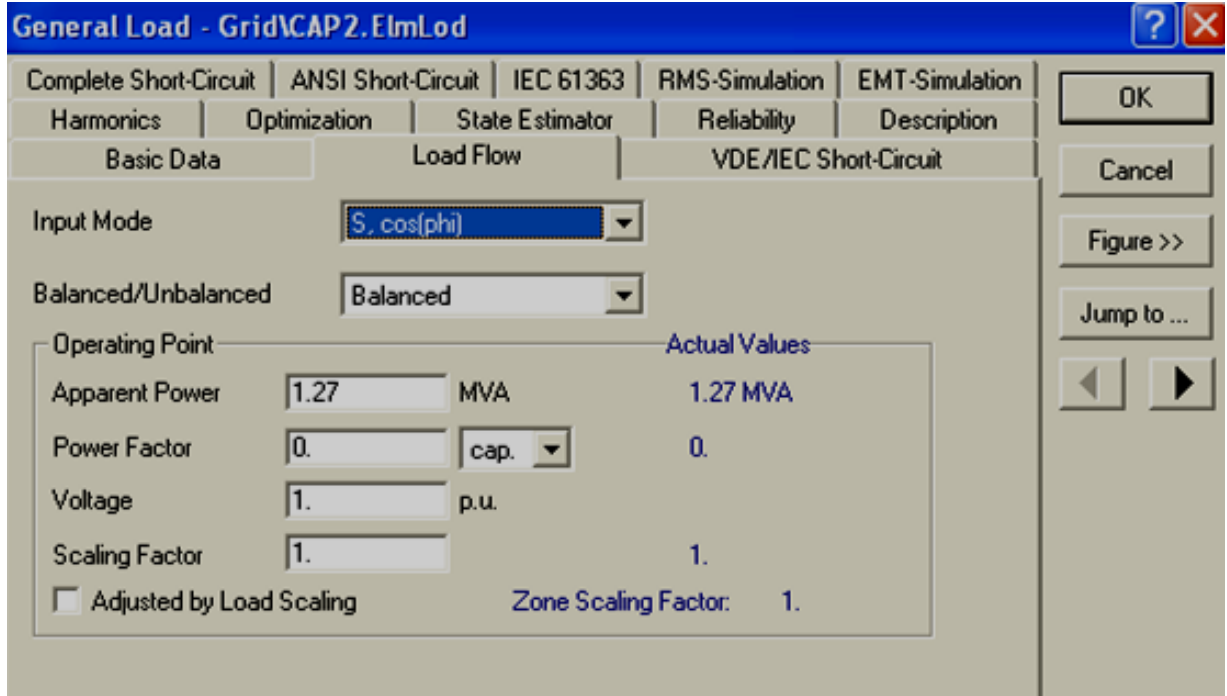
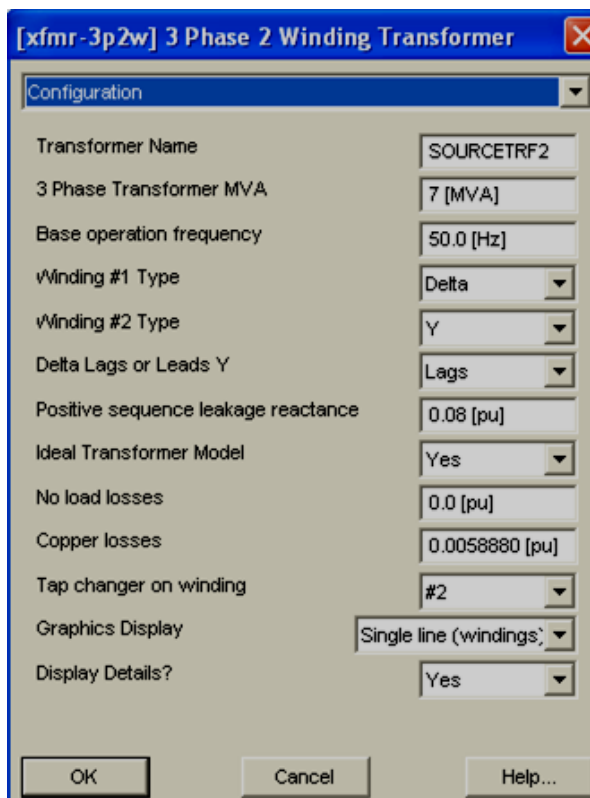


Figure A.6: Capacitor modelling

APPENDIX B PSCAD components modelling

B. PSCAD components modelling



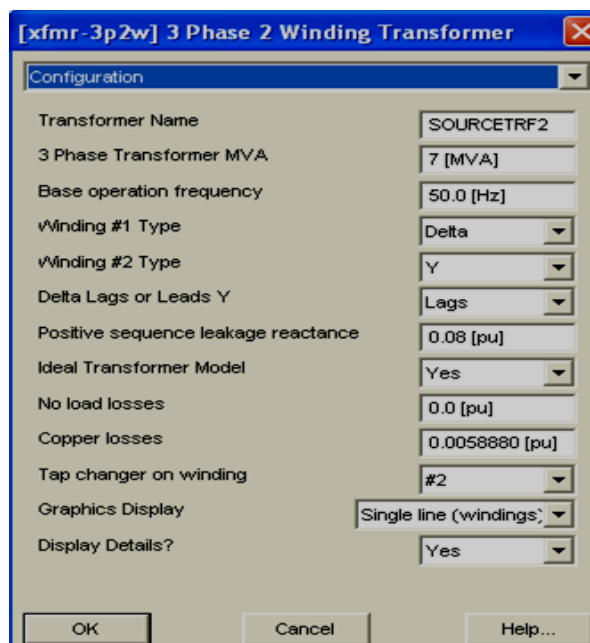
[xfmr-3p2w] 3 Phase 2 Winding Transformer

Configuration

Transformer Name	SOURCETRF2
3 Phase Transformer MVA	7 [MVA]
Base operation frequency	50.0 [Hz]
Winding #1 Type	Delta
Winding #2 Type	Y
Delta Lags or Leads Y	Lags
Positive sequence leakage reactance	0.08 [pu]
Ideal Transformer Model	Yes
No load losses	0.0 [pu]
Copper losses	0.0058880 [pu]
Tap changer on winding	#2
Graphics Display	Single line (windings)
Display Details?	Yes

OK Cancel Help...

Figure B.1: Ideal voltage source



[xfmr-3p2w] 3 Phase 2 Winding Transformer

Configuration

Transformer Name	SOURCETRF2
3 Phase Transformer MVA	7 [MVA]
Base operation frequency	50.0 [Hz]
Winding #1 Type	Delta
Winding #2 Type	Y
Delta Lags or Leads Y	Lags
Positive sequence leakage reactance	0.08 [pu]
Ideal Transformer Model	Yes
No load losses	0.0 [pu]
Copper losses	0.0058880 [pu]
Tap changer on winding	#2
Graphics Display	Single line (windings)
Display Details?	Yes

OK Cancel Help...

Figure B.2: Transformer modelling

Parameter	Value	
I	Number (1-99999)	1
NAME	Name	BUS1
BASKV	Bus base voltage	11
IDE	Type Code	0
GL	Shunt conductance	0
BL	Shunt admittance to gnd	0
AREA	Area Number (1-100)	1
ZONE	Zone Number (1-999)	0
VM	Voltage magnitude	11
VA	Voltage angle	0
OWNER	Owner	1

Figure B.3: Busbar modelling

T-LINE NAME	Line1A
Enter Imped./Admit. Data in:	R,XI,Xc (Ohms)
Nominal PI or Coupled PI Model:	Nominal
Line Rated Frequency	50.0 [Hz]
Line Length	2450 [m]
Enter 0 Seq Data, or Estimate:	Enter
Graphics Display	Single line view

Figure B.4: Cable modelling

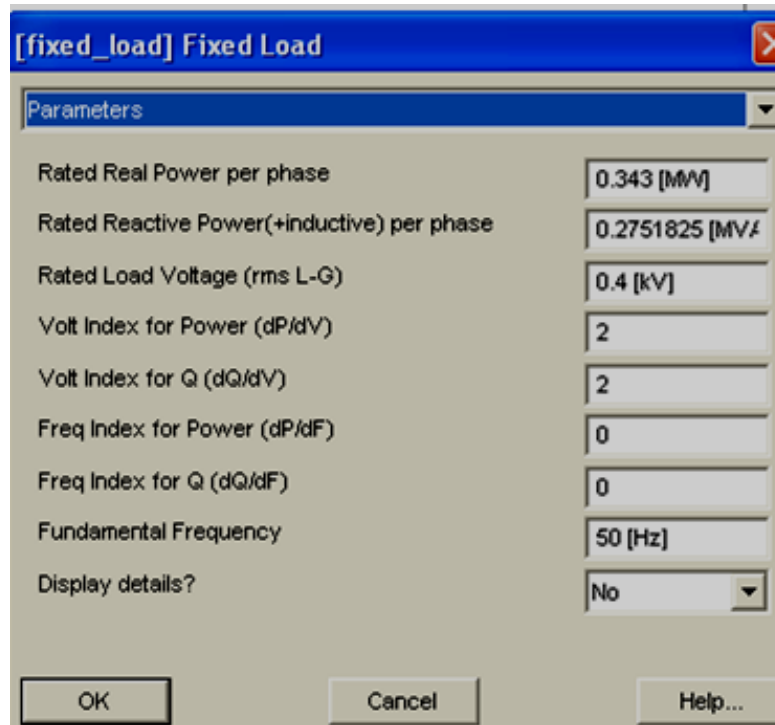


Figure B.5: Linear load modelling

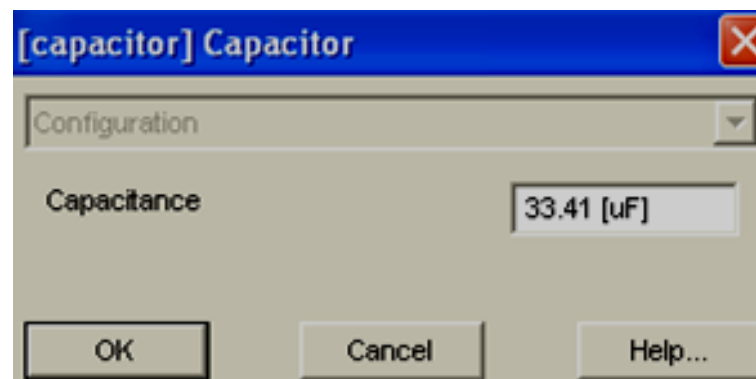


Figure B.6: Capacitor modelling

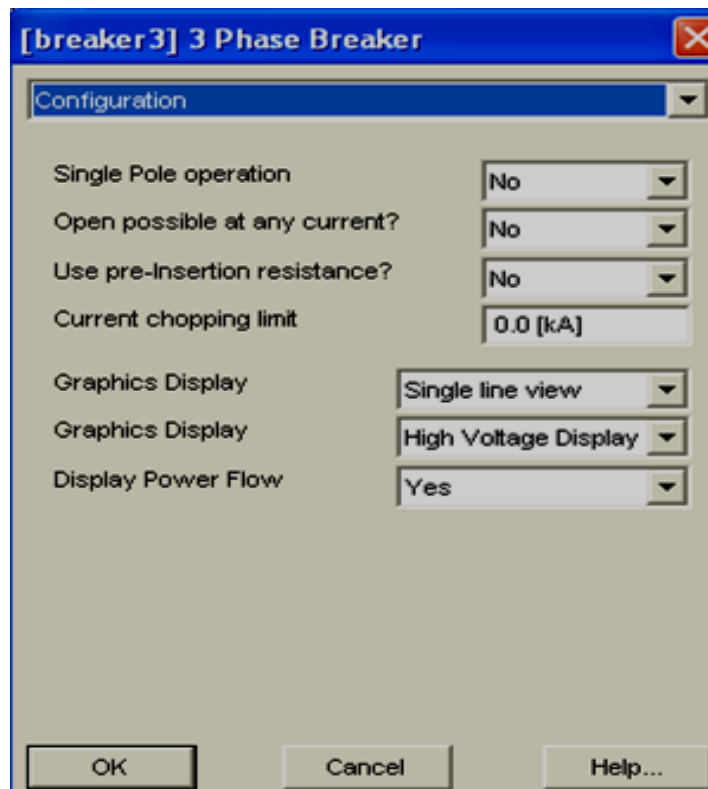


Figure B.7: Circuit breaker modelling

APPENDIX C

C. Case study 1

RM2 Normal operation results

Table C.1: Normal operating voltage profile for RM2

Load bus	Voltage (kV)	% Deviation
LV8	0.368	8.00%
LV9	0.374	6.50%
LV10	0.374	6.50%
LV11	0.373	6.75%
LV12	0.372	7.00%
LV13	0.37	7.50%
LV14	0.371	7.25%
LV15	0.371	7.25%
LV16	0.379	5.25%

Table C.1 shows that during the normal operations of the RM2, all the Load buses voltage levels are within the 10% limit as governed by the NRS 048-2.

Table C.2: Normal operating cable loadings for RM2

Cable	Current (kA)	% Loading
Cable 1B	0.081	54.00%
Cable 2B	0.052	34.67%
Cable 3B	0.133	88.67%
Cable 4B	0.026	26.00%
Cable 5B	0.027	27.00%
Cable 6B	0.059	59.00%
Cable 7B	0	0.00%
Cable 8B	0.026	26.00%
Cable 9B	0.013	13.00%
Cable 10B	0.04	40.00%
Cable 11B	0.06	60.00%
Cable 12B	0.087	58.00%

Table C.2 depicts that during normal operations of RM2, all the cables operate within their maximum current carrying capacities.

Power loss and overall efficiency

- **RM2 overall power losses**

- The overall power losses obtained from the original configuration are:

$$P_{\text{loss (overall)}} = \sum P_{\text{loss (Cables)}} + \sum P_{\text{loss (TRFR)}} \\ = 170 \text{ kW}$$

- **RM2 Overall efficiency**

The input power supplied by RM2 VS2 is $\sum P_{\text{in(RM2)}} = 4.071 \text{ MW}$, and $\sum P_{\text{out(RM2)}}$ is 3.901 MW. Hence the overall efficiency is:

$$\eta_{\text{overall}} = \frac{\sum P_{\text{out(RM2)}}}{\sum P_{\text{in(RM2)}}} \times 100\% = \frac{3.901}{4.071} \times 100\% = 95.82\%$$

C.2 RM2 steady-state results after Load 6 and Load 7 were transferred to RM2

Table C.3: RM2 Load bus voltage levels

Load bus	Voltage (kV)	%Deviation
LV8	0.380	4.92%
LV9	0.375	6.32%
LV10	0.376	6.05%
LV11	0.374	6.39%
LV12	0.373	6.77%
LV13	0.372	7.12%
LV14	0.369	7.75%
LV15	0.372	7.01%
LV16	0.372	6.95%

Table C.4: RM2 Cable loadings

Cable	Current (kA)	Loading
Cable 1B	0.089	59.21%
Cable 2B	0.058	38.81%
Cable 3B	0.150	100.15%
Cable 4B	0.018	17.70%
Cable 5B	0.034	34.19%
Cable 6B	0.066	66.17%
Cable 7B	0.000	0.00%
Cable 8B	0.030	30.05%
Cable 9B	0.006	5.70%
Cable 10B	0.031	30.67%
Cable 11B	0.052	51.77%
Cable 12B	0.079	52.33%

- **Overall power losses for RM2**
- The new power loss obtained from RM2 is:

$$\begin{aligned}
 P_{\text{loss (overall)}} &= \sum P_{\text{loss (Cables)}} + \sum P_{\text{loss (TRFR)}} \\
 &= 219.4 \text{ kW}
 \end{aligned}$$

- **Overall efficiency for RM2**

The input power supplied by RM2 VS2 is $\sum P_{\text{in(RM2)}} = 4.920 \text{ MW}$, and $\sum P_{\text{out(RM2)}}$ is 4.701 MW. Hence the overall efficiency is:

$$\eta_{\text{overall}} = \frac{\sum P_{\text{out(RM2)}}}{\sum P_{\text{in(RM2)}}} \times 100\% = \frac{4.701}{4.920} \times 100\% = 95.54\%$$

APPENDIX D

D. Case study 2

a) RM2 results

Since in the optimal configuration RM1 is completely dependent on RM2, the steady-state results for RM2 were analysed to check if the interconnection caused any constraint violation on RM2.

- RM2 voltage profile analysis

Figure D.1 shows the voltage profile of the normal operations and the voltage profile after RM1 load was transferred to RM2.

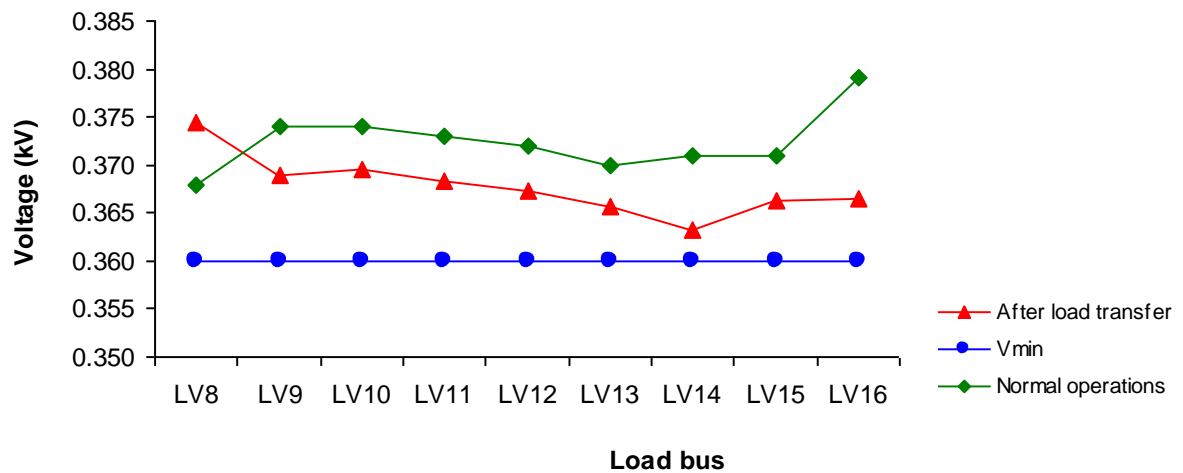


Figure D.1: RM2 Voltage profile for case study 2

Figure D.1 shows that all the voltage levels are within the 10% limit.

- RM2 cable loading

Figure D.2 shows the cable loadings obtained before and after the load transfer.

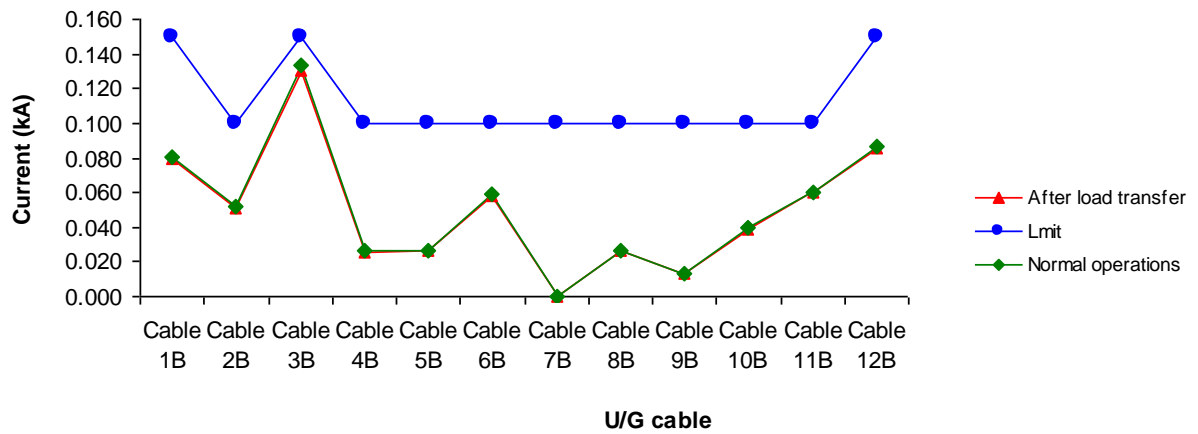


Figure D.2: RM2 cable loadings for case study 2

The cable loading profile obtained after the RM1 load was transferred to RM2 in Figure D.2 shows that all the cables are within their maximum current carrying capacities.

This clearly shows that the interconnection did not cause any overloading or under voltage on the RM2 busbar. This proves the configuration to be optimal.

- RM2 volt-drop Analysis

Table D.1: RM2's highest volt-drop obtained for the different configurations

	Normal operations	After load transfer
Volt-drop(%)	3.18% (Cable 3B)	3.13% (Cable 3B)

- Overall power loss for RM2

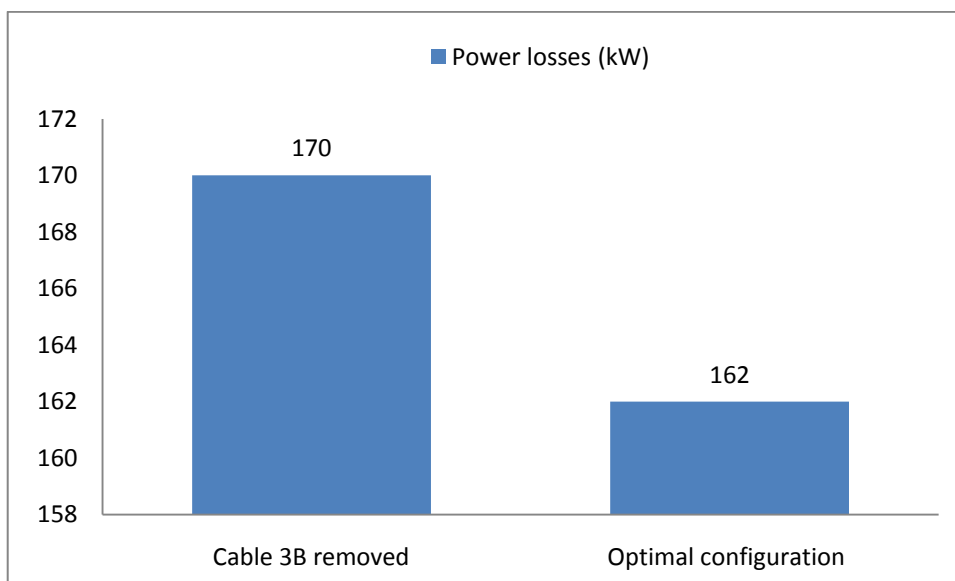


Figure D.3: RM2 Power losses for case study 2

The load transferred to RM2 did not cause any power loss increase on the RM2 network as it would be expected, instead it has caused a decrease in the power loss of the network. The losses of RM2 have decreased by:

$$\begin{aligned} \%P_{\text{loss(increase)}} &= \frac{P_{\text{loss (Normal Op)}} - P_{\text{loss (Cable 1A removed)}}}{P_{\text{loss (Normal Op)}}} \times 100\% \\ &= \frac{170 - 162}{162} \times 100\% = 4.71\% \end{aligned}$$

- Overall efficiency for RM2

The input power supplied by RM2 VS2 is $\sum P_{\text{in(RM2)}} = 3.97 \text{ MW}$, and $\sum P_{\text{out(RM2)}}$ is 3.97MW.

Hence the overall efficiency is:

$$\eta_{\text{overall}} = \frac{\sum P_{\text{out(RM2)}}}{\sum P_{\text{in(RM2)}}} \times 100\% = \frac{3.808}{3.97} \times 100\% = 95.91\%$$

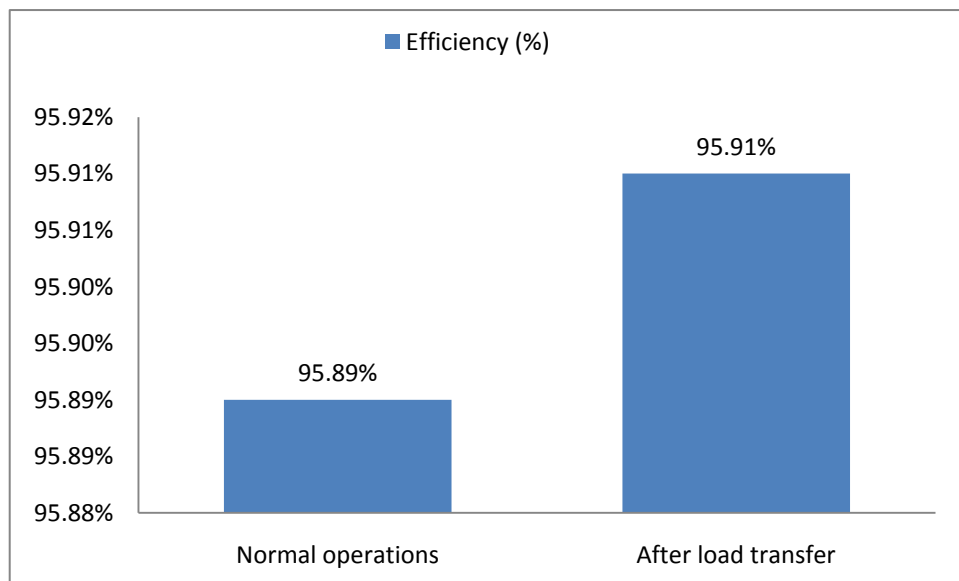


Figure D.4: RM2 Overall efficiency for case study 2

Figure D.4 shows that after the RM1 load was transferred to RM2, the RM2 efficiency increased from 95.89% to 95.91%.